The Dissertation Committee for Hua Li Certifies that this is the approved version of the following dissertation:

Metal-Catalyzed Oxidation of Polybutadiene in Oxygen Scavenging Packaging Applications

Committee:

Richard A. Jones, Supervisor

Benny D. Freeman, Co-Supervisor

Donald R. Paul

Alan H. Cowley

Bradley J. Holliday

O. Max Ekiner

Metal-Catalyzed Oxidation of Polybutadiene in Oxygen Scavenging Packaging Applications

by

Hua Li, B.S., M.S.

Dissertation

Presented to the Faculty of the Graduate School of

The University of Texas at Austin

in Partial Fulfillment

of the Requirements

for the Degree of

Doctor of Philosophy

The University of Texas at Austin

May, 2010

Dedication

To my parents for their constant love, encouragement and support

Acknowledgements

My Ph.D. years at the University of Texas at Austin and this dissertation had mentorship from numerous outstanding individuals both from within the university and outside of it. It is to these individuals that my heartfelt gratitude and thanks go out to, for without their help, this dissertation would not have been possible.

First and foremost I would gratefully acknowledge the enthusiastic supervision of Dr. Benny Freeman, who introduced me to the world of polymer membranes. I would like to deeply thank Dr. Richard Jones, Dr. Donald Paul, Dr. Max Ekiner, Dr. Alan Cowley and Dr. Bradley Holliday, for their warm encouragement and thoughtful guidance. I would also express my thanks to Dr. Richard Lagow, who gave me the opportunity to start my Ph.D. study at The University of Texas at Austin and supervise me in research regarding fluorine chemistry.

I thank Dr. Mark Stewart and Dr. Jason Jenkins at Eastman Company for their valuable suggestions and help in the OxySense$^®$ system and oxygen scavenging materials. I would also like to thank Dr. Yangming Sun and Dr. Huge Celio's for their help in XPS and SEM/EDS analysis, Dr. Domingo Ferrer for his help in TEM experiments and Dr. Steve Swinnea for his help in WAXD analysis. Many thanks to Ms. Pam Cook; she spent a lot of time helping me revising all my papers and thesis manuscripts.

I really enjoyed the research in Dr. Freeman's group everyday; this membrane research group is simply uncommon. You can rarely see such an enjoyable group of smart and kind people fitting together so well. A special thank goes to Kevin Tung, who is not only a great co-worker but also a great friend; also many thanks to Keith Ashcraft, for his cooperation, suggestions and educational discussions, the project could not have reached success without their help. The following members have been extremely helpful to this research: Dr. Victor Kusuma, Dr. Haiqing Lin, Dr. Scott Matteucci, Dr. Brandon Rowe, Dr. Maria-Chiara Ferrari, Dr. Hao Ju, Dr. Claudio Reberio Jr., Dr. Ho Bum Park, Dr. Bryan McCloskey, David Sanders and Zachary Smith. I am also grateful to the former and current members of Dr. Freeman's group for their various forms of support during my graduate study.

Most importantly, none of this would have been possible without the love and patience of my parents, Lixing Li and Guifang Jiang. It was under their watchful eye that I gained so much drive and ability to face challenges. Finally, I thank Ms. Shu Shen for her support, encouragement, quiet patience and unwavering love and for walking with me through the highs and lows for the past years.

Metal-Catalyzed Oxidation of Polybutadiene in Oxygen Scavenging Packaging Applications

Hua Li, Ph.D.

The University of Texas at Austin, 2010

Supervisors: Richard A. Jones, Benny D. Freeman

To better characterize the fundamentals of oxygen scavenging as a means to prepare high oxygen barrier polymer films, the oxidation of 1,4-polybutadiene, in the presence of a transition metal salt catalyst, cobalt neodecanoate, was studied at 30°C. 1,4-Polybutadiene was subjected to several purification steps to remove oxidation antioxidants that are typically added during the industrial scale preparation of this polymer. The importance of the purification method and residual antioxidant on oxidation was determined. Oxygen uptake of 1,4-polybutadiene films was measured as a function of cobalt neodecanoate concentration. In these samples, oxygen mass uptake values as high as 15 weight percent were observed, and the oxidation process occurred over approximately one week.

Oxygen mass uptake was measured in 1,4-polybutadiene films of different thicknesses undergoing cobalt-catalyzed oxidation in air at 30ºC. FTIR and XPS analysis

suggest that the oxidation was heterogeneous, with the film surface being highly oxidized and the film center being less oxidized. Interestingly, the oxygen uptake exhibited a maximum with catalyst loading, which is believed to be related to the heterogeneous nature of the oxidation process. Films thicker than approximately 50 µm showed a decrease in oxygen uptake per unit polymer mass as film thickness increased, while oxygen uptake per unit film area remained independent of thickness, suggesting that oxidation was heterogeneous and proceeded essentially as an oxidized front penetrating into the film from the surfaces exposed to oxygen. In contrast, oxidation in thin films appears to proceed homogeneously, with oxygen uptake per unit mass being essentially independent of thickness. The dividing line between thick and thin films, the so-called critical thickness for oxidation, appears to be about 28 µm. In oxidized samples, oxygen and nitrogen permeability decreased by more than two orders of magnitude relative to permeability values in unoxidized samples. A two-phase model was used to describe the permeability data.

Experiments were also conducted at different temperatures and oxygen partial pressures. Thick films oxidized at 45ºC showed heterogeneous oxidation similar to that reported above, while films oxidized at 5ºC showed a much longer oxidation time scale and higher oxygen mass uptake value. SEM images demonstrated that the structures of cross sections in films oxidized at different temperatures were also different; the oxidized layer structure was not observed in samples oxidized at 5ºC. Oxygen partial pressure experiments were conducted under the conditions that environmental oxygen content was less than 21%. It is observed that increasing oxygen partial pressure leads to faster oxidation kinetics and higher oxygen mass uptake in polybutadiene films.

Table of Contents

List of Tables

List of Figures

Chapter 1: Introduction

1.1   Packaging with Barrier Films

The demand for polymer barrier films in the packaging industry has grown in recent decades[1]. Packaging for foods and beverages like coffee, beer, fruit, and meat must usually be capable of excluding oxygen; in some cases limiting both oxygen and carbon dioxide, to preserve freshness and avoid changes in flavor, texture and color[2]. In other high value added products, like pharmaceuticals, both oxygen and water resistance are important[2]. Table 1.1 provides oxygen and water permeation protection data required for a number of foods.

Plastic packaging have replaced metal and glass in many applications[3]. One important reason is that consumers prefer to see products such as fruit and meat, so packaging materials need to be transparent and flexible. These materials can be made effectively using flexible polymers. The first practical polymeric film used by the packaging industry was cellophane, which provides an excellent gas barrier when dry but loses barrier capability at high humidities[2].   Because cellophane is neither thermoplastic nor heat sealable, processing can be difficult.

Polyvinyl chloride (PVC), vinylidene chloride (PVDC), polyacrylonitrile (PAN), and their copolymers are economical thermoplastic materials with good barrier properties to gases and water[4]. But the presence of low level residual toxic monomers limits their use for food packaging.

Table 1.1   Food and beverage protection requirements for one year shelf life at 25°C[5]

Food or Beverage	Estimated maximum tolerable oxygen gain, ppm	Estimated maximum water gain or loss, wt %	Required oxygen permeability, Barrer**
Canned milk, meats, canned vegetables	1 to 5	-3	$5.6 - 28 \times 10^{-7}$
Beer, ale, wine*	1 to 5*	-3	$5.6 - 28 \times 10^{-7}$
Instant coffee	1 to 5	+2	$5.6 - 28 \times 10^{-7}$
Canned fruits	5 to 15	-3	$2.8 - 8.4 \times 10^{-6}$
Nuts, snacks	5 to 15	+5	$2.8 - 8.4 \times 10^{-6}$
Fruit juice, drinks	10 to 40	-3	$5.6 - 22 \times 10^{-6}$
Carbonated soft drinks	10 to 40*	-3	$5.6 - 22 \times 10^{-6}$
Oils, shortenings, salad dressings	50 to 200	+10	$2.8 - 11 \times 10^{-5}$
Liquors	50 o 200	-3	$2.8 - 11 \times 10^{-5}$

* Less than 20% loss of CO_2 is also required.

**1 year shelf life. Package dimensions: 500 cm^3, wall thickness 11 mil, ΔP_{O_2}= 20 cm Hg

Ethylene-vinyl alcohol (EVOH) copolymers are excellent oxygen barrier materials and do not have the problem of toxic monomers[4]. They became popular soon after their introduction in the United States in the mid 1970's. Their strong hydrogen bonds and partially crystalline structures lead to very low permeability to oxygen when dry. However, like cellophane, EVOH loses barrier capability at high humidity[4].

Since condensation polymerization yields much lower levels of residual monomers, condensation polymers such as poly(ethylene terephthalate) (PET) are now widely used in food packaging[6]. PET is the material of choice for the carbonated beverage market. Since the permeability of PET is not as low as PVDC or EVOH, PET is often combined with other materials to reach better barrier properties[1].

There are several ways to improve the barrier properties of polymeric membranes: by reducing the membrane permeability, by increasing tortuosity, and by changing reactivity. The first strategy involves incorporating impermeable organic or inorganic materials, usually in the form of flakes[7-10], or recently, nanoparticles[11, 12], into barrier films. When polymer materials contain flakes, their direction will strongly affect permeation. Flakes perpendicular to the film surface will have very little effect on permeation; when flakes are aligned parallel to the film surface, limiting the diffusion path, the film's permeability to penetrant gas can be less than one-tenth that of the pure polymer films[10].

A second route is to prepare multi-layer rather than single layer packaging films. Although numerous polymers with good barrier properties have been discovered and designed, all have limitations that restrict their application. Common constraints include mechanical properties, humidity/chemical resistance, and cost. Multilayer structures can often resolve these problems efficiently: barrier polymers combined in layered structures often enhance the strengths of each material. For example, EVOH has very low oxygen permeability, but it is very sensitive to humidity because of the hydroxyl group in the polymer chain. Thus, it is often coextruded or laminated as a thin layer between other

3

barrier materials, such as PET, in food packaging applications[1]. The PET layers block excess humidity from the environment to keep the EVOH functional, and simultaneously reduce the cost of the barrier film. Multilayer films made from polymer materials that have similar melting temperatures and viscosities can be produced via coextrusion [1]. Figure 1.1 shows a typical structure of a nine-layer film prepared using coextrusion.

Nonpolymeric materials can also be introduced into layer structures by coating and lamination processes. Epoxy-amine organic coatings have been used to improve oxygen barrier properties of PET bottles, while laminations of aluminum foil and aluminum oxide have significantly improved the barrier properties of poly(propylene), PET, and nylons[13].
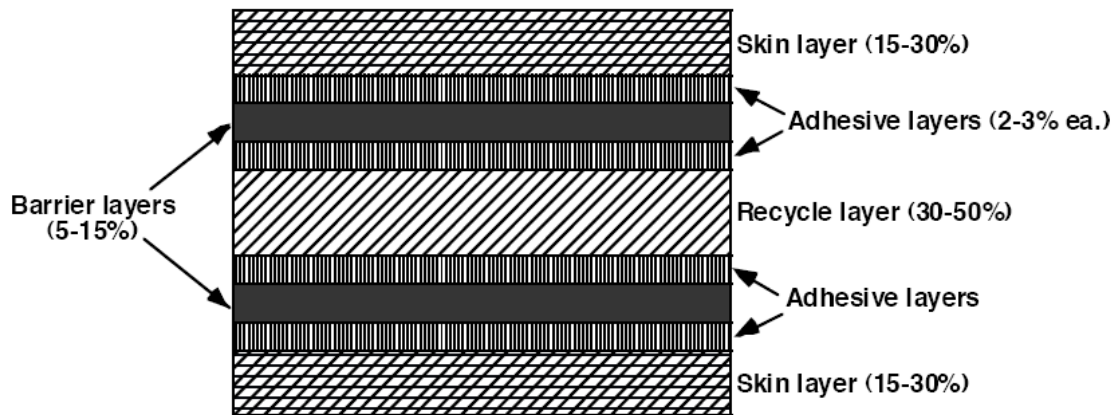
Figure 1.1   Nine-layer coextruded barrier film structure[14]

A third strategy is to incorporate other materials that will interact with the internal and external environments rather than merely providing an inert barrier. These are called "active" packaging materials, as opposed to traditional "passive" packaging materials[13]. The interaction processes may be either physical (e.g., absorption and adsorption) or chemical (e.g., reactive materials). The reactive sites can be either the functional groups on the packaging material itself, i.e., block copolymers with reactive blocks, or one or more polymer components in polymer blends. Methods two and three are often combined to prepare films with optimized barrier properties[13].

1.2   Oxygen Scavenging Materials

Packaging is defined as active (compared with traditional passive packaging) when it not only provides an inert barrier to external conditions, but also interacts with or responds to the environment[13]. Active packaging has developed as a series of responses to unrelated problems in maintenance of food quality and safety. Inherent in the definition is the point that active packaging plays a role in protecting the food, in addition to the classic purpose of any packaging.

Oxygen scavenging materials are important in active packaging. The removal of headspace oxygen and providing barriers to environmental oxygen have long been targets in the packaging of oxygen-sensitive products[15]. Early attempts at removing oxygen used vacuum packaging and inert gas flushing[16]. The use of sachets containing oxygen scavengers in low oxygen transmission conditions was also reported[17].

5

In recent decades there has been considerable interest in using reactive polymer films in oxygen scavenging systems, in part because conventional packaging materials, such as PET, do not by themselves have sufficiently low oxygen permeation properties to meet certain applications, e.g., packaging beer in long-shelf life plastic bottles[1]. Early attempts introduced salts, such as potassium sulfite or sodium sulfite, into the barrier polymers[18]. Metal complexes are also used as agents in oxygen scavengers[19]. Unlike the potassium and sodium salts, the metal ions are the components that will be oxidized.

Oxygen scavenging polymeric films provide an additional mechanism, above and beyond that which can be obtained by conventional passive barrier packaging, for reducing oxygen transmission into packages by chemically oxidizing a sacrificial polymer layered or embedded into some or all of a package wall[2]. In a packaging film containing or consisting of an oxygen scavenging polymer, any oxygen diffusing across the film is susceptible to being consumed by chemical reaction with the oxidizable polymer, where it may be incorporated into the oxidized polymer, thereby arresting its transport across the film[9].

Oxygen scavenging systems that incorporate reactive hydrocarbon polymers doped with transition metals have been reported by Speer *et al*.[20]. Blends containing small amounts of high barrier polyamides, such as poly(m-xylylene adipamide), typically known commercially as MXD6, with polyesters such as PET, enhance PET's barrier properties [21-24]. Figure 1.2 illustrates the ability of adding 4% of an oxygen

scavenging material (MXD-6 with cobalt catalyst) to reduce the oxygen permeability of PET and increase shelf life.
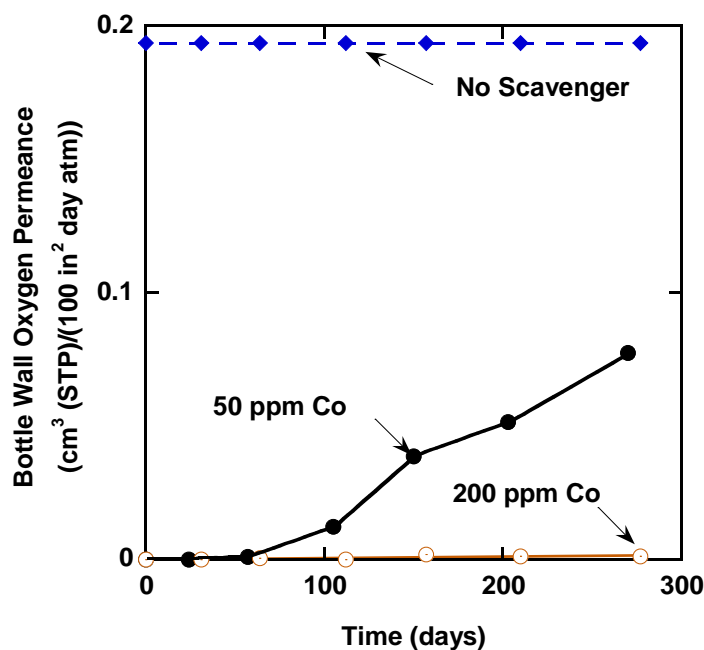
Figure 1.2   Effect of scavenger loading and catalyst concentration on oxygen permeance through a PET bottle wall, reproduced from [25].

The presence of oxygen at even ppm levels can cause certain foods and beverages to experience rapid deleterious oxidation or other aerobic degradation processes[26]. Incorporation of oxygen scavengers into otherwise passive barrier polymers can markedly reduce oxygen permeability and extend the shelf-life of oxygen sensitive products to levels rivaling those of glass and metal packaging over time spans of several years[15, 20, 27, 28]. Few studies of the chemistry of oxygen scavenging films have been published in peer-reviewed journals. However, numerous patents and some

conference proceeding give sufficient detail to allow a comparison of the systems reported. The most marked trend in oxygen scavenging system development during the past 20 years has been the increasing number of patent applications for compositions and designs based on plastics. Very few of these involve actual polymer oxidation but rather require the reactive ingredients to be dispersed within the polymer matrix or sandwiched between film layers.

The use of active oxygen scavengers, which chemically remove oxygen migrating through the walls of the package, can very effectively reduce the oxygen transmission rates of plastics used in packaging. While currently available scavengers have found some utility, they also suffer from a variety of drawbacks[15]. For example, oxygen uptake in scavenging systems is not sufficiently high enough for some applications[15]. In some instances, these deficiencies can be partially addressed by increasing the amount of oxygen scavenger in the package structure. However, this typically increases the final cost of the package and has undesirable effects on appearance, such as adding haze or color to the packaging[15]. In addition, increasing the concentration of oxygen scavenger can complicate manufacture and recycling of the package. Thus, there is a need for improved oxygen scavenging materials that rapidly achieve high scavenging rates.

1.3   Organizations of the Dissertation

There are eight chapters, including this introductory chapter, in this dissertation. Chapter 2 provides the background theory of gas permeation and sorption in barrier films,

and reaction mechanisms of polymer oxidation and degradation. Materials and experimental techniques used in this work, including the building and calibration of the OxySense® system, are presented in chapter 3.

Chapters 4 to 6 concentrate on the oxygen scavenging properties of polymer films based on commercial 1,4-polybutadiene. Chapter 4 presents the effect of antioxidants on polybutadiene oxidation and characterization of oxygen mass uptake in 1,4-polybutadiene films. The effect of catalyst concentration on oxygen mass uptake and oxidation rates is also discussed in this chapter. In chapter 5, the effect of film thickness on oxidation in polybutadiene films is discussed, and the critical oxidized layer thickness in 1,4-polybutadiene films was estimated using different methods. The effects of reaction temperature and initial oxygen content on oxygen scavenging are presented in chapter 6. There is one extra chapter on a separate research project: poly(urethane urea)s for CO_2 removal from other gases. This research project involved polymer synthesis, physical properties characterization and gas separation property measurement and is presented in Chapter 7. Chapter 8 contains the conclusions and recommendations for future work.

1.4 References

1. S. N. Dhoot, B. D. Freeman, and M. E. Stewart. Barrier polymers. In: Kroschwitz J. I., editor. Encyclopedia of Polymer Science and Technology, vol. 5. Wiley-Interscience, New York, 2003, 193-263.

2. W. J. Koros. Barrier polymers and structures: overview. In: Koros W. J., editor. Barrier Polymers and Structures. American Chemical Society, Washington, DC, 1990, 1-22.

3.   S. Solovyov and A. Goldman. Mass Transport & Reactive Barriers in Packaging: Theory, Applications & Design. DEStech Publications, Inc., Lancaster, Pennsylvania, 2008, 1-11.

4.   P. DeLassus. Barrier polymers. In: Kirk R. E. and Othmer D. F., editors. Kirk Othmer Encyclopedia of Chemical Technology, vol. 3. John Wiley & Son, Inc., Hoboken, New Jercy, 2002, 375-407.

5.   *Plastics Engineering*, **May 1984**, 47.

6.   Pira Forecasts PET Consumption. http://www.packworld.com/view-21883.

7.   E. L. Cussler, S. E. Hughes, W. J. Ward, and R. Aris. Barrier membranes. *Journal of Membrane Science*, **1988**, 38(2), 161-174.

8.   W. R. Falla, M. Mulski, and E. L. Cussler. Estimating diffusion through flake-filled membranes. *Journal of Membrane Science*, **1996**, 119(1), 129-138.

9.   C. Yang, E. E. Nuxoll, and E. L. Cussler. Reactive Barrier Films. *AIChE Journal*, **2001**, 47(2), 295-302.

10.   N. K. Lape, C. F. Yang, and E. L. Cussler. Flake-filled reactive membranes. *Journal of Membrane Science*, **2002**, 209(1), 271-282.

11.   T. M. Aminabhavi and N. N. Mallikarjuna. Polymeric membranes: Polymeric nanocomposites: Barrier properties and membrane applications. *Polymer News*, **2004**, 29(6), 193-195.

12.   M. Frounchi, S. Dadbin, Z. Salehpour, and M. Noferesti. Gas barrier properties of PP/EPDM blend nanocomposites. *Journal of Membrane Science*, **2006**, 282(1+2), 142-148.

13.   M. L. Rooney. Overview of active food packaging. In: Rooney M. L., editor. Active Food Packaging, vol. 1. Blackie Academic & Professional, London, 1995, 1-37.

14.   W. A. Jenkins and J. P. Harrington. Packaging foods with plastics. Technomic Publishing Co., Lancaster, 1991, 326-327.

15.   M. L. Rooney. Active packaging in polymer films. In: Rooney M. L., editor. Active food packaging, vol. 4. Blackie Academic & Professional, London, 1995, 74-110.

16.   A. L. Brody. Modified atomsphere packaging of seafoods. In: Brody A. L., editor. Controlled/Modified Atmosphere/Vacuum Packaging of Foods. Food and Nutrition Press, Trumbull, 1989, 59-60.

17.   Y. Abe and Y. Kondoh. Oxygen absorbers. In: Brody A. L., editor. Controlled/Modified Atmosphere/Vacuum Packaging of Foods. Food and Nutrition Press, Trumbull, 1989, 151.

18.   C. J. Farrell and B. C. Tsai. Oxygen Scavenger. U. S. Patent, 4,536,409, **1985**

19.   B. Zenner, E. Decastro, and J. Ciccone. Ligand extracting composition-containing chelated transition metal immobilised on solid phase, especially for scavenging oxygen in containers. U. S. Patent, 5,096,724, **1992**

20.   D. V. Speer, W. P. Roberts, and C. R. Morgan. Method and compositions for oxygen scavenging. U. S. Patent, 5,211,875, **1993**

21.   Y. S. Hu, V. Prattipati, S. Mehta, D. A. Schiraldi, A. Hiltner, and E. Baer. Improving gas barrier of PET by blending with aromatic polyamides. *Polymer*, **2005**, 46(8), 2685-2698.

22.   A. Polyakova, R. Y. F. Liu, D. A. Schiraldi, A. Hiltner, and E. Baer. Oxygen-barrier properties of copolymers based on ethylene terephthalate. *Journal of Polymer Science Part B-Polymer Physics*, **2001**, 39(16), 1889-1899.

23.   T. Shimotori, E. L. Cussler, and W. A. Arnold. Diffusion of mobile products in reactive barrier membranes. *Journal of Membrane Science*, **2007**, 291(1-2), 111-119.

24.   R. A. Siegel and E. L. Cussler. Reactive barrier membranes: some theoretical observations regarding the time lag and breakthrough curves. *Journal of Membrane Science*, **2004**, 229(1-2), 33-41.

25.   M. A. Cochran, R. Folland, J. W. Nicholas, and M. E. R. Robinson. Packaging. U. S. Patent, 5,021,515, **1991**

26.   L. Vermeiren, F. Devlieghere, M. van Beest, N. de Kruijf, and J. Debevere. Developments in the active packaging of foods. *Trends in Food Science & Technology*, **1999**, 10(3), 77-86.

27.   T. Y. Ching, K. Katsumoto, S. P. Current, and L. P. Theard. Compositions having ethylenic backbone and benzylic, allylic, or ether-containing side-chains, oxygen scavenging compositions containing same, and process for making these

compositions by esterification or transesterification of a polymer melt. U. S. Patent, 5,627,239, **1997**

28.   D. V. Speer and W. P. Roberts. Oxygen scavenging compositions for low temperature use. U. S. Patent, 5,310,497, **1993**

Chapter 2: Background

2.1   Fundamentals of Permeations in Polymers

The currently accepted solution-diffusion mechanism of penetrant transport in a dense or nonporous polymer membrane was first suggested by Graham in 1866[1]. In this model, gas transport though a polymer membrane is described as a three step process: penetrants first dissolve into the high pressure (i.e., upstream) surface of the membrane, diffuse through the membrane, and then desorb from the low pressure (i.e., downstream) surface. The steady state rate of transport of gas A through a polymer membrane is expressed by the permeability coefficient, P_A, defined as[2, 3]:

$$P_A = \frac{N_A l}{p_2 - p_1} \tag{2.1}$$

where N_A is the steady state gas flux through the membrane (cm^3(STP)/(cm^2·s)), l is the membrane thickness (cm), and p_2 and p_1 are upstream and downstream partial pressures of gas A (cmHg). Permeability coefficients are often expressed in barrers, where 1 barrer $= 1 \times 10^{-10} \frac{cm^3(STP) \cdot cm}{cm^2 \cdot s \cdot cmHg}$. At steady state, the gas flux, N_A, through the polymer film can be described by Fick's first law[4, 5]:

$$N_A = \frac{D_{loc}}{1 - w_A} \frac{dC_A}{dx} = -D_{eff} \frac{dC_A}{dx} \tag{2.2}$$

where D_{loc} is the binary mutual diffusion coefficient of gas A in the polymer, D_{eff} is the effective mutual diffusion coefficient in the polymer, C_A is the local concentration of

dissolved gas, w_A is the weight fraction of gas A in the film, and x is the distance across the film. Combining Eqs. (2.1) and (2.2) and integrating from $x = 0$ ($C = C_2$) to $x = l$ ($C = C_1$) yields:

$$P_A = \frac{1}{p_2 - p_1} \int_{C_1}^{C_2} D_{eff} dC_A \tag{2.3}$$

where C1 and C2 are the gas concentrations in the polymer at the upstream and downstream faces, respectively. This relationship can also be written as[4]:

$$P_A = D_A \frac{C_2 - C_1}{p_2 - p_1} \tag{2.4}$$

where D_A, the concentration averaged effective diffusion coefficient, is defined as follows:

$$D_A = \frac{1}{C_2 - C_1} \int_{C_1}^{C_2} D_{eff} dC_A \tag{2.5}$$

In experiments, the downstream pressure p_1 and gas concentration C_1 are often significantly lower than those at the upstream side of the film, and Equation (2.4) can be written as[4]:

$$P_A = D_A \times S_A \tag{2.6}$$

where

$$S_A = \frac{C_2}{p_2} \tag{2.7}$$

S_A is the apparent solubility coefficient of the penetrant in the polymer. Based on Equation (2.6), two factors influence permeability, P. The first factor is solubility, S_A, which determines the number of gas molecules sorbed by the polymer matrix. This is a thermodynamic term. The kinetic term, diffusion coefficient, D_A, characterizes the gas

14

molecules' mobility as they diffuse through the polymer membrane. Penetrant gas molecular size, polymer morphology, and polymer segmental dynamics can strongly affect the diffusion coefficient[4], and the penetrant gas condensability influences solubility[4].

Another important membrane property in gas separation studies is selectivity. The ideal selectivity is defined as[4]:

$$\alpha_{AB} = \frac{P_A}{P_B} \qquad (2.8)$$

where P_A and P_B are the permeability coefficients of different gases. Selectivity is usually expressed as a number ≥ 1, so the more permeable gas is taken as gas A. Combining Eqs. (2.6) and (2.8), the ideal selectivity can be express as follows:

$$\alpha_{AB} = \left(\frac{D_A}{D_B}\right)\left(\frac{S_A}{S_B}\right) = \alpha_{AB}^D \alpha_{AB}^S \qquad (2.9)$$

where D_A and D_B are the diffusion coefficients of different gas species, and S_A and S_B are their solubilities. The ideal selectivity between gas A and B depends upon diffusivity selectivity, $\alpha_{AB}{}^D$, and solubility selectivity, $\alpha_{AB}{}^S$.

2.2   Oxidation Mechanism in Polymers

2.2.1   Polymer Degradation

The exposure of polymers to certain environmental conditions often leads to gradual polymer degradation that usually involves chemical processes[6]. Many factors can play a role in this degradation, including thermal, radiative, chemical, and biological

processes, or some combination of these. The polymer physical properties (mechanical strength, elasticity, density, etc.) and chemical structures will change, depending on the extent of degradation[7]. Although in many circumstances, these changes need to be prevented, degradation can be useful in other applications (e.g., pollution caused by waste materials).

Metal-catalyzed oxidation can be categorized as homolytic and heterolytic[8]. Homolytic catalysis utilizes soluble transition metal salts, necessitates the transitioning of the metal species between oxidation states, and yields free radicals as intermediates from organic substrates. Heterolytic catalysis, on the other hand, involves reactions of organic substrates coordinated to transition metals. In both mechanisms, important characteristics of the transition metal include its accessibility to several oxidation states and the accommodation of various coordination numbers.

2.2.2   *Oxidative Degradation in the Presence of Metal Catalysts*

Like other radical reactions, the oxidative degradation generally follows three steps: initiation, propagation, and termination[9]. The first step, the chain initiation reaction, is usually caused by a free radical donor, such as α,α-azobisisobutyronitrile, or peroxides. Hydroperoxides may be present during oxidation because they have been added to the reaction medium or as a result of their formation during the oxidative process. However, not all autoxidation reactions are initiated by hydroperoxides. Some oxidation reactions occur in the absence of initiators; their initiation is exemplified by the following reactions[10]:

16

$$RH \xrightarrow{hv,\Delta} R\cdot \tag{2.10}$$

$$RH + O_2 \longrightarrow R\cdot + HO_2\cdot \tag{2.11}$$

$$M + O_2 \longrightarrow M^{\delta+}O_2^{\delta-} \quad \text{(M = metal complex)} \tag{2.12}$$

$$MO_2 + RH \longrightarrow M + R\cdot + HO_2\cdot \tag{2.13}$$
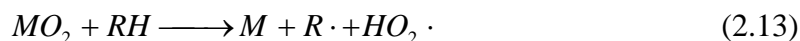
The propagation step, usually described as polymer chain elongation in other reactions, involves addition of oxygen to alkyl free radicals and abstraction of hydrogen atoms from polymers in oxidative degradation[8]. Intramolecular and intermolecular oxidation are also considered part of the propagation reactions. These reactions can be written as[8]:

$$R\cdot + O_2 \xrightarrow{k_0} RO_2\cdot \tag{2.14}$$

$$RO_2\cdot + RH \xrightarrow{k_p} ROOH + R\cdot \tag{2.15}$$

$$RO_2\cdot + RH \xrightarrow{k_p'} ROO\dot{R}H \tag{2.16}$$

As reported in the literature, intramolecular propagation will be important only in cases where the reaction is sterically favored[11]. It was observed most often in autoxidation of branched alkanes (e.g., polypropylene)[11].

Transition metal ions play an important role in the redox decomposition of alkyl hydroperoxides (ROOH, where R represents the polymer structure)[8]. This kind of decomposition is the most commonly reported pathway for catalysis in metal-catalyzed polymer autoxidation[8]. There is a wide selection of transition metal ions: silver, cerium, iron, copper, and most commonly, cobalt and magnesium. Introducing a transition metal

complex into the polymer will increase the production rate of alkoxy and alkylperoxy radicals, both of which are important in the propagation step. This increase in reaction rate is caused by a change in activation energy. For example, in regular alkyl hydroperoxides, thermal decomposition has an activation energy of about 40 kcal/mole, while the activation energies in reactions between cobalt complexes and hydroperoxides are around 10-20 kcal/mole, depending on the type of hydroperoxide[8]. The likely catalysis mechanism is an oxidation-reduction catalytic cycle composed of two reactions by two valence states of metal ions[10]:

$$ROOH + M^{n+} \longrightarrow RO \cdot + M^{(n+1)+} + OH^-$$ (2.17)

$$ROOH + M^{(n+1)+} \longrightarrow RO_2 \cdot + M^{n+} + H^+$$ (2.18)

$$RO \cdot + RH \longrightarrow ROH + R \cdot$$ (2.19)
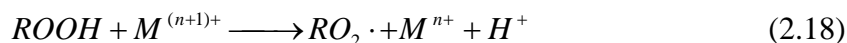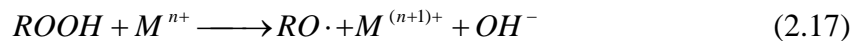
This mechanism was first proposed in iron-hydroperoxide complex[12] and later in other transition metals[13-16]. The termination steps, in which two free radicals react together and generate inactive product, consist of three types of reactions[10]:

$$2R \cdot \longrightarrow products$$ (2.20)

$$RO_2 \cdot \longrightarrow products$$ (2.21)

$$2RO_2 \cdot \longrightarrow products + O_2$$ (2.22)

In the presence of oxygen, reactions (2.20) and (2.21) can be neglected because the concentration $[RO \cdot] \gg [R \cdot]$, and reaction (2.14) is very fast. Thus, reaction (2.22) becomes the primary termination reaction during oxidation.

Based on the above reactions, the transition metal ions help produce free radicals not only in the initiation steps, but also in the propagation steps. However, these effects happen only at low transition metal catalyst concentrations. The reaction rate is related to the metal catalyst concentration until the catalyst reaches a certain concentration, above which addition of metal catalyst no longer impacts the reaction rate[17]. Furthermore, when the metal ion concentration reaches a critical concentration), the reaction rate starts to decrease rapidly with increasing concentration of metal ions[18-20]. In this case, the role of the transition metal complex is no longer a catalyst but an inhibitor of the reaction.

This catalyst-to-inhibitor transition may caused by reactions between free radicals and the metal complex. These termination steps can be written as[11]:

$$RO_2 \cdot + MA_2 \xrightarrow{k_t} RO_2MA_2 \tag{2.23}$$

or

$$RO_2 \cdot + MA_2 \xleftarrow{K_t} RO_2MA_2 \tag{2.24}$$

$$RO_2MA_2 + RO_2 \xrightarrow{k_t'} products \tag{2.25}$$

At relatively high transition metal complex concentrations, termination steps such as (2.23) and (2.25) become more important; thus, the oxidation rate decreases as the amount of catalyst is increased. This effect is observed in autoxidation catalyzed by both magnesium and cobalt catalysts[11].

2.3 Diffusion Limited Oxidation

If oxidation is slow compared with the diffusion of oxygen in the polymer film, and if oxygen uptake occurs when oxygen is in excess, oxidation will be homogenous and the oxygen uptake often follows first order kinetics[21]:

$$\frac{dn'(t)}{dt} \propto x(t) = -kx(t) = -k\left[x_i - n_0 + n'(t)\right] \tag{2.26}$$

where $n'(t)$ is the number of moles of oxygen remaining in the gas phase at time t, n_0 is the initial number of moles of oxygen, $x(t)$ is the number of moles of reactive centers in polymer at time t, and x_i is the number of reactive centers in the polymer.

Integrating equation (2.26) between time 0 and t, the number of moles of oxygen that have reacted with the polymer, $n(t)$, can be expressed as[21]:

$$n(t) = x_i(1 - e^{-kt}) \tag{2.27}$$

If oxidation is fast relative to oxygen diffusion in the polymer, heterogeneous oxidation will occur, and the oxidation reaction takes place only in a narrow zone at the film surface, i.e., reaction is localized in a wavefront. In this circumstance[22, 23],

$$L_d^*(t) = \sqrt{\frac{2DC_{out}t}{\mu R_0}} \tag{2.28}$$

where $L_d^*(t)$ is the front position thickness at time t, D is the diffusion coefficient of polymer, C_{out} is oxygen concentration in environment, R_0 is the initial concentration of reactive sites, and μ is the scavenger reactive capacity (based on mass of oxygen consumed per mole of reactive sites).

Under conditions that foster high oxidation rates, such as high temperature and photo-oxidation, oxidation in the polymer may consume oxygen more rapidly than it can be supplied via diffusion. This condition, known as diffusion-limited oxidation (DLO), gives rise to heterogeneous oxidation profiles in films, with surface oxidation being greater than interior film oxidation[24].

Penetrant diffusion in polymers can be divided into two categories, i.e., Fickian (which obeys Fick's law of diffusion) and non-Fickian. In the Fickian diffusion-controlled kinetics of permeation through a plane film, the time required to reach steady state, t_{ss}, is given by[25]:

$$t_{ss} = \frac{L^2}{D}$$ (2.29)

where L is the thickness of the thin plane film. L should be much smaller than the film width or length. Fickian behavior is usually exhibited when penetrants transport through rubbery polymers and at low activity in glassy polymers. Non-Fickian diffusion behavior can be found in glassy polymers; for example, organic vapors sorb into amorphous glassy polymers at relatively high activity. With non-Fickian diffusion behavior, the time required to reach steady-state transport might be much longer than that predicted by Equation (2.29).

Since the gas transport properties of polymer materials continue changing during the oxidation process, the polymer's oxidation rate is affected not only by the kinetics parameters of the reaction but also by the rate of oxygen transport through the polymer film surfaces[24, 26-28]. In Daynes's studies of thermal degradation in rubber[29], as the

rate and extent of oxidation increased, the rate of diffusion decreased, and as the surface layers of the polymer oxidized, the oxygen absorption rate decreased sharply.

In thermo-oxidation of polybutadiene, Bauman[30] observed that the oxygen consumption rate showed an acceleration step in the beginning and later exhibited a deceleration step. The amount of oxygen consumed until the consumption rate reached its maximum was measured and is presented in Figure 2.1. In this figure, the films all had the same surface areas and were aged in air at various temperatures. Unfortunately, Bauman did not report the film mass or area, so it is impossible to normalize the data and compare them quantitatively with the results from this study. Additionally, it is not clear from Bauman's study whether the volume of oxygen absorbed is being reported at standard temperature and pressure (i.e., STP) or not. Nevertheless, Bauman proposed that if the oxidation reaction were not diffusion limited, then oxygen could readily penetrate to the center of the film. Otherwise, if the reaction were diffusion limited, the amount of oxygen that could reach the film center (and, therefore, participate in the oxidation process) would depend upon film thickness, so the amount of oxygen absorbed by the sample would decrease as film thickness increased. At 50ºC, the sorbed volume of oxygen is independent of film thickness, suggesting that oxidation was homogenous, so there was no diffusion limitation. In contrast, in samples oxidized at 90ºC, which exhibited faster oxidation rates, the amount of oxygen taken up by the polymer decreased as film thickness increased because the oxidation at the film surface inhibited transport of oxygen into the film, thereby limiting the amount of oxygen that could be consumed.
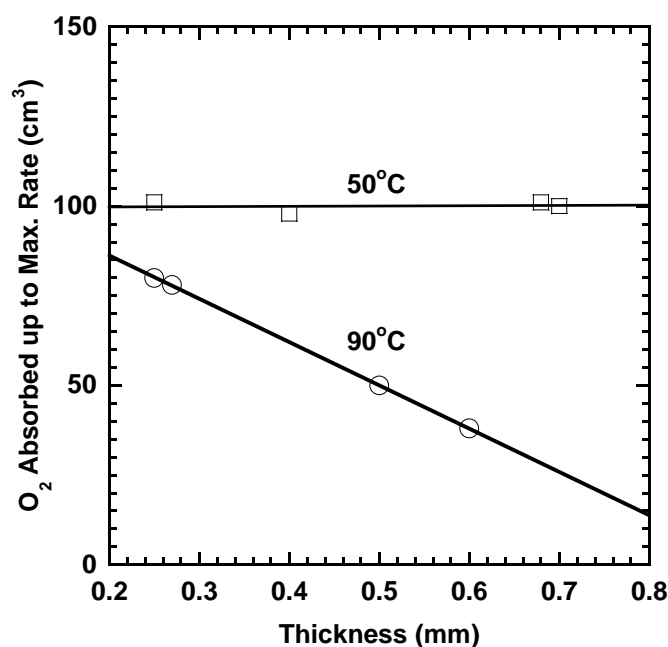
Figure 2.1   Influence of film thickness and temperature on the amount of oxygen absorbed by polybutadiene films in the initial stage of oxygen uptake, before the rate of oxidation reached its maximum value and, thereafter, decreased. These data are reproduced from[30].

2.4   References

1.   U. Graham. On the absorption and dialytic separation of gases by colloid septa Part I.-Action of a septum of caoutchouc. *Philosophical Magazine*, **1866**, 32, 401-420.

2.   K. Ghosal and B. D. Freeman. Gas separation using polymer membranes: an overview. *Polymers for Advanced Technologies*, **1994**, 5, 673-697.

3.   J. G. Wijmans and R. W. Baker. The solution-diffusion model: a review. *Journal of Membrane Science*, **1995**, 107, 1-21.

4.   S. Matteucci, Y. Yampolskii, B. D. Freeman, and I. Pinnau. Transport of gases and vapors in glassy and rubbery polymers. In: Yampolskii Y., Freeman B. D., and Pinnau I., editors. Material Science of Membranes for Gas and Vapor Separation. John Wiley & Sons, New York, 2006, 1-47.

5.   W. J. Koros. Barrier polymers and structures: overview. In: Koros W. J., editor. Barrier Polymers and Structures. American Chemical Society, Washington, DC, 1990, 1-22.

6.   M. C. Celina, R. L. Clough, and G. D. Jones. Interactive behavior in polymer degradation. In: Celina M. C. and Assink R. A., editors. Polymer Durability and Radiation Effects. American Chemical Society, Washington, DC, 2007, 37-47.

7.   L. Audouin, V. Langlois, J. Verdu, and J. C. M. Debruijn. Role of oxygen diffusion in polymer aging - kinetic and mechanical aspects. *Journal of Materials Science*, **1994**, 29(3), 569-583.

8.   R. A. Sheldon and J. K. Kochi. Metal-Catalyzed Oxidations of Organic Compounds. Academic Press, Inc. , New York City, New York, 1981, 33-70.

9.   J. Wise, K. T. Gillen, and R. L. Clough. Quantitative model for the time development of diffusion-limited oxidation profiles. *Polymer*, **1997**, 38(8), 1929-1944.

10.   L. Reich and S. S. Stivala. Autoxidation of Hydrocarbons and Polyolefins Marcel Dekker, Inc., New York, 1969.

11.   L. Reich and S. S. Stivala. Elements of Polymer Degradation McGraw-Hill, Inc., New York, 1971.

12.   G. L. Banks, A. J. Chalk, J. E. Dawson, and J. F. Smith. Catalysis of olefin autoxidation by heavy-metal ions in nonpolar media. *Nature*, **1954**, 174, 274-275.

13.   A. J. Chalk and J. F. Smith. Catalysis of cyclohexane autoxidation by trace metals in nonpolar media. II. Metal salts in the presence of chelating agents. *Transactions of the Faraday Society*, **1957**, 53, 1235-1245.

14.   J. F. Black. Metal-catalyzed autoxidation. The unrecognized consequences of metal-hydroperoxide complex formation. *Journal of the American Chemical Society*, **1978**, 100(2), 527-535.

15.   M. E. Ladhabhoy and M. M. Sharma. Absorption of oxygen by 2-ethylhexanaldehyde. *Journal of Applied Chemistry*, **1970**, 20(9), 274-280.

16.   G. C. Allen and A. Aguilo. Metal-ion catalyzed oxidation of acetaldehyde. *Advances in Chemistry Series*, **1968**, 76, 363-381.

17. Y. Kamiya and E. Niki. Oxidative degradation. In: Jellinek H. H. G., editor. Aspects of Degradation and Stabilization of Polymers, vol. 3. Elsevier Scientific Publishing Company, Amsterdam, The Netherland, 1978, 79-148.

18. A. T. Betts and N. Uri. Catalyst-inhibitor conversion in autoxidation reactions. *Advances in Chemistry Series*, **1968**, 76, 160-181.

19. A. T. Betts and N. Uri. Conversion of metal catalysts into inhibitors of autoxidation. *Makromolekulare Chemie*, **1966**, 95, 22-39.

20. Y. Kamiya and K. U. Ingold. The metal-catalyzed autoxidation of Tetralin. IV. The effect of solvent and temperature. *Canadian Journal of Chemistry*, **1964**, 42(11), 2424-2433.

21. S. W. Bigger and O. Delatycki. New approach to the measurement of polymer photooxidation. *Journal of Polymer Science Part A: Polymer Chemistry*, **1987**, 25(12), 3311-3323.

22. S. E. Solovyov. Theory of transient permeation through reactive barrier films I. Steady state theory for homogeneous passive and reactive media. *International Journal of Polymeric Materials*, **2005**, 54, 71-91.

23. S. E. Solovyov. Theory of transient permeation through reactive barrier films II. Two layer reactive passive structures with dynamic interface. *International Journal of Polymeric Materials*, **2005**, 54, 93-115.

24. S. G. Kiryushkin and Y. A. Shlyapnikov. Diffusion-controlled polymer oxidation. *Polymer Degradation and Stability*, **1989**, 23(2), 185-192.

25. R. L. Clough and K. T. Gillen. Oxygen diffusion effects in thermally aged elastomers. *Polymer Degradation and Stability*, **1992**, 38(1), 47-56.

26. C. R. Boss and J. C. W. Chien. Oxygen diffusion limitation in autoxidation of polypropylene. *Journal of Polymer Science, Part A-1: Polymer Chemistry*, **1966**, 4(6), 1543-1551.

27. M. Iring, T. Kelen, and F. Tudos. Thermal oxidation of polyolefins. II. Effect of layer thickness on the rate of oxidation in the melt phase. *European Polymer Journal*, **1975**, 11(9), 631-636.

28. N. C. Billingham and T. J. Walker. Autoxidation of poly(4-methyl-1-pentene). I. Role of diffusion in autoxidation kinetics. *Journal of Polymer Science, Polymer Chemistry*, **1975**, 13(5), 1209-1222.

29. H. A. Daynes. The Permeability of Rubber and Methods of Testing It. *Transactions, Institution of the Rubber Industry*, **1928**, 3, 428-453.

30. R. G. Bauman and S. H. Maron. Oxidation of polybutadiene. I. Rate of oxidation. *Journal of Polymer Science*, **1956**, 22, 1-12.

Chapter 3: Materials and Techniques

3.1   Materials

Pure gases, such as nitrogen, oxygen, and carbon dioxide, were purchased from Airgas Southwest Inc. (Corpus Christi, TX) and had a purity of 99.9%. Mixed gas cylinders (i.e., O_2/N_2 mixtures of different compositions) were also purchased from Airgas Southwest Inc. (The Woodlands, TX), and the purity was UHP level. All gases were used as received.

1,4-Polybutadiene (36% cis, 55% trans, and 9% vinyl, M_n=230,000) was purchased from Scientific Polymer Products, Inc. (Ontario, NY). Cobalt neodecanoate (12 wt % in mineral oil) was purchased from Shepherd Chemical Company (Norwood, Ohio) and was diluted 100 times (v:v) using cyclohexane in a volumetric flask before use. The chemical structures of the polymers and reagents and the physical properties of 1,4-polybutadiene are shown in Figure 3.1 and Table 3.1, respectively.

Table 3.1   Physical properties of 1,4-polybutadiene

Polymer	Component	Mn	ρ (g/cm^3)	T_g (°C)	Permeability*, P (Barrer)	
					N_2	O_2
1,4-PB	36% cis, 55% trans, 9% vinyl	230,000	0.89	-92	10.4	24.1

* Gas permeability was measured at 35°C.

Cyclohexane (anhydrous, 99.5%), toluene (anhydrous, 99.8%) and methanol (anhydrous, 99.8%) were purchased from Sigma-Aldrich and used as received. Silicon wafers (5 inch and 6 inch diameter) were purchased from Addison Engineering Inc. (San Jose, CA). SEM stub specimen mounts were ordered from Ted Pella Inc. (Redding, CA).
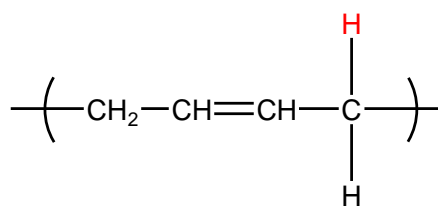
(A)
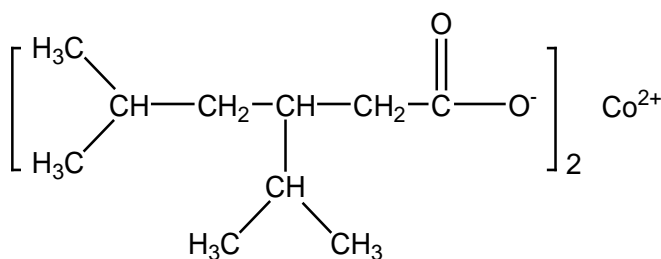
(B)

Figure 3.1   Chemical structures of polymers and catalyst   (A) 1,4-polybutadiene, (B) cobalt neodecanoate

The 1,4-polybutadiene was purified as follows: 50 grams of 1,4-polybutadiene were dissolved in 450 ml of dry toluene in a 1000 ml three-necked flask equipped with a mechanical stirrer at 65ºC under nitrogen. The polymer was then precipitated from solution by pouring the solution into 2000 ml of methanol at room temperature. The precipitated 1,4-polybutadiene was placed in a seven-speed laboratory blender (Waring

Laboratory, Torrington, CT), cut into small pieces, and dried under vacuum in a vacuum oven overnight at ambient temperature until the residual methanol was removed. These steps were repeated several times, with the exact number of purification cycles being a variable in this study. The purified 1,4-polybutadiene was stored in an amber glass bottle filled with nitrogen until needed.

3.2   Film Formation and Characterization

3.2.1   Solution Casting

A normalized film making process was developed to keep all experimental data comparable. Films between 10 and 400 μm thick were prepared by solution casting. The polymer was dissolved in cyclohexane at 2 wt % solids while stirring in an amber glass bottle. Then, a prescribed amount of cobalt neodecanoate solution was added to the solution while stirring. Once the solution was well-mixed, the casting solution was poured into a glass casting ring (2 inch diameter) on a Teflon plate and kept under nitrogen in a glove box covered with aluminum foil for 8 hours to permit the cyclohexane to slowly evaporate, as shown in Figure 3.2. Then the films were stored in a vacuum oven at room temperature for an additional 6 hours. In tests to determine the oxidized layer thickness, the films were cast onto thick aluminum foil. The films were left on aluminum foil during oxidation so that oxygen could only diffuse into the films from one side.

Nitrogen environment

Polymer Solution

Glass ring $\longrightarrow$

Teflon[®] plate
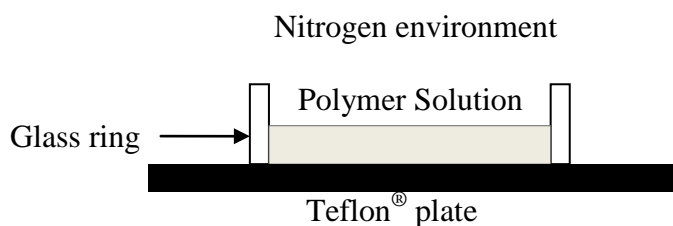
Figure 3.2   Experimental set-up for solution casting of polymer films

3.2.2 *Spin Coating*

The mechanism of film formation by spin coating has been well described elsewhere[1, 2]. Films thinner than 10 µm were prepared by spin coating polybutadiene solution (8 wt % in cyclohexane) onto the clean native-oxide (100) surface of a silicon wafer using a Laurell WS-400B-8NPP/LITE model spin coater (North Wales, PA). Polybutadiene solutions were filtered through a 0.1 µm Whatman[®] PURADISC[TM] Teflon syringe filter before use. The spin coater was set to 1000 rpm for 60 seconds. Films were left on the silicon wafer to oxidize for oxygen mass uptake experiments. If a thicker film was needed, one or two extra layers of polymer solution were coated onto the first polymer layer, and the thickness of such polymer films could reach 10 to 15 µm. For samples prepared for permeation experiments, the thin films were first cut to 3cm x 3cm coupons using a razor blade. Then, this coupon was detached from the wafer surface by immersing the polymer coated wafer in deionized water. The resulting films were transferred carefully onto a thin wire frame[3] and dried in a vacuum oven at ambient temperature for 1 hour before use.

30

3.2.3 *Thickness measurement*

Film thicknesses were measured two ways. Thicknesses of thicker films, prepared by solution casting, were determined using a Mitutoyo Litematic VL-50A instrument (Mitutoyo Corporation, Japan), which is specifically designed to measure the thickness of soft polymeric samples, such as rubbery 1,4-polybutadiene. A cover glass was used on both sides of the polymer film during the measurement to prevent direct contact of the measuring tip of the instrument with the soft film.

For thin, spin-coated films, thickness was measured using a KLA-Tencor Instrument Alpha-step 200 profilometer (Milpitas, CA) while the polymer film was still on the silicon wafer. Using a razor blade, a small nick was cut in a sample on the wafer. The depth of the nick, which is also the thickness of the spin-coated film, was measured by physical contact of the profilometer tip with the film and the wafer.

3.2.4 *Polymer Density Measurement*

Film density was characterized using a Mettler Toledo Balance (Model AG204) and a density kit. The film density was calculated as follows[4]:

$$\rho_p = \frac{M_A}{M_A - M_L} \cdot \rho_0 \tag{3.1}$$

where M_A was the film weight in air, M_L was the film weight in the auxiliary liquid, and ρ_0 was the density of the auxiliary liquid used. To reduce the sorption of the auxiliary liquid into the polymer sample and increase the density difference between the polymer and the auxiliary liquid, a high density perfluorinated liquid was used as the auxiliary

liquid. The perfluoroalkane FC-77 was purchased from Acros Organics. The density of this liquid is 1.766 g/cm^3 at 25°C[5].

3.3 Oxygen Mass Uptake

3.3.1 OxySense® System and Sample Container

Oxygen transmission rates of high barrier materials are commonly measured with an Ox-Tran (Mocon, Inc.) oxygen transmission rate measurement system[6]. This system uses a patented coulometric sensor to detect oxygen transmission through flat films and packages[6]. However, high barrier materials that include OSPs are nearly impermeable to oxygen until the scavenging capacity is exhausted; therefore, oxygen transmission rates can be negligible for long periods of time[7]. Scavenging performance is more efficiently characterized via oxygen uptake measurements, and headspace analysis is useful for such studies[8].

To measure oxygen uptake via headspace analysis, a polymer sample is first loaded into a vessel of known volume, which is then charged with a gas of known oxygen composition. Then, the gas in the headspace is sampled using an oxygen sensor or a gas chromatograph to determine the headspace oxygen concentration. Based on the known initial amount of oxygen charged to the system and the known volume, temperature, pressure and composition in the headspace, a mass balance is used to determine the amount of oxygen taken up by the film. By sampling the headspace oxygen concentration as a function of time, the rate of oxygen scavenging and total amount of

oxygen scavenged can be determined. Because excessive sampling can introduce leaks or contaminants into the headspace, a non-invasive measurement of headspace oxygen concentration is desirable.

Figure 3.3 presents a schematic of the system used for non-invasive headspace measurements. The oxygen analyzer is an OxySense® 200T purchased from OxySense, Inc. (Dallas, TX), and this sensor has been previously used in oxygen scavenging studies[9]. This analyzer consists of the 200T instrument, a bifurcated fiber optic cable bundle with an infrared detector attached to a reader-pen, and oxygen-sensitive films (OxyDot®). The OxySense® measures the oxygen concentration inside a transparent, sealed container by monitoring the fluorescence of the OxyDot® upon illumination with the reader-pen. Dynamic quenching by oxygen molecules causes the OxyDot® fluorescence lifetime to decrease in proportion to the oxygen partial pressure in the container. The temperature of the OxyDot® is measured simultaneously via the infrared sensor contained in the reader pen. In the system shown in Figure 3.3, the OxySense® 200T interfaces with a Dell 2400 personal computer through a USB port. The OxyDots® are mounted inside the transparent sample container with clear, silicon rubber (GE 284, GE Sealants and Adhesives, Huntersville, NC).
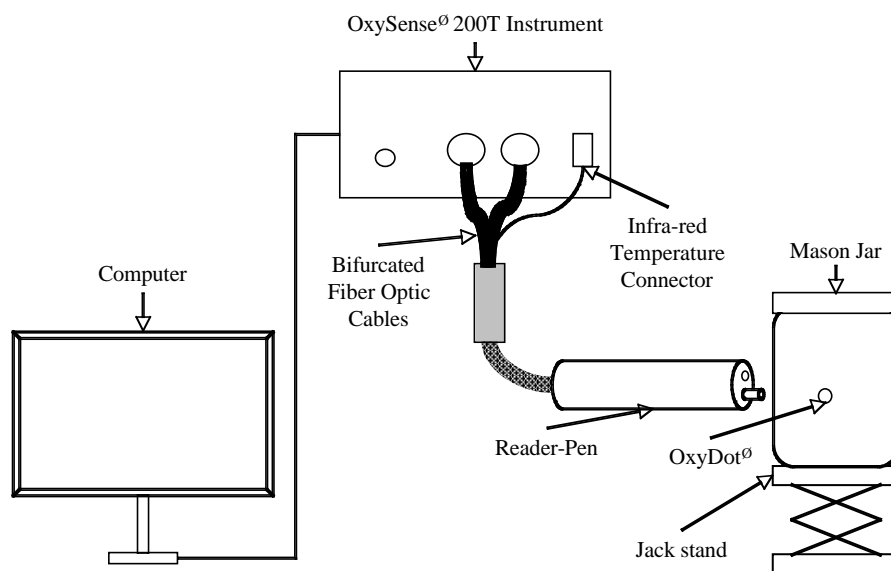
Figure 3.3   Schematic diagram of OxySense® non-invasive oxygen analyzer system.

The sample container, in which the polymer sample is sealed and oxygen is scavenged, is a 1/2 pint Ball® Mason jar. Mason jars are inexpensive and easy to seal, and the jars can sustain sub-atmospheric pressures for long periods of time. The interiors of hermetically sealed ampoules, which were considered as an alternative to the Mason jars, were difficult to access due to their small diameter opening. As a result, mounting OxyDots® was laborious, and residual adhesive from the mounting process could create pinhole leaks in the ampoule seal. Figure 3.4 presents headspace oxygen concentration data for various transparent containers that were initially filled with 100% nitrogen. After approximately two months of storage in air, Mason jars exhibited the slowest rate of oxygen ingress, and the rate of oxygen concentration increase, 0.003%/day, was well below the experimental error observed in the control sample, which was a sample jar open to ambient air. The upward drift in oxygen concentration in the control sample can

34

be attributed to signal drift, which is reported by the manufacturer to be < 5% of the

reading.
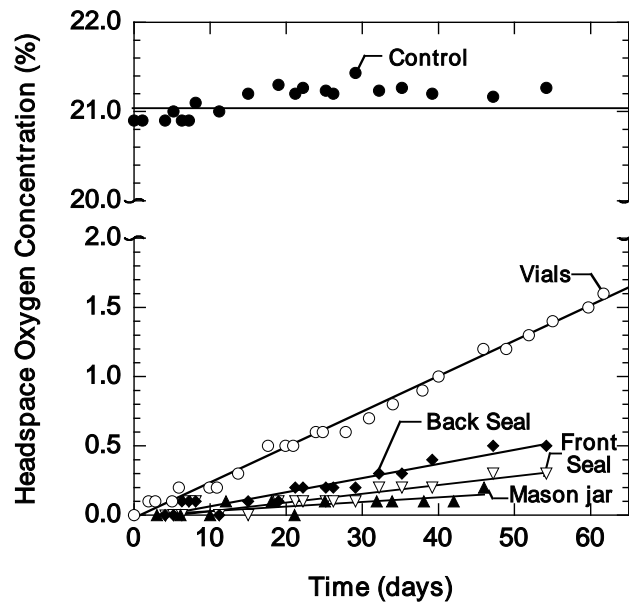
Figure 3.4   Oxygen headspace measurements of various nitrogen filled enclosures (○ glass vial with phenolic screw cap; ♦ glass vial with Teflon® plug and back sealing o-ring; ∇ glass vial with Teflon® plug and front sealing o-ring; ▲ 1/2 pint Ball® regular Mason jar; ● unsealed glass vial, open to atmosphere).

The ability of the 1/2 pint Ball® Mason jars to hold vacuum was verified using a

technique illustrated in Figure 3.5. A 1/4" stainless steel tube was routed through a

Mason jar lid and affixed with metal epoxy. Pressure inside the Mason jar was reduced

with a vacuum pump, and the reduced pressure inside the jar was monitored with the

OxySense® and simultaneously confirmed with an external pressure gauge. Using this

technique, 1/2 Pint Ball® Mason jars are found to maintain pressures below 1 psia for over 1 month.
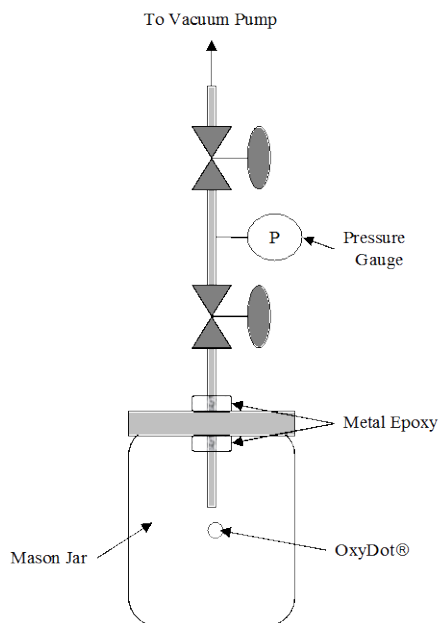
Figure 3.5   Schematic diagram of Mason jar vacuum testing apparatus.

Effective OSPs can consume 50 cm^3 (STP) O_2/gram of polymer (or more) at rates as high as 5.0 cm^3 (STP) O_2/gram of polymer/day. Therefore, a small amount of OSP (~ 100 mg) can scavenge substantial amounts of oxygen (~ 5 cm^3 (STP)) at a rate of approximately 0.5 cm^3 (STP)/day.[10] The reported oxygen detection limit of the OxySense® 200T is 0.13 cm^3 (STP); therefore, the use of just 100 mg of an OSP generates a measurable change in oxygen concentration inside a 1/2 pint Ball® Mason jar. The small sample requirement also facilitates concurrent testing of many samples since these small Mason jars are conveniently stored and readily available.

3.3.2 Oxygen Mass Uptake Calculation

Scavenging performance of polymeric materials is often characterized by the amount of oxygen reacted with the polymer, i.e., the amount of oxygen consumed by the polymer. When using the OxySense® system, oxygen uptake (mass of oxygen consumed/mass of polymer) is calculated from measured oxygen partial pressures inside the Mason jars as follows:

The number of moles of free oxygen in the Mason jar at time t, n_t, is calculated from the corresponding partial pressure measured at time t, P_t, according to the ideal gas law[11]:

$$n_t = \frac{P_t \times (Vol_{jar} - Vol_{polymer})}{R \times T} \tag{3.2}$$

where Vol_{jar} is the internal volume of Mason jar, $Vol_{polymer}$ is the volume of the polymer, R is the ideal gas constant, and T is the temperature of the OxyDot®.

The mass uptake of oxygen at time t, M_t, is calculated by subtracting n_t from the initial number of moles of oxygen in the jar, n_0. The mass uptake is then normalized by the weight of the film as follows:

$$M_t = \frac{(n_0 - n_t) \times MW}{m_0} \tag{3.3}$$

where MW is the molecular weight of oxygen, and m_0 is the initial film mass.

An accurate value of Vol_{jar} is obtained from the difference in weight before and after the addition of deionized water to a sealed Mason jar. Water is added to the jars via

a small hole drilled through the lid, and the weight of water at room temperature is readily converted to volume using the tabulated density of water[11]. $Vol_{polymer}$ is found by dividing the polymer film mass by the film density, ρ.

Figure 3.6 presents an example of the conversion of oxygen partial pressure data to mass uptake values for a model scavenging polymer. The solubility of oxygen in typical polymers is very low compared to the amount of oxygen that can react with an oxygen scavenging polymer. For example, the solubility of oxygen in 1,4-polybutadiene is 0.957 x 10^{-6} cm^3(STP)/(cm^3g Pa)[12], and this value, corresponding to 0.003 wt% at ambient conditions, is negligible compared to the total amount of oxygen scavenged by 1,4-polybutadiene, which, according to Figure 3.2, is on the order of 14 wt%.
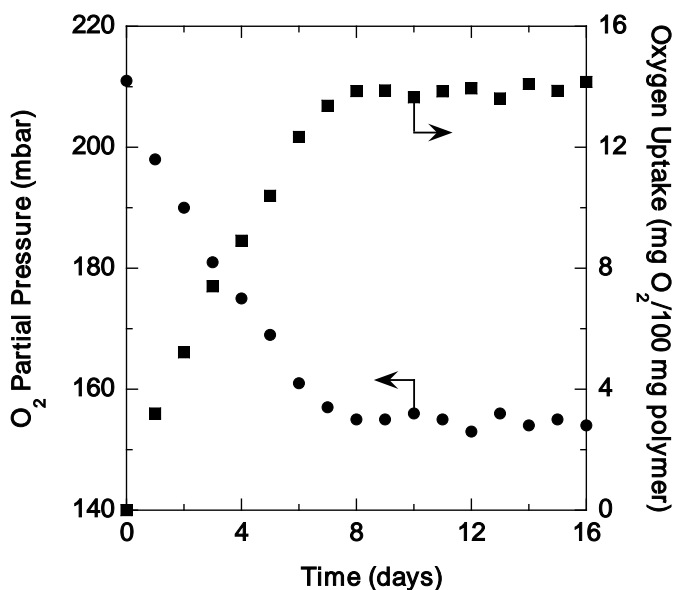
Figure 3.6   Conversion of raw headspace measurements to mass uptake values for poly(1,4-butadiene) loaded with 200 ppm cobalt at 30°C. Film mass and film thickness is 124.9 mg and 100 µm, respectively. Cobalt added as cobalt neodecanoate.

3.3.3   *Validation of Analysis Method*

Three uptake experiments were conducted with the cobalt doped, 1,4-polybutadiene films, and the results from these experiments are shown in Figure 3.5. The first experiment, referred to as "Integral OxySense[®]," tracked the mass uptake of a film stored in a single Mason jar over a period of sixteen days. This experiment followed the operation procedures outlined previously.

The use of the OxySense[®] technique to measure mass uptake requires a change in oxygen partial pressure inside the Mason jar, but if mass uptake is determined gravimetrically, then no change in oxygen partial pressure is required. The mass uptake can simply be tracked by recording changes in sample mass using an analytical balance in ambient air. However, oxygen partial pressure can have a significant effect on polymer scavenging kinetics[13]. Therefore, to validate the OxySense[®] method using a gravimetric technique, samples must be stored in Mason jars so the films are exposed to oxygen partial pressures similar to those in the OxySense[®] experiments.

Therefore, in the experiment referred to as "Analytical Balance," sixteen samples of 1,4-polybutadiene films were prepared, ranging in mass from 107 to 126 mg, and these samples were sealed in separate Mason jars (labeled Jar 1, Jar 2, etc.). Mason jars were exposed to air at ambient temperature before loaded with 1,4-polybutadiene films, so the original total pressure inside Mason jars is one atmosphere. The original oxygen partial pressure inside Mason jars was determined by measuring with an OxySens[®] instrument.

After one day, the film in Jar 1 was removed, and the film mass at time t, m_t, was recorded with an analytical balance. The oxygen uptake, M_t, was calculated as follows:

$$M_t = \frac{m_t - m_0}{m_0} \qquad (3.4)$$

where m_0 is the initial film mass. On day two, the oxygen uptake in Jar 2 was measured using the analytical balance, and on day three, Jar 3 was measured, etc. This process continued until the oxygen uptake of all sixteen samples was determined. The use of individual samples during the "Analytical Balance" experiment ensured that the mass uptake measured with the analytical balance on day 16, for example, would account for a change in oxygen partial pressure similar to the change observed in the "Integral OxySense®" experiment.

Prior to removal of each film in the "Analytical Balance" experiment, oxygen partial pressure inside the jar was recorded with the OxySense® system, and the corresponding oxygen uptake, M_t, was calculated according to Equations (3.3) and (3.4). These data constitute the "Incremental OxySense®" curve shown in Figure 3.7, and these data agree very well with the "Analytical Balance" values. Little deviation is also observed between the "Integral OxySense®" and "Incremental OxySense®" experiments. Close agreement between these experimental data is expected since similar changes in oxygen partial pressure were maintained throughout the three independent experiments.
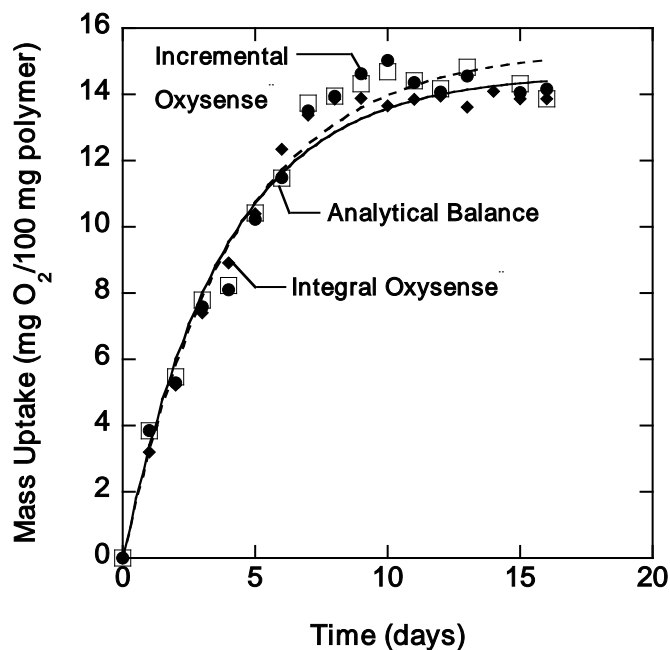
Figure 3.7   Comparison of analytical balance and OxySense® data for oxygen uptake of poly(1,4-butadiene) doped with 200 ppm cobalt at 30°C ($\square$ Analytical Balance, $k = 0.23 \pm 0.04$ days^{-1}, $M_f = 15.6 \pm 0.8$ mg O$_2$/100 mg polymer; $\bullet$ Incremental OxySense®, $k = 0.24 \pm 0.03$ days^{-1}, $M_f = 15.4 \pm 0.4$ mg O$_2$/100 mg polymer; $\blacklozenge$ Integral OxySense®, $k = 0.27 \pm 0.04$ days^{-1}, $M_f = 14.6 \pm 0.5$ mg O$_2$/100 mg polymer). The solid and dashed curves represent the least-squares fit of the Integral OxySense® and Analytical Balance data, respectively, to the first order kinetic model given in equation (3.4). Cobalt added as cobalt neodecanoate.

The rate of oxygen uptake follows first order kinetics in the presence of excess oxygen; therefore, the first order rate constant k and final oxygen uptake M_f are obtained from a best fit of the data to the following equation[14]:

$$M_t = M_f (1 - e^{-kt}) \qquad (3.5)$$

The values of k and M_f determined from these independent experiments are listed in Table 3.2, and these values are in excellent agreement. The rate constants determined

41

from the sixteenth jar, "Analytical Balance" and "OxySense® Incremental" experiments are 0.23 ± 0.04 and 0.24 ± 0.03 days^{-1}, respectively. The final oxygen uptake is 15.6 ± 0.8 mg O_2/100 mg polymer in the "Analytical Balance" experiment and 15.4 ± 0.4 mg O_2/100 mg polymer in the "Incremental OxySense®" experiment. For the "Integral OxySense®" experiment, the rate constant is 0.27 ± 0.04 days^{-1}, and the final oxygen uptake is 14.6 ± 0.5 mg O_2/100 mg polymer. Parameter uncertainties were estimated using a nonlinear least-squares method, where the uncertainty in the parameters corresponds to a change of 1 in χ^2 from its minimum value.[15] Therefore, within the precision of this technique, all three experimental protocols yield the same results.

Table 3.2 Summary of oxygen uptake methods and experimental results.

Method	Description	k (days)	M_f (mg O_2/100 mg polymer)
Analytical Balance	• OSP sample removed from jars on each of their scheduled test day and manually weighed • Each of the 16 data points is a separate sample	0.23 (± 0.04)	15.6 (± 0.8)
Incremental OxySense®	• OxySense® measurement of "Analytical Balance" sample prior to removal of the sample from the jar • Each of the 16 data points is a separate sample	0.24 (± 0.03)	15.4 (± 0.4)
Integral OxySense®	• Repeated OxySense® measurement of the same OSP sample, without opening jar • All 16 data points are from a single sample	0.27 (± 0.04)	14.6 (± 0.04)

There are several sources of uncertainty in determining the oxygen uptake of scavenging polymers with the OxySense® system: uncertainty in measuring P_t (± 1 mbar),

uncertainty in measuring Vol_{jar} (± 1 cc), uncertainty in measuring $Vol_{polymer}$ (± 0.001 cc), uncertainty in measuring T (± 0.1 ^{o}C), and uncertainty in measuring m_0 (± 0.5 mg). The uncertainty in determining oxygen uptake is dominated by the uncertainty in measuring P_t and Vol_{jar}, and the uncertainty in measuring these values is about $\pm 0.5\%$. Using a standard propagation of errors analysis, uncertainties in oxygen uptake, M_t, were estimated, and these values ranged from $\pm 3\%$ to $\pm 14\%$, depending on the uncertainty in the OxySense$^{®}$ measurement. Uncertainties in OxySense$^{®}$ measurements are highest when the total amount of oxygen consumed is smallest, i.e., at the beginning of the experiment, and lowest when the total amount of oxygen consumed is high, usually towards the end of an experiment.

3.4   Ultraviolet (UV) Spectroscopy

The amount of residual antioxidant in the polymer was determined by ultraviolet (UV) spectroscopy. UV spectra were recorded on a Shimadzu Mini UV spectrometer (Columbia, MD). Untreated and purified polybutadienes were dissolved in cyclohexane to prepare 5 wt. % solutions. Solutions were filtered through a 0.1 µm Whatman$^{®}$ PURADISC^{TM} Teflon syringe filter to remove any solid impurities.   Then, the polybutadiene solutions were transferred to quartz cuvettes using glass pipettes for UV tests. Pure cyclohexane was used as reference background before each sample test.

3.5 Fourier Transform Infrared Spectroscopy (FTIR)

Fourier transform infrared spectroscopy (FTIR) is a typical method to detect the functional group change in polymer films[16-19]. It has been widely used in monitoring thermo-oxidation in polybutadiene. Both qualitative and quantitative changes can be measured using FTIR by tracking the changes of peak wave number and peak strength.

Attenuated total reflection Fourier transform infrared spectroscopy (FTIR-ATR) was performed using a Thermo Nicolet Nexus 470 FT-IR spectrophotometer (Madison, WI) equipped with an ATR Smart Avatar Miracle attachment (Zinc Selenide crystal). The measurements were conducted at 1 cm^{-1} nominal resolution, 256 scans, and the region from 675 to 4000 cm^{-1} was recorded for each spectrum. The data were collected and analyzed using Omnic software from the spectrometer manufacturer.

Small portion samples and non-membrane samples were prepared by mixing and grinding with anhydrous KBr (Sigma-Aldrich). The powder mixtures were then compressed into pellet samples and examined using transition FTIR. The scanning condition was the same as those of the ATR tests.

3.6 X-ray Photoelectron Spectroscopy (XPS)

X-ray photoelectron spectroscopy (XPS) was used to characterize changes in the polymer structure due to oxidation. XPS spectra were obtained using a Kratos Axis Ultra Electron Spectrometer (Kratos Analytical Inc., Chestnut Ridge, NY) equipped with a monochromatic Al Kα (hv=1456.6 eV) X-ray source. Operating conditions were: 1×10^{-9}

Torr background pressure; 15KV; 200W X-ray power. For XPS analysis of the center of an oxidized film, the film was fractured by bending. A sandwich structure was readily visible across the cross section of the film, consisting of a brittle, highly oxidized surface layer and a softer, less oxidized core layer. A razor blade was used to cut through the sample to expose the surface of the center of the film, and XPS analysis was conducted immediately on the new generated surface (i.e. the film center of an oxidized 1,4-polybutadiene film). This step was undertaken just before loading the sample into the XPS apparatus to limit any additional oxidation of the sample prior to performing the XPS measurements.

3.7 Pure Gas Permeability Measurements

Gas permeability of nitrogen and oxygen in polybutadiene films was measured using a constant pressure/variable volume apparatus[20, 21]. A liquid nitrogen trap was installed between the permeation apparatus and vacuum pump to prevent any possible vacuum oil contamination of the permeation system.

Oxygen is of direct interest because oxygen-scavenging films are typically designed to reduce the transport of oxygen across a package wall. Nitrogen is of interest because it acts an inert (i.e. non-oxidizable) probe gas molecule of similar size to oxygen, so it can be used to determine changes in permeability in samples in various states of oxidation without concerns about the film undergoing further oxidation during the permeation measurement. Films with thicknesses ranging between 80 and 130 μm were prepared for

permeability tests by solution casting films. Films were partially masked using impermeable aluminum tape on their upstream and downstream sides. For thin film (thickness between 1 µm and 10 µm) permeability tests, a thin film sample located on the copper wire support mentioned earlier was carefully placed at the center of a Whatman Anodisc® for mechanical support, as described previously[3]. Impermeable aluminum tape, having an opening in the center to permit gas permeation during the experiment, was then applied to both sides. The pure gas permeability coefficients are reported in units of Barrer, where 1 Barrer = 10^{-10} cm^3(STP) cm/(cm^2 s cmHg). The permeability of a film was calculated using the following equation:

$$P_A = \frac{V \cdot l}{p_1 \cdot A \cdot R \cdot T} \left[\left(\frac{dp_2}{dt} \right)_{ss} - \left(\frac{dp_2}{dt} \right)_{leak} \right] \tag{3.6}$$

where V is the downstream volume (cm^3), l is the film thickness (cm), p_1 is the upstream absolute pressure (cmHg), A is the film area (cm^2), T is absolute temperature (K), R is the gas constant (0.278 cmHg cm^3/(cm^3(STP)K)), and $(dp_2/dt)_{ss}$ and $(dp_2/dt)_{leak}$ are the pseudo-steady state rate of pressure change at the downstream side of a sample exposed to a fixed upstream pressure and under vacuum (cmHg/s), respectively. All measurements were taken at downstream pressures, p_2, of less than 10 Torr. The permeability selectivity of a polymer for penetrant gas A relative to gas B is defined as the ratio of the permeability coefficients of the two gases:

$$\alpha_{A/B} = \frac{P_A}{P_B} \tag{3.7}$$

3.8   Scanning Electron Microscopy (SEM)

The cross sections of film samples were characterized using a Zeiss NEON 40 FE-SEM (Carl Zeiss SMT Inc., Peabody, MA) operated at 5kV and at approximately 20 mm working distance.   Unoxidized and oxidized film samples were cut to 2 mm×3mm coupons, and they were microtomed using an RMC-Boeckeler PowerTome PT-XL (Boeckeler Instruments Inc., Tucson, AZ) just before the SEM test to prevent further oxidation of the microtomed cross sections. The operating temperature was set to -125°C using liquid nitrogen, and the cutting speed was 0.8 mm/sec. Films were polished first with a glass knife and then with a diamond knife (Micro Star Technologies, Huntsville, TX).   Before the SEM tests, samples were mounted perpendicularly on low profile 45°/90° SEM mounts (Ted Pella Inc., Redding, CA) using carbon tape and coated with indium in an Emitech K575X sputter coater (Quorum Technologies Ltd., West Sussex, United Kingdom) operated at 150 µW for 10 seconds. An indium layer approximately 10 nm thick was generated on top of the sample.

3.9   Differential Scanning Calorimeter (DSC)

DSC experiments were conducted using a Q-100 DSC equipped with a liquid nitrogen cooling system (LNSC) from TA instruments (New Castle, DE).   Polymer samples for DSC analysis weighed 6 to 10 mg. Samples were placed in aluminum DSC pans, and helium, flowing at 25 ml/min, was used as the blanketing gas in the DSC. The DSC sweep began by taking the sample from ambient to -180°C and then holding

at -180ºC for 5 minutes to equilibrate and stabilize the system. Then, the sample was scanned from -180 to 250 ºC at a heating rate of 10 ºC/min. The glass transition temperature (T_g) was taken as the midpoint of the measured step change in heat capacity. The degree of crystallinity in polymer was evaluated from the area under the melting endotherm in the scan.

3.10   Thermal Gravimetric Analysis (TGA)

TGA analysis was conducted using a TGA Q500 V 6.3 equipped with a standard furnace (TA instruments, New Castle, DE). Samples weighed about 10 mg was loaded into a platinum pan, and they were heated from 25ºC to 800ºC at 5ºC/min in nitrogen (flow rate: 50 ml/min). Both DSC and TGA data were analyzed using the Universal Analysis 2000 software provided by TA instruments.

3.11   Wide Angle X-Ray Diffraction (WAXD)

WAXD was performed at room temperature using a Scintag X1 theta–theta diffractometer with Cu Kα radiation of 1.54 Å wavelength (power settings of 45 kV and 50 mA) and a solid state (Si(Li)) detector. The software used for data processing was Jade v. 7.5 from Materials Data Inc. (Livermore, CA).

3.12 References

1.   D. E. Bornside, C. W. Macosko, and L. E. Scriven. On the modeling of spin coating. *Journal of Imaging Technology*, **1987**, 13(4), 122-130.

2.   A. Weill and E. Dechenaux. The spin-coating process mechanism related to polymer solution properties. *Polymer Engineering and Science*, **1988**, 28(15), 945-948.

3.   Y. Huang and D. R. Paul. Experimental methods for tracking physical aging of thin glassy polymer films by gas permeation. *Journal of Membrane Science*, **2004**, 244(1-2), 167-178.

4.   P. Zoller and D. Walsh. Standard Pressure-Volume-Temperature Data for Polymers, 1st ed. Technomic Publishing Company, Inc., Lancaster, 1995.

5.   A. Car, C. Stropnik, W. Yave, and K. V. Peinemann. PEG modified poly(amide-b-ethylene oxide) membranes for CO2 separation. *Journal of Membrane Science*, **2008**, 307(1), 88-95.

6.   S. N. Dhoot, B. D. Freeman, and M. E. Stewart. Barrier polymers. In: Kroschwitz J. I., editor. Encyclopedia of Polymer Science and Technology, vol. 5. Wiley-Interscience, New York, 2003, 193-263.

7.   G. Strupinsky and A. L. Brody. A Twenty-Year Retrospective on Plastics: Oxygen Barrier Packaging Materials. Polymers, Laminations and Coating Conference. San Francisco, 1998. pp. 119-140.

8.   T. Y. Ching, K. Katsumoto, S. P. Current, and L. P. Theard. Compositions having ethylenic backbone and benzylic, allylic, or ether-containing side-chains, oxygen scavenging compositions containing same, and process for making these compositions by esterification or transesterification of a polymer melt. U. S. Patent, 5,627,239, **1997**

9.   M. E. Stewart, R. N. Estep, B. B. Gamble, M. D. Cliffton, D. R. Quillen, L. S. Buehrig, V. Govindarajan, and M. J. Dauzvardis. Blends of oxygen scavenging polyamides with polyesters which contain zinc and cobalt. United States Patent Application Publication, US 2006/0148957, **2006**

10.   D. V. Speer, W. P. Roberts, and C. R. Morgan. Methods and Compositions for Oxygen Scavenging. 5,211,875722,067, **1993**

11. J. M. Smith, H. C. Ness, and M. M. Abbott. Introduction to Chemical Engineering Thermodynamics, 5th ed. McGraw-Hill, Inc., New York, 1996.

12. G. J. van Amerongen. Influence of structure of elastomers on their permeability to gases. *Journal of Polymer Science*, **1950**, 5, 307-332.

13. L. Reich and S. S. Stivala. Elements of Polymer Degradation McGraw-Hill, Inc., New York, 1971.

14. S. W. Bigger and O. Delatycki. New approach to the measurement of polymer photooxidation. *Journal of Polymer Science Part A: Polymer Chemistry*, **1987**, 25(12), 3311-3323.

15. P. R. Bevington and D. K. Robinson. Data Reduction and Error Analysis for the Physical Sciences. 3rd ed. McGraw-Hill, Inc., New York, 2003.

16. C. Adam, J. Lacoste, and J. Lemaire. Photo-oxidation of elastomeric materials. 1. Photooxidation of polybutadienes. *Polymer Degradation and Stability*, **1989**, 24(3), 185-200.

17. S. W. Beavan. Mechanistic studies on the photo-oxidation of commercial poly(butadiene). *European Polymer Journal*, **1974**, 10, 593-603.

18. M. Coquillat, J. Verdu, X. Colin, L. Audouin, and R. Neviere. Thermal oxidation of polybutadiene. Part 1: Effect of temperature, oxygen pressure and sample thickness on the thermal oxidation of hydroxyl-terminated polybutadiene. *Polymer Degradation and Stability*, **2007**, 92(7), 1326-1333.

19. M. Piton and A. Rivaton. Photooxidation of polybutadiene at long wavelengths (λ>300nm). *Polymer Degradation and Stability*, **1996**, 53(3), 343-359.

20. V. I. Bondar, B. D. Freeman, and I. Pinnau. Gas transport properties of poly(ether-b-amide) segmented block copolymers. *Journal of Polymer Science Part B-Polymer Physics*, **2000**, 38(15), 2051-2062.

21. H. Lin and B. D. Freeman. Permeation and diffusion. In: Czichos H., Smith L. E., and Saito T., editors. Handbook of Materials Measurement Methods. Springer, New York, 2006, 371-387.

Chapter 4: Characterization of Oxygen Scavenging Films Based on 1,4-Polybutadiene

4.1   Introduction

Although the use of polymers in packaging has grown rapidly, polymers have not replaced glass and metal in a number of applications[1]. One reason for the lack of penetration into certain markets is that polymer packaging systems based on passive diffusion alone cannot always provide adequate barrier properties to gases such as oxygen. There is considerable interest in using reactive polymer membranes in oxygen scavenging systems[2-7], in part because conventional packaging materials, such as poly(ethylene terephthalate) (PET), do not have low enough oxygen permeation properties, by themselves, to meet certain applications, such as the packaging of beer in long-shelf life plastic bottles[8]. The presence of oxygen at even ppm levels causes certain foods and beverages to experience deleterious oxidation or other aerobic degradation processes[9]. Incorporation of oxygen scavengers into otherwise passive barrier polymers can markedly reduce oxygen transmission and extend the shelf-life of oxygen sensitive products to levels rivaling those of glass and metal packaging over timescales of use for food and beverage applications[9-11].

Polybutadiene is an important synthetic rubbery polymer that is readily oxidized upon exposure to even low levels of atmospheric oxygen at room temperature. Many studies of thermo-oxidation[12-16], photo-oxidation[17-21], and ozonolysis[22] of polybutadiene have been conducted during the last fifty years, and several oxidation

mechanisms have been suggested[16, 18, 23]. However, most of these studies have focused on preventing oxidation of polybutadiene under processing or use conditions. Only a few studies have examined oxidation rate, mass uptake, or application of polybutadiene in oxygen scavenging materials[11, 24]. In such cases, it is typical to add a small amount of a transition metal catalyst to the polybutadiene to accelerate the oxidation. In this regard, cobalt neodecanoate is a popular choice in the patent literature[11, 24-26].

This study reports the influence of preparation and reaction conditions on oxidation of 1,4-polybutadiene. Commercial 1,4-polybutadiene samples contain antioxidants that can be largely removed prior to preparing oxygen scavenging films. However, UV tests show that antioxidants are not totally removed in a single purification step, and oxygen sorption experiments confirm that oxygen uptake and oxidation rate are affected by the number of purification steps (i.e., extent of antioxidant removal). Oxygen uptake and oxidation rate stabilize after a sufficient number of purification steps, suggesting that antioxidants can be removed at least to a level that they no longer measurably influence oxygen scavenging. In this study, oxygen mass uptake by 1,4-polybutadiene was measured using a non-invasive oxygen sensor based system[27]. The oxygen uptake experiments show that oxygen uptake can reach values as high as 15 weight percent. The effects of catalyst concentration on oxygen uptake rate and amount were determined. Because crosslinking was observed during the oxidation process, the effect of crosslinking on oxygen uptake was also studied.

4.2 Results and Discussion

UV spectroscopy is one method to characterize antioxidant concentration in 1,4-polybutadiene since many common oxidation antioxidants are strongly UV-active. Figure 4.1 presents the UV spectra of purified and unpurified (i.e., as-received) polybutadiene samples. The peak between 240 nm and 280 nm is ascribed to the antioxidant. After one purification cycle, the peak height decreases, as shown in Figure 4.1. The peak decreases to the point that it is no longer resolvable after five purification cycles. However, even very small amounts of antioxidant can influence the oxidation of 1,4-polybutadiene[28]. In our experiments, we made one additional cycle of purification (i.e., a sixth cycle) and compared the oxygen mass uptake from samples with various numbers of purification steps.

53
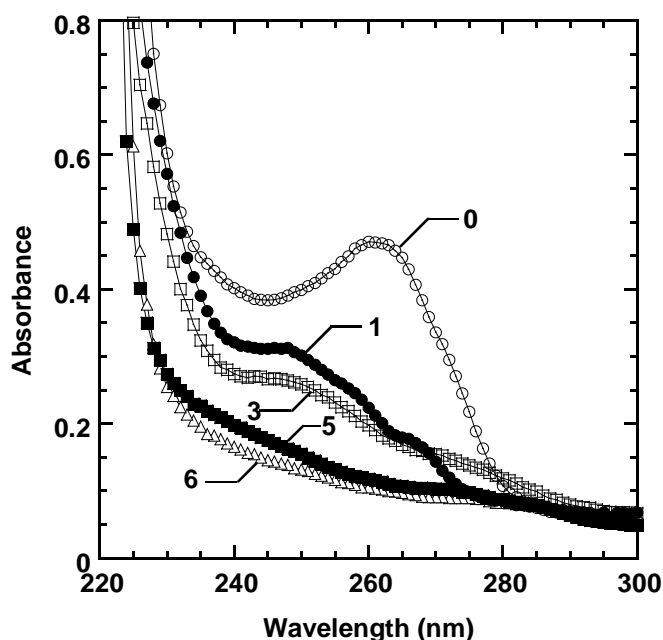
Figure 4.1   UV spectrum of unpurified and purified 1,4-polybutadiene. ○: Unpurified 1,4-polybutadiene (i.e., 0 purification cycles). ●: 1,4-polybutadiene after 1 purification cycle. □: 1,4-polybutadiene after 3 purification cycles. ■: 1,4-polybutadiene after 5 purification cycles. Δ: 1,4-polybutadiene after 6 purification cycles. The numbers shown next to the spectra indicate the number of dissolution/reprecipitation purification cycles that the sample was subjected to prior to acquiring the spectrum.

In commercial 1,4-polybutadiene, antioxidants are added to prevent oxidation and crosslinking[29]. If there are antioxidants in cobalt-catalyzed 1,4-polybutadiene films, the free radicals generated at the beginning stages of oxidation will be consumed by the antioxidant, leading to an induction period in oxygen uptake. That is, there will be a period of time at the beginning of the experiment when there is no measurable oxygen uptake (i.e., oxidation), followed by a period where oxygen uptake increases as the sample oxidizes. Figure 4.2 presents oxygen mass uptake data as a function of the number of purification cycles. For each fixed number of purification cycles, three or four

54

different cobalt neodecanoate concentrations were used in preparing the polymer membranes.

The unpurified 1,4-polybutadiene film exhibited an induction period approximately four days long in a sample containing 1000 ppm of cobalt neodecanoate. Even more time was required to initiate measurable oxidation in a sample containing less cobalt neodecanoate (e.g., 400 ppm) (cf., Figure 4.2A). The sample containing 200 ppm of catalyst did not exhibit measurable oxygen uptake even after one month, suggesting that the sample was stable against oxidation, due to the presence of the oxidation antioxidants, for at least one month at this catalyst concentration.

As indicated previously, both Co^{2+} and Co^{3+} species participate in the steps of oxidation and help generate free radicals. More specifically, the oxidation reactions proposed in the literature are[30]:

$$O_2 + RH \rightarrow ROOH$$

$$Co^{2+} + ROOH \rightarrow Co^{3+} + OH^- + RO\cdot$$

$$Co^{3+} + ROOH \rightarrow Co^{2+} + H^+ + ROO\cdot$$
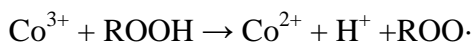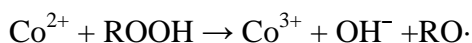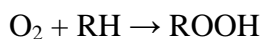
where RH is a section of the 1,4-polybutadiene molecule susceptible to oxidation. Typically, the allylic carbon-hydrogen bonds would be the most susceptible linkages to undergo oxidative degradation, because of their lower bond energy (85 kcal/mol) compared with the tertiary C-H bond energies in saturated hydrocarbons (90-103 kcal/mol) and vinylic C-H bond energy (105 kcal/mol)[31]. Of course, oxidation of the double bonds to form epoxides[17], and generation of carboxylic acid from aldehyde[19], etc., are other potential sources of oxygen uptake.

Upon increasing cobalt neodecanoate concentration, the free radical generation rate will increase. Simultaneously, antioxidants in the polymer consume free radicals and terminate the reaction before chain transfer occurs, preventing the polymer film from being oxidized before all the antioxidants are consumed[28]. After the antioxidant has been consumed, the reactions noted above can occur to a greater extent. Then, significant oxidation begins to be observed and continues until the surface of the film is highly oxidized [17] At this point, the rate of oxygen mass uptake slows since, presumably the highly oxidized surface is much less permeable to oxygen, and the oxidation rate decreases sharply and oxygen mass uptake stabilizes[32, 33].

An induction period is also observed in the sample prepared with three purification cycles and 100 ppm of catalyst (cf., Figure 4.2B), but the induction time is shorter than in the unpurified samples. In films with higher catalyst concentration (200, 400, and 1000 ppm), the induction period disappears altogether.

Some studies suggest that an induction period followed by acceleration is typical of an autoxidation reaction[14], because chain transfer reactions occur after photo initiation[34] as part of an autocatalytic reaction. This behavior was not observed in the present work. The induction period disappears in Figure 4.2B (samples undergoing 3 purification cycles) at higher catalyst concentrations, and the induction period does not appear at all in Figures 4.2C and 4.2D, which present results from samples that have undergone 5 and 6 purification cycles, respectively. The disappearance of the induction period does not mean that antioxidants no longer affect the oxidation reaction. If one compares Figures 4.1, 4.2B and 4.2C, there is a still significant difference in oxidation as

56

well as in the UV spectra. One potential hypothesis to explain the disappearance of the induction period is that the samples may still be exposed to a small amount of oxygen during the film-making process, and this adventitious oxygen may generate enough peroxide free radicals to consume the residual antioxidant before the oxygen uptake measurements were started.

Figure 4.2B shows the highest oxygen mass uptake in samples containing 400 ppm of cobalt neodecanoate, while Figure 4.2C exhibits the highest oxygen mass in samples containing 200 ppm of cobalt neodecanoate. The oxygen mass uptake of a sample containing 100 ppm of cobalt neodecanoate in Figure 4.2B is lower than that in Figure 4.2C. While UV tests show a significantly reduced peak at 250 nm for the sample having three purification cycles relative to the as-received polymer, the oxygen mass uptake data show obvious effects of residual antioxidants on the oxidation kinetics and uptake.
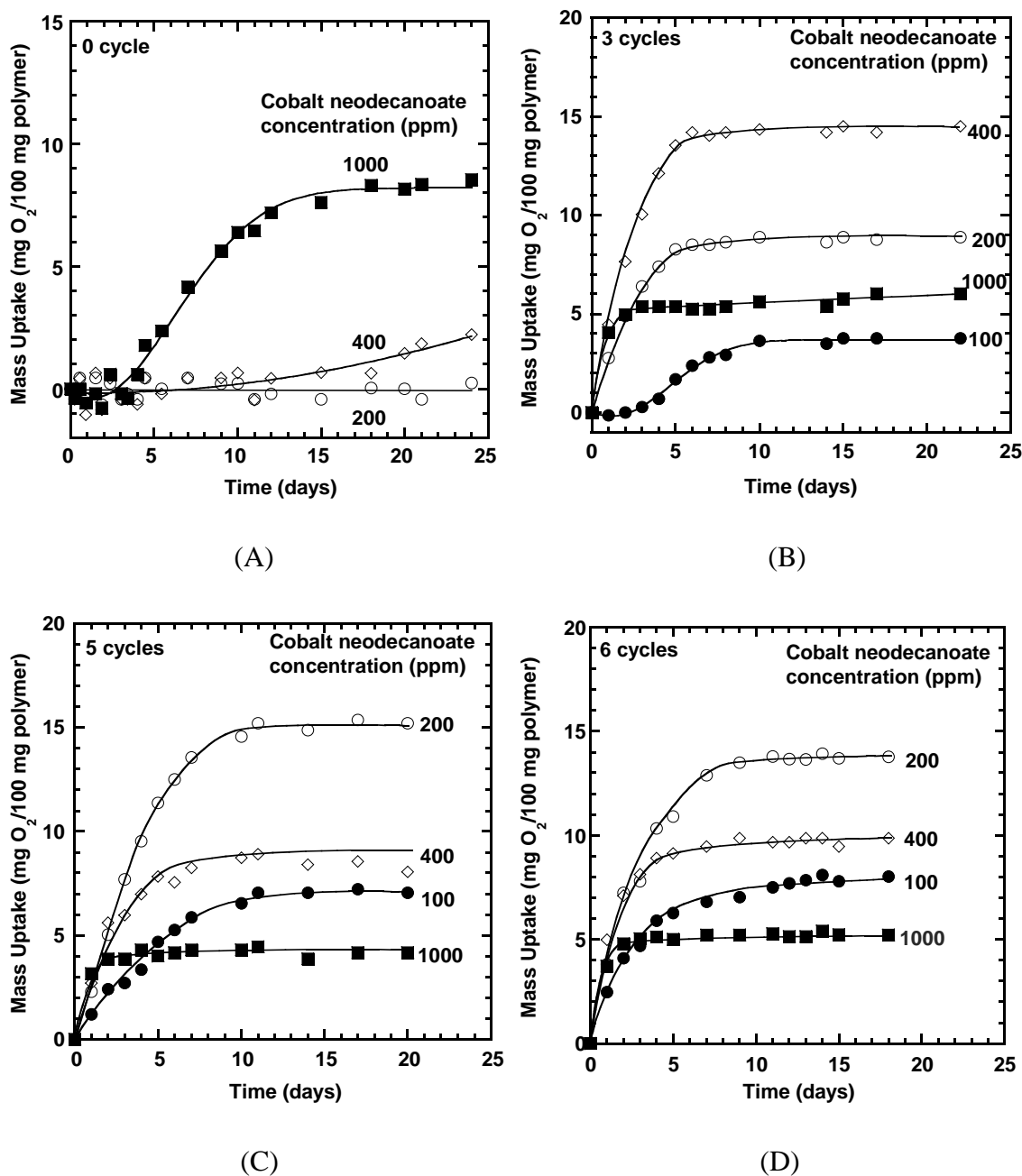
Figure 4.2   Influence of cobalt neodecanoate (Co) concentration and number of purification cycles on oxygen mass uptake. The cobalt neodecanoate concentrations are the numbers beside each data set (e.g., 100 ppm Co). (A) Unpurified (B) Three cycles (C) Five cycles (D) Six cycles

The oxygen mass uptake of 1,4-polybutadiene subjected to six purification cycles is presented in Figure 4.2D. The highest oxygen mass uptake (14.5 wt. %) is obtained in the sample containing 200 ppm of cobalt neodecanoate. This result is similar to that in the sample subjected to five purification cycles (cf., Figure 4.2C), which exhibited maximum oxygen uptake (15 wt. %) in a sample containing 200 ppm of cobalt neodecanoate. Additionally, the oxygen mass uptake values at 100, 400, and 1000 ppm of cobalt neodecanoate are similar in the samples that were subjected to either five or six purification cycles. Thus, it appears that the antioxidants are removed to the point that they have little effect on the oxidation kinetics and uptake after five purification cycles. To put the oxygen uptake values in perspective, the solubility coefficient for oxygen in 1,4-polybutadiene, is $0.957 \times 10^{-6} cm^3 (STP)/(cm^3 Pa)$[35]. This value, corresponding to 0.003 wt % oxygen uptake at ambient conditions, is negligible compared to the total amount of oxygen scavenged by 1,4-polybutadiene, which, according to Figure 4.2C and 2D, is on the order of 15 wt%.

The oxidation half-life is defined, in these studies, as the time required for the oxygen mass uptake to reach 50% of its ultimate value. It provides a crude, model-independent way to characterize the oxidation kinetics. The half-lives of the oxidation reactions are presented in Figure 4.3. The half-life values show the effect of purification cycles and catalyst loading on oxidation reaction rates. As the number of purification cycles increases, the half-life of the reaction decreases, and the half-lives of samples with low catalyst loading (i.e., 100 ppm) are more sensitive to the number of purification cycles than that of samples with high catalyst loading (i.e., 1000 ppm). For example, the

59

half-life for oxidation decreases to a low value that is independent of the number of purification cycles after only 3 purification cycles when using a catalyst loading of 1000 ppm. For a sample containing 100 ppm of catalyst, the half-life is higher than that in the 1000 ppm sample and still decreasing even after 6 purification cycles. This sample is the one which showed negligible oxygen uptake after 30 days when using polymer that was not subjected to any purification steps (cf. Figure 4.2A), so presumably the half-life for this sample at zero purifcation steps would be well above the upper limit of Figure 4.3.
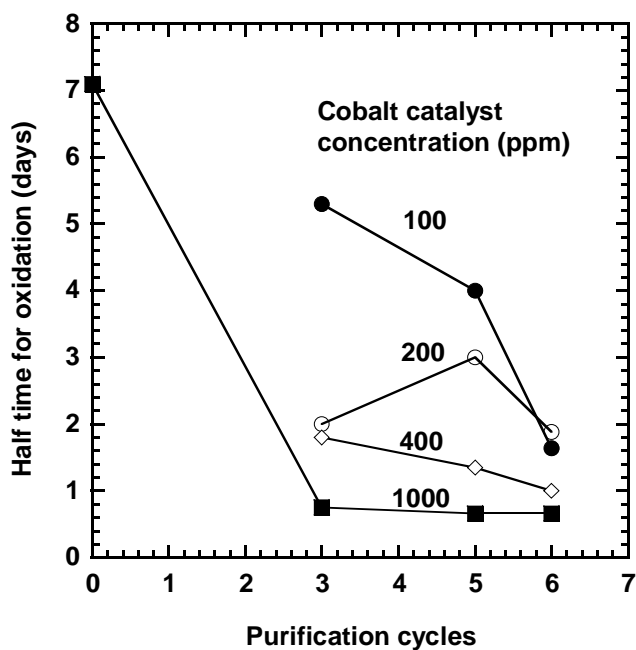
Figure 4.3   Effect of purification cycles on half life of oxidation in 1,4-polybutadiene films containing ●: 100 ppm, ○: 200 ppm, ◊: 400 ppm and ■: 1000 ppm of cobalt neodecanoate. The half-life values (i.e., the time at which half of the final oxygen mass uptake is reached) were obtained from Figure 4.2.

60

Previous studies reported not only oxidation, but also crosslinking when 1,4-polybutadiene was exposed to air[18, 19]. To determine the influence of crosslinking on the results of this study,

After the evaporation of cyclohexane in a nitrogen-filled glove box, polybutadiene films were stored in a vacuum oven to remove residual solvent. However, experiments showed that the observed oxygen mass uptake values depend on the length of time of vacuum storage. To study this effect, 1,4-polybutadiene films were stored under vacuum for various periods of time beyond the 6 hours stated in the Experimental section before being transferred to the Mason® jars for oxidation. The results of this study are presented in Figure 4.4. This experiment used 1,4-polybutadiene samples that had been subjected to 6 purification cycles and contained 200 ppm of cobalt neodecanoate. The films were prepared as described in the experimental section except they were stored under vacuum for different amounts of time, from 6 hours to 168 hours. They were then transferred to Mason® jars, where their oxygen mass uptakes were measured. Based upon the results presented in Figure 4.4 the maximum oxygen mass uptake decreases as vacuum storage time increases. For the sample stored under vacuum for 6 hours, oxygen uptake reaches a maximum, after about seven days, of approximately 15 wt. %. Samples stored under vacuum for longer times show less oxygen uptake. For example, the sample stored under vacuum for 168 hours, the maximum oxygen uptake is only about 9 wt. %.

Since there was no oxygen in the vacuum oven, no oxidation reaction (and, therefore, no mass uptake) would occur inside the vacuum oven. Adventitious oxygen

could be present during the film-making process, but the small amount of oxygen would not lead to large differences in the subsequent oxygen uptake experiment. Obviously, some changes in the film occur during vacuum storage. Although a complete understanding of this phenomenon is not available, we believe there could be several reasons for this behavior. Crosslinking can occur between the double bonds without the presence of oxygen, or it could be initiated by radicals produced by the adventitious oxygen present during the film preparation process. However, swelling experiments only showed a light extent of crosslinking in samples that were stored in vacuum for 96 and 168 hours. Figure 4.2 shows that the oxygen mass uptake values are very sensitive to cobalt catalyst concentration. Change in catalyst activity during vacuum storage time could affect the observed oxygen uptake. Catalyst activity might be affected by either chemical or physical processes. For example, the state of dispersion of cobalt catalyst in the polymer film might change due to the loss of some of the mineral oil into which the catalyst was originally dispersed.

Since vacuum storage is required for residual solvent removal, this step cannot be eliminated before oxygen uptake experiments. To standardize the oxygen uptake experiment, the vacuum storage time during the film preparation process was fixed. All films (except those discussed in Figure 4.4) were stored under vacuum for six hours before testing.
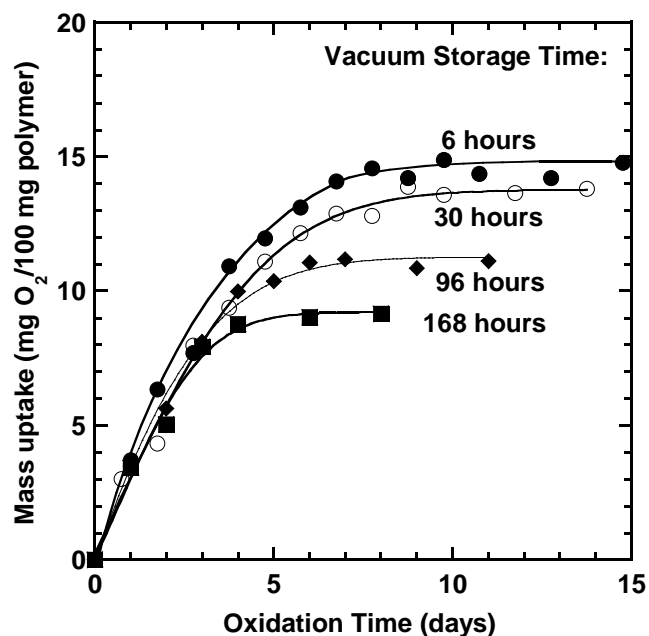
Figure 4.4   Effect of vacuum storage time on oxygen mass uptake. The abscissa (oxidation time) is measured from the moment that the films were initially exposed to air following removal from the vacuum oven.

FTIR and XPS analysis was used to characterize the chemical changes occurring in the polymer during oxidation, and the results are presented in Figures 4.5 and 4.6. Several new peaks were observed in FTIR spectra after two weeks of oxidation in air at room temperature. Based on their positions, the peak at 3450 cm^{-1} is assigned to hydroxyl groups, the one at 1715 cm^{-1} is consistent with the presence of carbonyl groups[17], and peaks at 1250 cm^{-1} and 805 cm^{-1} indicates the generation of epoxides[36]. The disappearance of the sharp peak at 965 cm^{-1} indicates the consumption of C=C bonds in the trans-1,4 structure[37]. These groups have been reported in other polybutadiene oxidation studies[17-19].
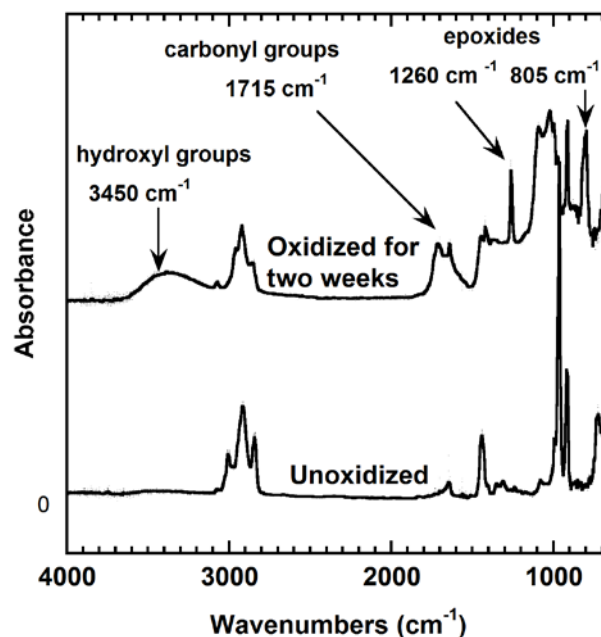
Figure 4.5   ATR-FTIR spectra of oxidized and unoxidized 1,4-polybutadiene films.

XPS was performed both on the film surface and the center of the film. In these studies, 1,4-polybutadiene was purified as described above. 200 ppm of cobalt neodecanoate was added to the casting solution, and the films were prepared by the process described above. The films were oxidized in air for two weeks at 30ºC. The carbon and oxygen spectra were obtained by XPS both on the surface and at the film center. To detect the oxygen content at the film center, the film surface layer was removed using a clean razor blade.

A survey spectrum of the surface of oxidized 1,4-polybutadiene is shown in Figure 4.6(A), and it shows the presence of carbon and oxygen. Because of the low concentration of cobalt neodecanoate catalyst, no cobalt peaks are observed in the survey spectrum. High resolution spectra were also taken of the C1s and O1s regions. The

binding energy for C1s is between 280 eV and 288 eV. For O1s, the binding energy is around 533 eV[38]. The peak at 286 eV is assigned to the carbon-oxygen double bond. High resolution C1s spectra of an unoxidized film, an oxidized film surface and an oxidized film center are presented in Figure 4.6(B). The main peak at 282 eV remained fundamentally unchanged before and after oxidation. Two new peaks appeared in the spectrum of the oxidized film surface. The shoulder peak around 284 eV beside the main peak is assigned to the C-O binding and the peak at 288 eV is attributed to the C=O binding, indicating the presence of a large amount of hydroxyl and carbonyl groups.

These two peaks can also be observed in the spectrum of the oxidized film center. However, the peak strength is much weaker. This result is consistent with the film surface being more highly oxidized than the film center. Carbon and oxygen atomic percentage were also calculated from the XPS analysis, and the results are recorded in Table 4.1. Based on the data in Table 4.1, there is a much higher concentration of oxygen in the oxidized film surface sample than at the film center. On the film surface, there is 24 mole percent of oxygen, while at the film center, the oxygen content is only 10 percent.
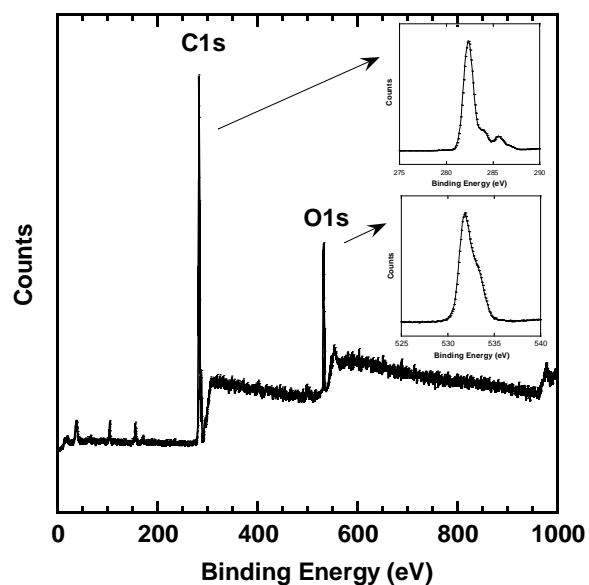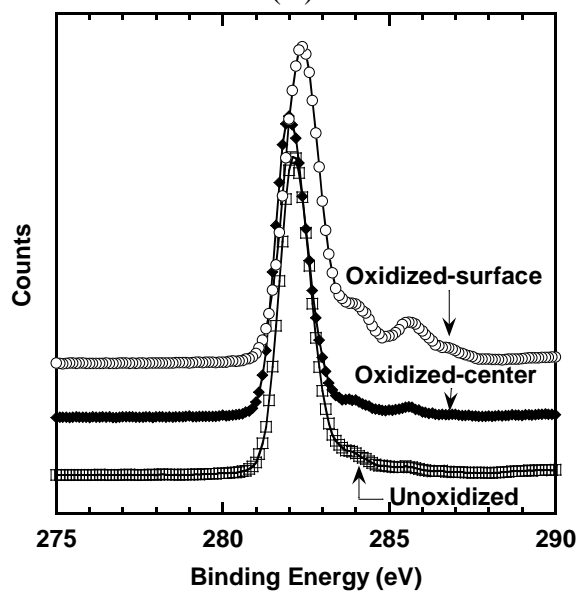
Figure 4.6   XPS spectra of oxidized and unoxidized 1,4-polybutadiene films. (A) A: Survey spectra of oxidized film surface. (B) C1s high-resolution spectrum of oxidized and unoxidized films □: Unoxidized 1,4-polybutadiene film. ♦: Oxidized 1,4-polybutadiene film center.   ○: Oxidized 1,4-polybutadiene film surface.

Table 4.1 XPS results from surface and center of oxidized and unoxidized 1,4-polybutadiene films

Atomic %	Unoxidized 200 ppm Cobalt	Oxidized 2 weeks, Center	Oxidized 2 weeks, Surface
Carbon	96.1	89.7	75.2
Oxygen	3.9	10.3	24.8

Based on these results, a highly oxidized layer is generated at the film surface during oxidation. Further studies, to be reported separately, demonstrate that the highly oxidized layer has more than two orders of magnitude lower oxygen permeability than the unoxidized polymer[39]. The formation of this highly oxidized, impermeable crust on the outside of these samples appears to markedly impede the transmission of oxygen to the center of the film and oxidation at the film center is, correspondingly, much lower than at the film surface. That is, the oxidation proceeds in a heterogeneous fashion, with a highly oxidized surface protecting (from oxygen penetration) a much less oxidized core. Of course, the extent of oxidation of the core versus the surface of the films should be sensitive to film thickness, among other variables, and a future study will report the influence of film thickness on the heterogeneity of oxidation[39].

4.3   Conclusions

Catalyst-promoted oxidation of commercially available 1,4-polybutadiene was studied as part of a project aimed at characterizing the oxygen scavenging properties of this material. The influence of the polymer purification protocol (i.e., number of

purification cycles and time under vacuum) on oxygen uptake and uptake kinetics were explored. These films eventually sorb up to 15 weight percent oxygen; for the thickness used here, the oxidation process occurs over approximately one week. FTIR and XPS studies show the presence of hydroxyl and carbonyl groups after oxidation. The films have a highly oxidized surface and a less oxidized film center, suggesting that the oxidation is heterogeneous.

4.4   References

1.   S. N. Dhoot, B. D. Freeman, and M. E. Stewart. Barrier polymers. In: Kroschwitz J. I., editor. Encyclopedia of Polymer Science and Technology, vol. 5. Wiley-Interscience, New York, 2003, 193-263.

2.   Y. S. Hu, V. Prattipati, S. Mehta, D. A. Schiraldi, A. Hiltner, and E. Baer. Improving gas barrier of PET by blending with aromatic polyamides. *Polymer*, **2005**, 46(8), 2685-2698.

3.   N. K. Lape, C. F. Yang, and E. L. Cussler. Flake-filled reactive membranes. *Journal of Membrane Science*, **2002**, 209(1), 271-282.

4.   A. Polyakova. Oxygen-Barrier Properties of Copolymers Based on Ethylene Terephthalate. *Journal of Polymer Science Part B: Polymer Physics*, **2001**, 39(16), 1889-1899.

5.   A. Polyakova, D. M. Connor, D. M. Collard, D. A. Schiraldi, A. Hiltner, and E. Baer. Oxygen-barrier properties of polyethylene terephthalate modified with a small amount of aromatic comonomer. *Journal of Polymer Science Part B-Polymer Physics*, **2001**, 39(16), 1900-1910.

6.   T. Shimotori, E. L. Cussler, and W. A. Arnold. Diffusion of mobile products in reactive barrier membranes. *Journal of Membrane Science*, **2007**, 291(1-2), 111-119.

7.   R. A. Siegel and E. L. Cussler. Reactive barrier membranes: some theoretical observations regarding the time lag and breakthrough curves. *Journal of Membrane Science*, **2004**, 229(1-2), 33-41.

8.   M. A. Cochran, R. Folland, J. W. Nicholas, and M. E. R. Robinson. Packaging. U. S. Patent, 5,021,515, **1991**

9.   L. Vermeiren, F. Devlieghere, M. van Beest, N. de Kruijf, and J. Debevere. Developments in the active packaging of foods. *Trends in Food Science & Technology*, **1999**, 10(3), 77-86.

10.   T. Y. Ching, K. Katsumoto, S. P. Current, and L. P. Theard. Compositions having ethylenic backbone and benzylic, allylic, or ether-containing side-chains, oxygen scavenging compositions containing same, and process for making these compositions by esterification or transesterification of a polymer melt. U. S. Patent, 5,627,239, **1997**

11.   D. V. Speer, W. P. Roberts, and C. R. Morgan. Method and compositions for oxygen scavenging. U. S. Patent, 5,211,875, **1993**

12.   M. Coquillat, J. Verdu, X. Colin, L. Audouin, and R. Neviere. Thermal oxidation of polybutadiene. part 1: Effect of temperature, oxygen pressure and sample thickness on the thermal oxidation of hydroxyl-terminated polybutadiene. *Polymer Degradation and Stability*, **2007**, 92(7), 1326-1333.

13.   M. Coquillat, J. Verdu, X. Colin, L. Audouin, and R. Neviere. Thermal oxidation of polybutadiene. part 3: Molar mass changes of additive-free non-crosslinked polybutadiene. *Polymer Degradation and Stability*, **2007**, 92(7), 1343-1349.

14.   R. G. Bauman and S. H. Maron. Oxidation of polybutadiene. I. Rate of oxidation. *Journal of Polymer Science*, **1956**, 22, 1-12.

15.   R. G. Bauman and S. H. Maron. The oxidation of polybutadiene. II. Property changes during oxidation. *Journal of Polymer Science*, **1956**, 22, 203-212.

16.   M. Coquillat, J. Verdu, X. Colin, L. Audouin, and R. Neviere. Thermal oxidation of polybutadiene. Part 2: Mechanistic and kinetic schemes for additive-free non-crosslinked polybutadiene. *Polymer Degradation and Stability*, **2007**, 92(7), 1334-1342.

17.   C. Adam, J. Lacoste, and J. Lemaire. Photo-oxidation of elastomeric materials. 1. Photooxidation of polybutadienes. *Polymer Degradation and Stability*, **1989**, 24(3), 185-200.

18. S. W. Beavan. Mechanistic studies on the photo-oxidation of commercial poly(butadiene). *European Polymer Journal*, **1974**, 10, 593-603.

19. M. Piton and A. Rivaton. Photooxidation of polybutadiene at long wavelengths (λ>300nm). *Polymer Degradation and Stability*, **1996**, 53(3), 343-359.

20. J. F. Rabek and B. Ranby. Role of singlet oxygen in photooxidative degradation and photostabilization of polymers. *Polymer Engineering and Science*, **1975**, 15(1), 40-43.

21. J. F. Rabek and B. Ranby. Studies on the photooxidative mechanism of polymers 7. Role of singlet oxygen in the dye photosensitized oxidation of cis-1.4-polybutadiene and 1,2-polybutadiene and butadiene-styrene copolymers. *Journal of Applied Polymer Science*, **1979**, 23(8), 2481-2491.

22. M. P. Anachkov, S. K. Rakovski, and R. V. Stefanova. Ozonolysis of 1,4-cis-polyisoprene and 1,4-trans-polyisoprene in solution. *Polymer Degradation and Stability*, **2000**, 67(2), 355-363.

23. K. T. Gillen and R. L. Clough. Rigorous experimental confirmation of a theoretical-model for diffusition-limited oxidation. *Polymer*, **1992**, 33(20), 4358-4365.

24. W. J. Gauthier and D. V. Speer. Method and compositions for improved oxgyen scavenging. U. S. Patent, 5,981,676, **1999**

25. J. C. Jenkins, R. F. Morrow, and M. E. Stewart. Oxygen-scavenging polyesters useful for packaging. United States Patent Application Publication, US 2008/0161529, **2008**

26. M. E. Stewart, R. N. Estep, B. B. Gamble, M. D. Cliffton, D. R. Quillen, L. S. Buehrig, V. Govindarajan, and M. J. Dauzvardis. Blends of oxygen scavenging polyamides with polyesters which contain zinc and cobalt. United States Patent Application Publication, US 2006/0148957, **2006**

27. H. Li, D. K. Ashcraft, B. D. Freeman, M. E. Stewart, M. K. Jank, and T. R. Clark. Non-invasive headspace measurement for characterizing oxygen-scavenging in polymers. *Polymer*, **2008**, 49(21), 4541-4545.

28. M. Coquillat, J. Verdu, X. Colin, L. Audouin, and M. Celina. A kinetic evaluation of the thermal oxidation of a phenol stabilised polybutadiene. *Polymer Degradation and Stability*, **2008**, 93(9), 1689-1694.

29. R. H. Whitfield and D. I. Davies. Novel nitrogen-containing antidegradants for polybutadiene. *Polymer Photochemistry*, **1981**, 1(4), 261-274.

30. R. A. Sheldon and J. K. Kochi. Metal-Catalyzed Oxidations of Organic Compounds. Academic Press, Inc. , New York City, New York, 1981, 33-70.

31. R. A. Sheldon and J. K. Kochi. Metal-Catalyzed Oxidations of Organic Compounds. Academic Press, Inc. , New York City, New York, 1981, 22.

32. R. L. Clough and K. T. Gillen. Oxygen diffusion effects in thermally aged elastomers. *Polymer Degradation and Stability*, **1992**, 38(1), 47-56.

33. C. Adam, J. Lacoste, and J. Lemaire. Photo-oxidation of elastomeric materials. 2. Photo-oxidation of styrene-butadiene copolymer. *Polymer Degradation and Stability*, **1989**, 26(3), 269-284.

34. A. V. Tobolsky, D. J. Metz, and R. B. Mesrobian. Low temperature autoxidation of hydrocarbons: the phenomenon of maximum rates. *Journal of the American Chemical Society*, **1950**, 72, 1942-1952.

35. G. J. Armerongen. Influence of structure of elastomers on their permeability to gases. *Journal of Polymer Science*, **1950**, 5(3), 307-332.

36. R. V. Gemmer and M. A. Golub. Applications of Polymer Spectroscopy Academic Press, New York 1978, 79.

37. R. M. Silverstein, F. X. Webster, and D. J. Kiemle. Spectrometric Identification of Organic Compounds. 7 ed. John Wiley & Son, Hoboken, NJ 2005, 72-126.

38. G. Beamson and D. Briggs. High resolution XPS of organic polymers John Wiley & Sons Ltd., West Sussex, England, 1992.

39. H. Li, K. K. Tung, D. R. Paul, and B. D. Freeman. Effect of thickness on auto-oxidation in cobalt-catalyzed 1,4-polybutadiene films. In preparation.

4.5   Appendix
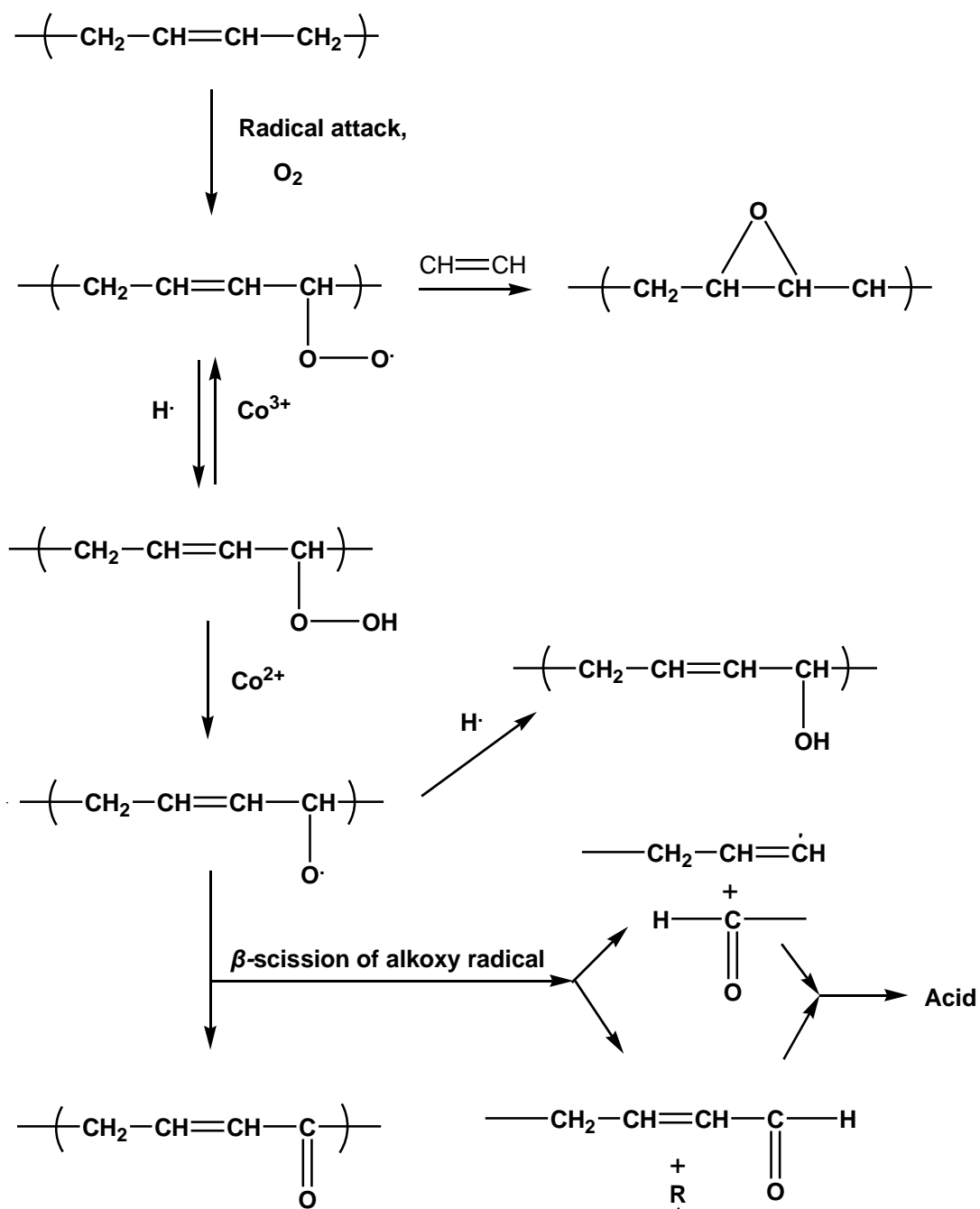
Figure 4.7   Possible mechanism for the cobalt-catalyzed oxidation of polybutadiene

Chapter 5: Effect of Film Thickness on Oxidation in Cobalt-Catalyzed 1,4-Polybutadiene Films

5.1   Introduction

Oxygen scavenging materials are used in active packaging of foods, beverages, and other products[1]. Removing headspace oxygen and providing an effective barrier to oxygen ingress from the environment surrounding packages have been of significant interest for packaging of oxygen-sensitive products[1]. Oxygen scavenging polymeric films provide an additional mechanism, above and beyond that which can be obtained by conventional passive barrier packaging, for reducing oxygen transmission into packages by chemically oxidizing a sacrificial polymer layered or embedded into some or all of a package wall[2]. In a packaging film containing an oxygen scavenging polymer, any oxygen diffusing across the film is susceptible to being consumed by chemical reaction with the oxidizable polymer, incorporating the oxygen into the oxidized polymer, thereby arresting its transport across the film. Additionally, as the polymer film oxidizes, its permeation properties change. In some systems, significant decreases in permeability have been reported, which provides another mechanism for impeding transport of oxygen (and other species) into packages containing oxygen-sensitive products. Such effects are reported in, for example, photo-oxidation and thermal oxidation of polybutadiene-containing rubbers[3, 4].

The rate of oxidation is often determined by a balance between the oxidation rate kinetics and the rate of transport of oxygen through a polymer film, which in turn governs

73

the capacity to replenish oxygen in the film and permit further oxidation[4]. These two rates determine whether a polymer film oxidizes homogeneously or heterogeneously. Rapid oxidation rate tends to result in heterogeneous oxidation, with an oxidized layer being formed at the film surface (e.g. polymers oxidized at high temperature)[5]. In contrast, slower oxidation rates lead to homogeneous oxidation[6]. Because oxygen enters a polymer via diffusion and because the timescale for diffusion depends on film thickness, oxidation can be homogenous in a thin film but become heterogeneous in thicker films. The film thickness at which the oxidation switches from being predominantly homogeneous to predominantly heterogeneous represents a critical thickness[7].

There are several studies of diffusion-controlled reaction in reactive polymeric films[8-15], and several models have been proposed to describe diffusion-controlled oxidation[3, 12-17]. IR spectroscopy has been used to track functional group concentration change in polymers undergoing oxidation[18, 19]. Modulus of polymer films has also been characterized as function of oxidation time[3]. In heterogeneous oxidation, large differences in these parameters can be observed at the film surface exposed to oxygen and in the core of the film[4]. Permeability in polymer films during oxidation has also been studied in some cases. For example, Audouin reported gas permeability changes upon radiochemical aging of low-density polyethylene.[20]. In this case, oxygen permeability at the film surface increased because of chain scission and decreased at the center of the film due to crosslinking. Clough and Gillin reported that the oxygen permeability of Neoprene rubber decreased two orders of magnitude after six

74

days of thermal oxidation, and approximately an order of magnitude decrease in oxygen permeability was reported for styrene-butadiene rubber upon oxidation[4].

Polybutadiene is of commercial interest as an oxygen scavenging polymer matrix for barrier packaging applications[21-26]. Typically, it is mixed with low levels of a transition metal catalyst, such as cobalt neodecanoate, which promotes oxidation at ambient conditions[21, 25, 26]. However, there are no systematic studies in the open literature describing the effect of important variables, such as catalyst concentration and film thickness, on oxidation in this polymer, and such studies are the focus of this paper. In a related study of cobalt-catalyzed auto-oxidation in 1,4-polybutadiene films, we observed heterogeneous oxidation[27]. The objective of the current study was to characterize the thickness of the oxidized and unoxidized zones in 1,4-polybutadiene films and to determine permeability changes in the polymer due to oxidation. Because the gas permeability of oxidized thick films of 1,4-polybutadiene was too low to measure, we prepared thin films (i.e. 1-5 µm thick) for these studies, which makes it possible to measure gas permeability coefficients in even highly oxidized 1,4-polybutadiene films. The relationship between permeability change and oxidized layer thickness is also presented.

5.2 Results and Discussion

5.2.1 *Effect of Film Thickness on Oxidation and Oxygen Mass Uptake*

Polybutadiene films with thicknesses between 50 and 400 μm were oxidized in air at 30ºC. All films were prepared with 200 ppm of cobalt neodecanoate because previous studies showed that 1,4-polybutadiene films in this thickness range oxidizing at 30°C in air exhibited a maximum oxygen mass uptake when the sample contained 200 ppm of cobalt neodecanoate[27]. The oxygen mass uptake was measured with an OxySense® system[28], and the oxygen uptake curves for 1,4-polybutadiene films, normalized by polymer mass and film area, are presented in Figure 5.1.

For all samples, oxygen uptake began as soon as the films were removed from the vacuum oven and exposed to air. In Figure 5.1(A), oxygen uptake is reported as mass of oxygen sorbed per unit mass of polymer. As film thickness increased, the maximum oxygen mass uptake decreased, from 19 % in a 66 μm thick film to 4 % in a 344 μm thick film. The slope of the oxygen uptake curves at short times, which is the initial oxidation rate, was lower in thicker films. The time required to reach maximum oxygen uptake in all films was approximately 5 to 6 days.

76
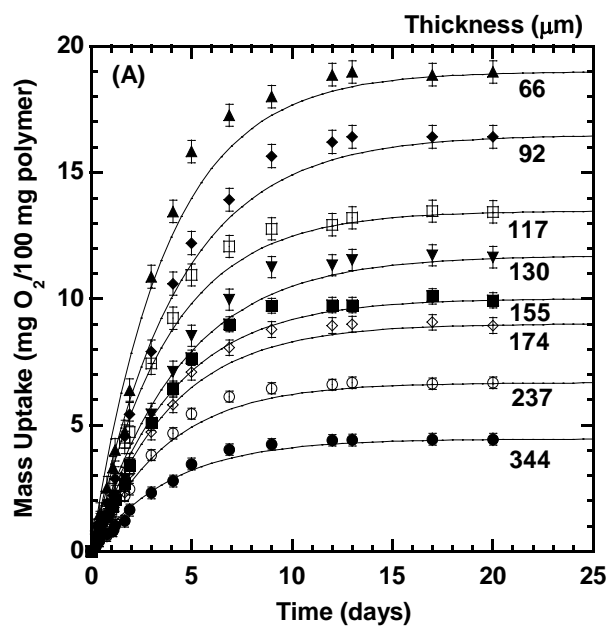
(A)
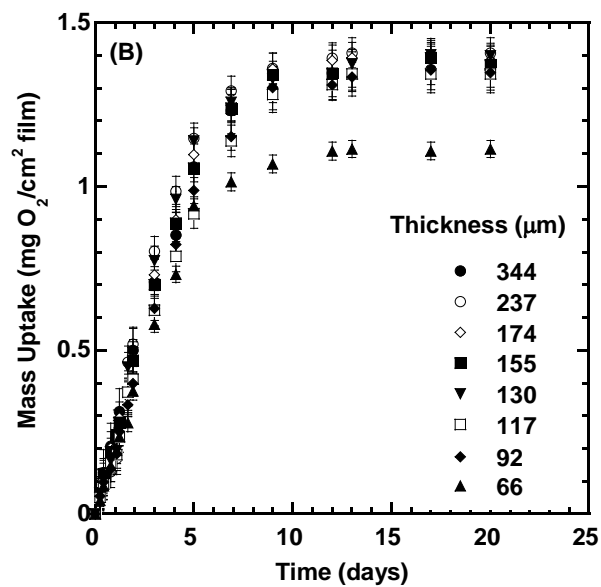
(B)

Figure 5.1   Effect of film thickness on oxygen mass uptake in thick 1,4-polybutadiene films containing 200 ppm of cobalt neodecanoate and oxidized at 30ºC in air. Oxygen uptake values are normalized with respect to: (A) polymer mass and (B) film area.

As shown in Figure 5.1(B), when the oxygen uptake was normalized by the surface area of the film, the uptake curves largely collapsed onto a single master curve (except for the thinnest film, 66 µm, which will be discussed separately), indicating that films with the same surface area (but different thicknesses) sorbed similar amounts of oxygen. The only exception was the thinnest sample (66 µm), which had the highest oxygen uptake in Figure 5.1(A) but the lowest oxygen uptake when oxygen uptake was normalized by film area (cf. Figure 5.1(B)). Similar effects were also observed in samples containing different cobalt catalyst concentrations. Table 5.1 presents oxygen uptake normalized by polymer mass and polymer area in films containing 100, 400 and 1000 ppm of cobalt neodecanoate, respectively.

Table 5.1 Effect of film thickness and cobalt neodecanoate concentration on oxygen uptake in 1,4-polybutadiene films.

Oxygen mass uptake	100 ppm Cobalt Neodecanoate					
	65 µm	79 µm	102 µm	121 µm	165 µm	271 µm
mg O_2/100 mg polymer	15.8	13.3	10.6	9.0	6.8	5.3
mg O_2/cm^2 polymer	0.94	0.97	0.99	1.0	1.0	1.1

Oxygen mass uptake	400 ppm Cobalt Neodecanoate				
	57 µm	82 µm	101 µm	160 µm	252 µm
mg O_2/100 mg polymer	15.9	11.4	9.3	5.6	3.9
mg O_2/cm^2 polymer	0.83	0.86	0.86	0.83	0.90

Oxygen mass uptake	1000 ppm Cobalt Neodecanoate				
	54 µm	72 µm	112 µm	168 µm	230 µm
mg O_2/100 mg polymer	10.7	7.2	5.4	3.4	2.7
mg O_2/cm^2 polymer	0.53	0.48	0.56	0.53	0.57

Bigger and Delatycki studied oxidation in polymers and analyzed the oxygen consumed by the polymer using the following empirical model:[6]

$$n(t) = x_i (1 - e^{-t/\tau}) \tag{5.1}$$

where $n(t)$ is moles of oxygen reacted with the polymer at time t, x_i is the number of reactive centers in the polymer, and τ is the oxidation timescale. Since the number of effective available reactive sites in 1,4-polybutadiene films depends on film thickness, and changes as the oxidation reaction proceeds, because the consumption of C=C bonds can limit the oxidation of the polymer[29], an infinite time oxygen consumption value, m_0, is used to replace the total reactive sites x_i in the equation. Thus, Equation (5.1) is written as follows:

$$m(t) = m_o (1 - e^{-t/\tau}) \tag{5.2}$$

where $m(t)$ and m_o are the oxygen mass uptakes at time t and infinite time, respectively. The lines shown in Figure 5.1(A) represent fits of this model to the experimental data. While the model does not perfectly fit the data, which suggests that the oxidation/diffusion phenomena occurring in these samples is more complex than can be completely captured by such a simple model, clearly the model captures much of the trends in the experimental data and provides a convenient way to characterize the overall behavior of the oxidation kinetics. Values of m_0 and τ are presented in Figure 5.2 as a function of film thickness. The time constant for oxidation is essentially independent of film thickness, and the oxygen uptake capacity, m_0, decreases with increasing thickness. These observations, as discussed in more detail below, help build a picture of the oxidation mechanism in these films.

(A)

(B)
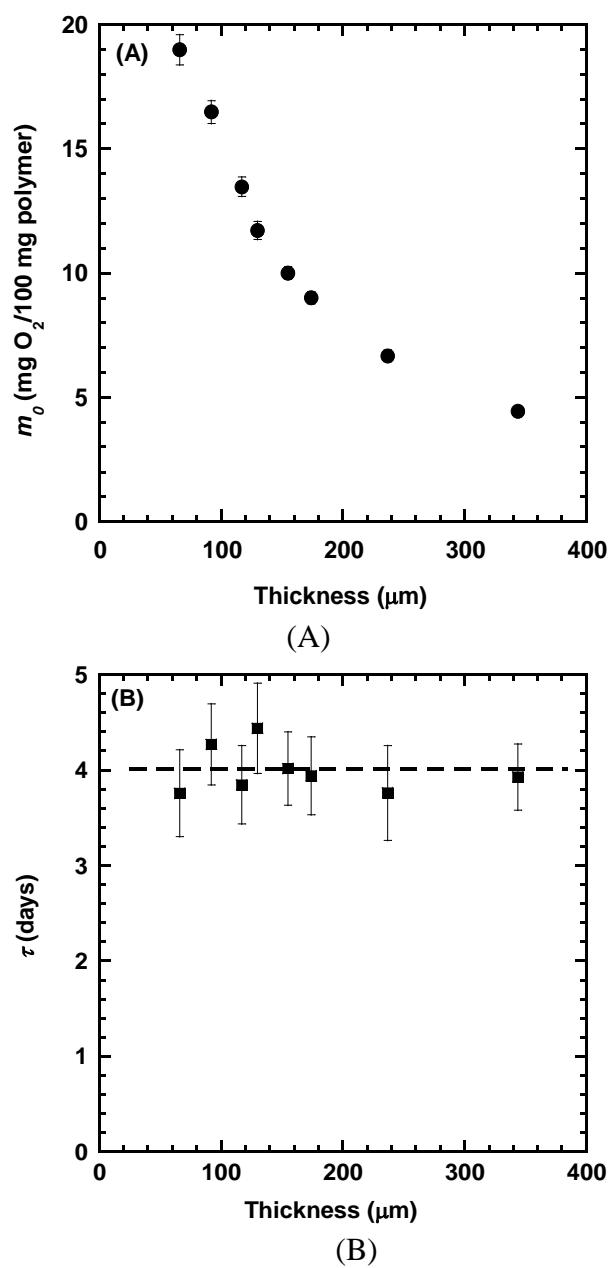
Figure 5.2   Effect of film thickness on the model parameters m0 and τ used to describe the experimental data in Figure 5.1.

If the oxidation reaction were homogeneous and limited only by the oxygen reaction kinetics, the polymer films would be evenly oxidized, and the oxygen uptake per unit mass of polymer should be independent of film thickness, which is not consistent with the experimental results presented in Figures 5.1(A) and 5.2(A). On the contrary, if the oxidation process were limited by the ability of the oxygen to diffuse through a very impermeable surface layer that is highly oxidized, then the oxidation of the polymer film would be heterogeneous. In the extreme limit of this scenario, oxygen uptake would only occur in a thin layer near the surface of the film, which would be the region accessible to oxygen. In this case, oxygen uptake per unit mass of polymer would depend on film thickness, but it would be independent of film surface area, which is consistent with most of the data in Figures 5.1 and 5.2. In a related study, XPS results showed that the oxygen content of an oxidized polybutadiene film surface was much higher than at the film center, supporting the hypothesis of heterogeneous oxidation in thick films[27].

Penetrant diffusion in rubbery polymers typically follows Fickian behavior. In Fickian diffusion-controlled kinetics of permeation through a film, the time required to reach steady state, t_{ss}, is given by[4]:

$$t_{ss} = \frac{L^2}{D} \quad\quad\quad (5.3)$$

where L is the thickness of the thin film. The reported oxygen diffusion coefficient of unoxidized polybutadiene at 25 °C is between 1.5×10^{-6}[30] and 1.7×10^{-6} cm^2/sec[31]. So, in a 100 μm thick film, the time to reach steady state is only tens of seconds. This value is

orders of magnitudes shorter than the oxidation time scale, so diffusion of oxygen through the native unoxidized polymer is not controlling the kinetics of oxygen uptake.

Thin polymer films (i.e. thicknesses below 10 µm) containing 200 ppm of cobalt neodecanoate were prepared by spin coating polymer solution onto silicon wafers, and oxygen mass uptake was studied. Since it is difficult to detach the thin films from the silicon wafers, they were left on the wafers during oxidation, so only one side of the film was exposed to air. However, as will be shown later, such thin films are believed to oxidize homogeneously, with the rate of mass uptake being controlled by the oxidation kinetics. Therefore, since diffusion of oxygen through the film is not limiting, there will be no difference in the oxygen mass uptake or kinetics of oxygen uptake in samples with only one side (rather than both sides) exposed to air. The oxygen mass uptake in these thin polybutadiene films are presented in Figure 5.3. The lines through the data represent least squares fits of Equation (5.2) to the results, and the model parameters are recorded in Table 5.2.

(A)

(B)
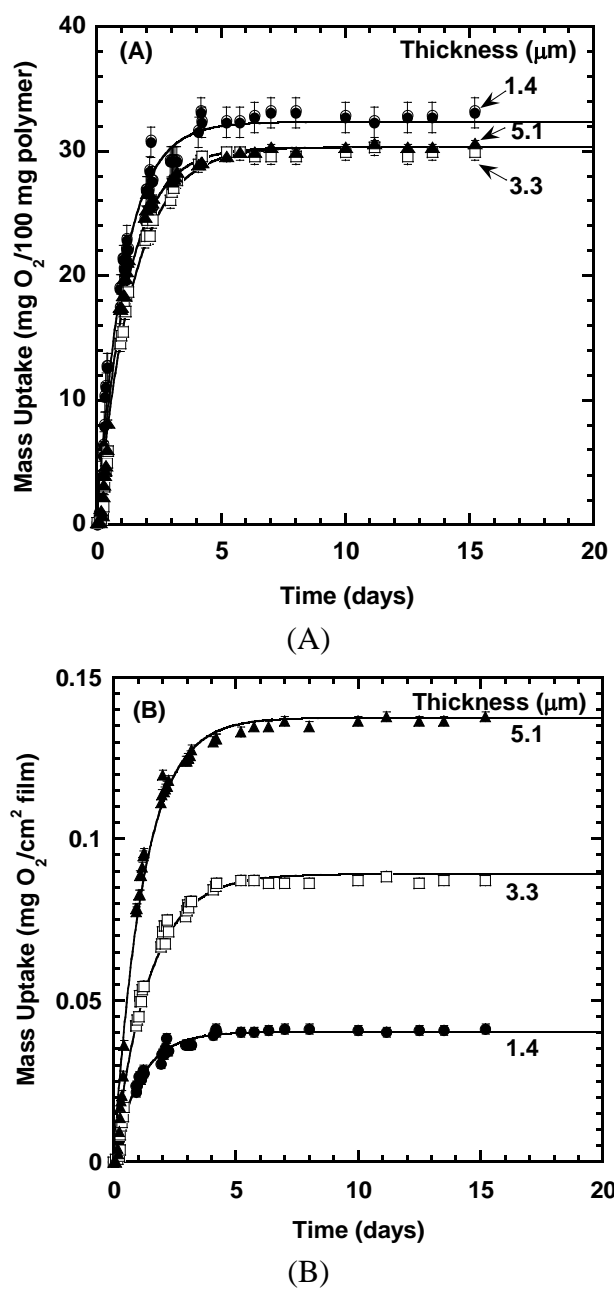
Figure 5.3   Effect of film thickness on oxygen mass uptake in thin spin-coated 1,4-polybutadiene films containing 200 ppm of cobalt neodecanoate. These films were oxidized at 30ºC in air. Oxygen uptake values are normalized with respect to: (A) polymer mass and (B) film area.

Table 5.2 Model parameters m_0 and τ used to describe the experimental data in Figure 5.3(A).

Film Thickness (μm)	m_0 (wt %)	τ (days)
1.4	32.3 ± 0.3	1.10 ± 0.04
3.3	30.4 ± 0.5	1.44 ± 0.06
5.1	30.3 ± 0.4	1.22 ± 0.05

Samples with different thicknesses had similar oxidation kinetics and maximum uptake values when the oxygen uptake was normalized with respect to initial polymer mass, as shown in Figure 5.3(A). Oxygen uptake in these thin films increased quickly at the beginning and slowed down over the next few days. The maximum oxygen uptake values were similar in thin films, ranging from about 33 wt % in a 1.4 μm thick film to about 30 wt % in 3.3 and 5.1 μm thick films. In thick films, as shown in Figures 5.1(A) and 5.1(B), oxygen uptake per unit mass of polymer depends on film thickness, and oxygen uptake per unit area is independent of film thickness. On the contrary, in thin films, thickness has essentially no effect on the oxygen uptake per unit polymer mass, while oxygen uptake per unit polymer area changes as film thickness changes. Taken together, these results suggest that in such thin films, oxidation is homogeneous, whereas it is heterogeneous in thick films. Further evidence to support this hypothesis will be presented below.

If one butadiene repeat unit reacted with one oxygen atom, the oxygen mass uptake would be 29.3 wt %, which is very close to the experimentally observed maximum uptake in Figure 5.3(A). But based on the chemical structure of 1,4-

polybutadiene, there are four α-position C-H bonds that potentially react with oxygen. One C-H bond can oxidize to either a hydroxyl or a carbonyl group, and if a carbonyl group is generated, no further oxidation can occur on that site. If a hydroxyl group is formed, the other hydrogen on the same carbon is still reactive, and breaking of this C-H bond will form a radical on the carbon. However, this radical tends to convert the hydroxyl group into carbonyl group, and no extra oxygen would be added to the polymer during such a reaction. The alpha C-H on the other side of double bond should be minimally affected by this oxidation, and it could, in principle, still be oxidized. Thus, the theoretical oxygen mass uptake in 1,4-polybutadiene would be higher than 29.3 wt %. There could be several reasons that the measured oxygen uptake is smaller than the theoretical value.

One possible cause is the generation of small molecules. Small molecules are often produced in thermal oxidization and photo-oxidation of rubbery polymers[32]. The small molecule by-products may diffuse out of the film, causing mass loss. However, the amounts of such by-products are affected by initiation conditions[33]. In our system, few small molecule by-products were generated at room temperature because the oxygen uptake data measured using an analytical balance (an open system) and an OxySense[®] system (a sealed system) were essentially identical[28]. Therefore, any mass loss from the production and subsequent loss of small molecule byproducts can be neglected.

Crosslinking may be another reason that oxygen uptake is lower than expected. In a metal-catalyzed auto-oxidation system, crosslinking is a major side reaction[34]. There may be more than one mechanism by which crosslinking occurs during oxidization; one

is crosslinking directly between double bonds. After crosslinking, C=C double bonds are consumed, and a new C-C network is built[34, 35]. Because of the saturation of carbon-carbon double bonds, the original alpha C-H bonds are much less active towards oxidation. Crosslinking could also be initiated by reaction between C=C bonds and peroxy radicals[35]. This reaction can lead to either a crosslinked network or an epoxide structure[36]. In photo-oxidation of polybutadiene without transition metal catalyst, a 25% consumption of double bonds caused the oxidation rate to fall to a very low level[29], and significant double bond consumption was observed for any butadiene structure (1-2, trans-1,4 or cis-1,4) in polybutadienes[37] and styrene-butadiene copolymers[38] oxidation.

Crosslinking is the most likely explanation for the oxygen uptake of these films being lower than one might expect based on the polymer structure. In other studies of oxidation in polybutadienes, the oxygen uptakes were even lower than the theoretical value mentioned earlier (29.3%), so not all the reactive sites were oxidized in those studies either[5, 7]. For example, in the study of thermal oxidation in polybutadiene at 100ºC in air, a fully oxidized 20 µm thick film showed about 13 wt % oxygen mass uptake[7].

The difference in oxidation kinetics in thick and thin films raises these questions: What is the thickness of the oxidized layer of 1,4-polybutadiene films, and what is the maximum oxygen uptake in such highly oxidized layers? Because 1,4-polybutadiene is a soft elastomer, to utilized its oxygen uptake capacity in barrier materials, it must be copolymerized, or formed in layered configuration with other polymers (e.g., polystyrene

or PET) for commercial oxygen scavenging applications[25]. A better understanding of the oxidized layer thickness in 1,4-polybutadiene films could help maximize the efficiency of oxygen scavenging packaging films.

A series of films of various thicknesses was produced to determine the critical thickness of the oxidized layer in 1,4-polybutadiene at the oxidation conditions considered in this study. In all cases, the oxidation of these films was conducted in air at 30°C using an analytical balance to measure mass uptake. Figure 5.4 presents the maximum mass uptake as a function of reciprocal thickness, L^{-1}. This method of presenting the data follows that presented in the literature for oxidation of polybutadiene via thermal processes[7]. The oxygen mass uptake data were obtained in experiments lasting more than 30 days, which was much longer than the time required for oxygen uptake to be complete, so these results are for samples that have essentially been oxidized to the largest extent possible. Oxygen mass uptake in thin films remained constant at approximately 30 wt %, even though only one surface of the polymer film was exposed to air. In such thin films, oxygen transport into the film is not the rate-limiting step in oxidation, and the films oxidize to the maximum amount possible in less than a week. As thickness approaches and exceeds 10 µm, the maximum mass uptake decreases with increasing thickness. Similar phenomena have been reported previously[7]. In these literature studies, the critical thickness of the oxidized layer, L_c, is identified as the intersection of the two lines shown in Figure 5.4. On this basis, the critical thickness is about 28 µm, similar to the reported critical thickness in thermally oxidized polybutadiene, which is 22±2 µm [7].
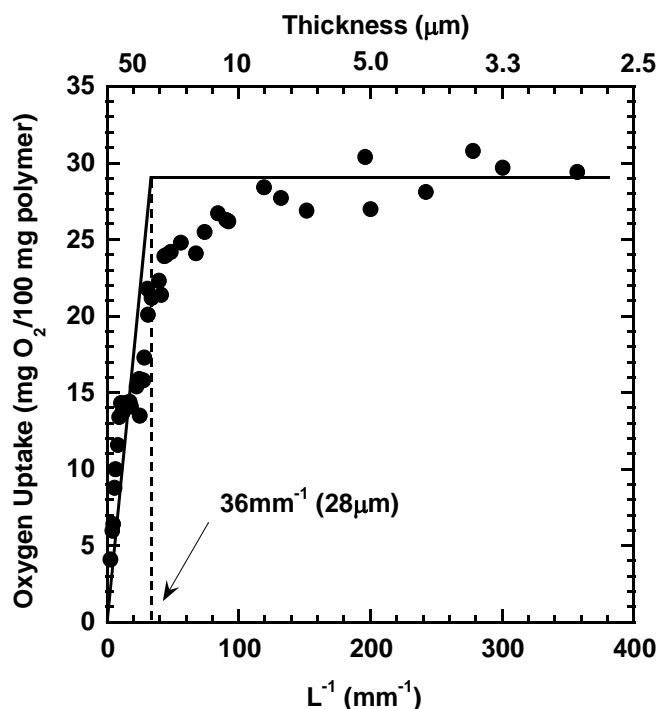
Figure 5.4   Influence of film thickness on oxygen mass uptake. The films were prepared with 200 ppm of cobalt neodecanoate and were oxidized in air at 30°C.

The oxidization products are localized primarily in surface layers approximately L_c thick. In film samples oxidized on both sides, in thin films (i.e. when $L<2L_c$), the mass uptake per unit polymer mass tends to be independent of L and the sample is homogeneously oxidized. In thick films, (i.e. when $L>2L_c$), the mass uptake per unit polymer mass depends on L, and the sample is heterogeneously oxidized, with the surfaces being highly oxidized to a depth of approximately L_c and much less oxidized deeper into the sample. Since the oxidation is presumed to occur approximately homogeneously in the oxidized layer, the oxygen content of the oxidized layer would also

be constant. Therefore, per unit area of film, the volume of the oxidized region and the oxygen uptake would be fixed and independent of film thickness. A schematic showing the suggested structure is presented in Figure 5.5. L_c and L_{no} are the critical oxidized layer thickness and non-oxidized core thickness, respectively.
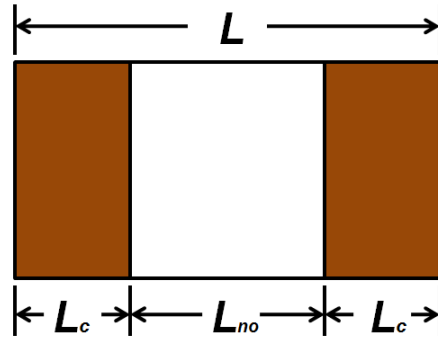
Figure 5.5   Schematic morphology of an oxidized 1,4-polybutadiene film.

If the scenario described above is approximately true, then the oxygen uptake data taken using thick films (i.e. $L>2L_c$) can be expected to follow a simple model with thickness. In film samples oxidized on both sides, the simplest model would be one in which all of the oxidation is confined to surface layers of thickness L_c. In these layers, the oxidation would be at its maximum extent, $m_{o_{max}}$, given approximately by the values observed at long times in the thin films, where the oxidation is homogeneous (cf. Figure 5.3(A)). In this case, the maximum oxygen uptake per unit polymer mass would be given by:

$$m_o = m_{o_{max}} \frac{2L_c}{L} \qquad\qquad (5.4)$$

or, equivalently,

$$\frac{1}{m_o} = \frac{L}{2L_c \cdot m_{o_{max}}} \qquad\qquad (5.5)$$
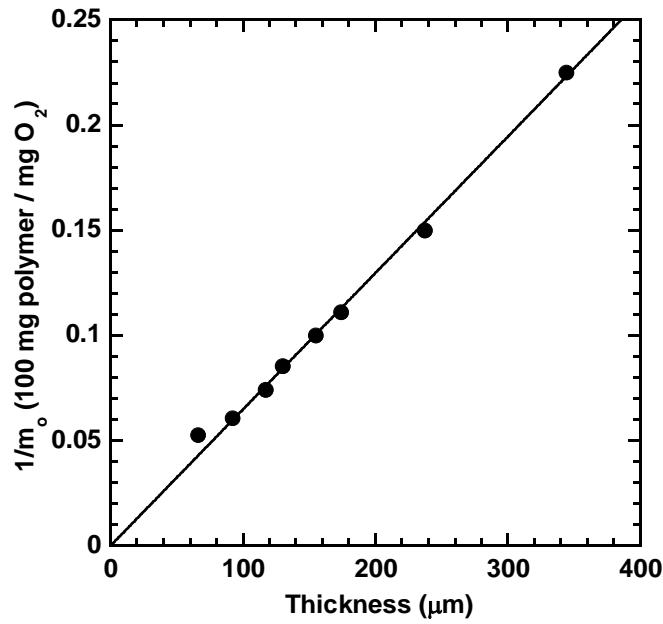
Figure 5.6   Effect of film thickness on reciprocal final oxygen mass uptake, m_0. The solid line is a least squares fit of all of the data, except the data point at 66 μm thickness, which is very near the limit of 2Lc. Based on Equation (5.5), the slope of the line should be $\dfrac{1}{2L_c \cdot m_{o_{max}}}$.

The data in Figure 5.2(A) are presented as suggested by Equation (5.5) in Figure

5.6. All of the data points, with the exception of the data point at 66 microns, which is

very near the limit of $2L_c$ where this model would no longer apply, lie on a straight line through the origin, as shown in Figure 5.6. The value of $m_{o_{max}}$, which was obtained independently from Figure 5.3(A) (about 30 mg O_2/100 mg polymer), and the slope from Figure 5.6 were used to calculate L_c. The resulting value is 26 µm, consistent with the value of L_c estimated from Figure 5.4 (about 28 µm), as expected.

The oxidation timescale difference between thin films ($\tau \approx 1$ day) and thick films ($\tau \approx 4$ days) may result from a difference in the rate-controlling mechanism for oxidation in thick and thin films. The reaction should be essentially fully controlled by the oxidation reaction kinetics in thin films, but there may be a significant contribution from diffusion-limited oxidation in thicker films, which acts to slow the observed oxidation response. Consequently, oxidation of 1,4-polybutadiene may involve two successive steps because of the significant decrease in oxygen permeability occurring during sample oxidation (experimental evidence of this permeability decrease is presented below). Near the surface, oxygen diffusion does not limit the oxidation, so the polymer is essentially homogenously oxidized. However, after a markedly less permeable thin oxidized layer was formed at the surfaces of thick films, the diffusion of oxygen through these thin, relatively impermeable layers can begin to limit the oxidation kinetics, and the oxidation process becomes a competition between oxygen diffusion and reaction. During this further oxidation, the increasingly limited ability of diffusion to bring oxygen to regions of the film where oxidation is possible can limit the increase in oxygen mass uptake and oxidized layer thickness. Eventually, the oxygen uptake stops increasing when the

oxidized layer thickness reaches L_c, due to the difficulty for oxygen to diffuse through the highly oxidized layers at rates and amounts sufficient to continue measurable oxidation kinetics over experimentally accessible timescales. It is possible that some very limited transport of oxygen through the oxidized layers would occur, allowing oxidation would continue, albeit at rates that are imperceptible over the timescales of our experiments.

5.2.2   *Characterization of Oxidized Layers*

When carboxy-terminated polybutadiene undergoes thermal oxidization at 250ºC, a jet-black surface layer is formed, and the interior of the film is reported to be protected against oxidation[39]. Layered structures have been observed by optical microscopy and other techniques in other diffusion controlled reaction systems [5, 12, 40-42]. In our studies, SEM was used to study the oxidized layers. Typical SEM images of microtomed surfaces from unoxidized and oxidized 1,4-polybutadiene films taken are shown in Figure 5.7.

(A)

(B)

(C)

(D)
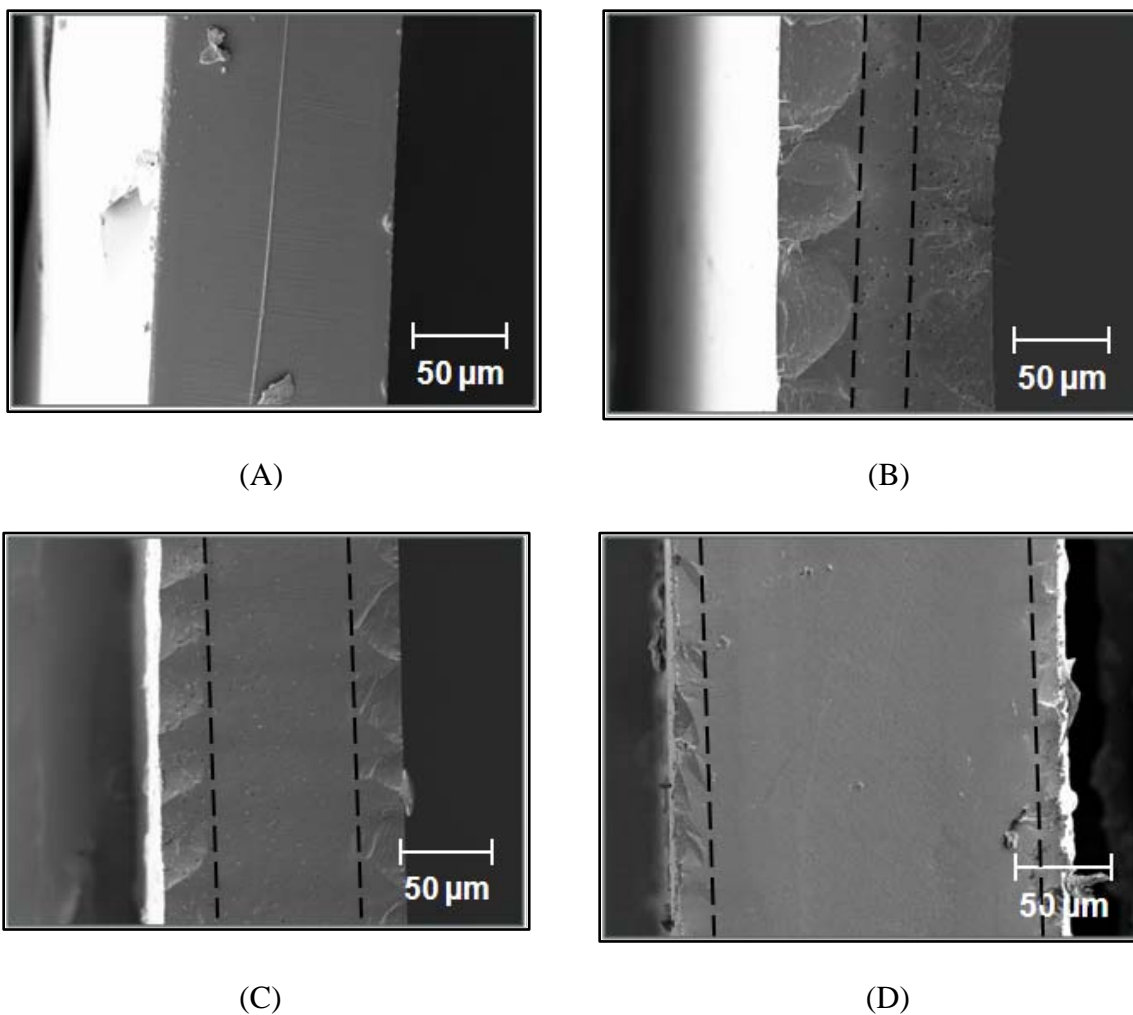
Figure 5.7   SEM images of cross-sections of oxidized 1,4-polybutadiene films containing: (A) 0 ppm, (B) 200 ppm, (C) 400 ppm and (D) 1000 ppm of cobalt neodecanoate. Samples were oxidized in air at 30ºC for 20 days and microtomed at -125ºC.

The unoxidized sample's cross-section is very smooth with no notable structures on the film surface or at the film center, indicating that the entire film is uniform. However, in oxidized 1,4-polybutadiene, a heterogeneous structure was observed in the

SEM images, which is similar to that reported for thermally oxidized polybutadiene[37]. In films containing 200 ppm of cobalt, a layered structure was observed that may be caused by differences in the mechanical properties of the film near the outer surfaces versus the center. The film center is still flat and smooth after microtoming, presumably because this region has mechanical properties similar to those of unoxidized 1,4-polybutadiene. The layer of material extending from the surface into the film exhibits a scalloped structure after microtoming, suggesting that the mechanical properties of outer layers are quite different from those of the core of the sample. Polymer oxidation is known to make the material brittle, and some studies suggest that the embrittlement is essentially confined to the oxidized surface [43-46]. Thus, this surface layer containing the scalloped structure could be viewed as the oxidized zone. The oxidized film in Figure 5.7 (i.e. Figure 5.7(B)) is about 140 μm thick, and the surface layer thickness appears to be about 40 µm, which is qualitatively consistent with the critical thickness determined from oxygen uptake experiments.
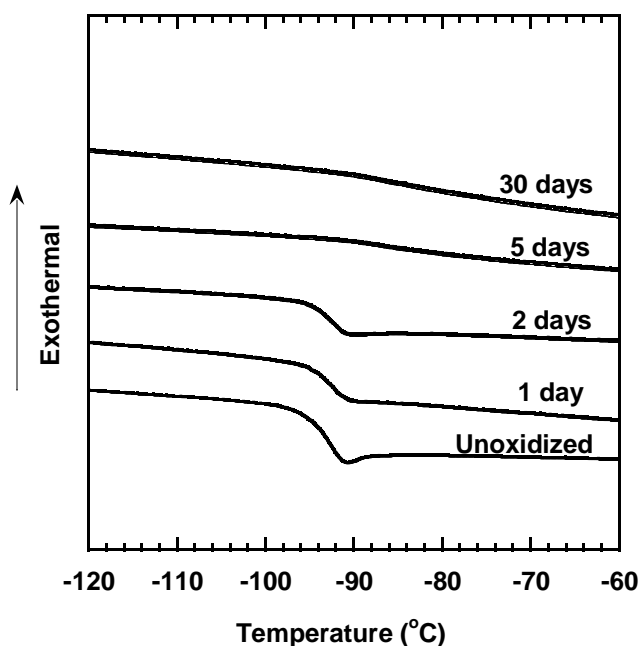
Figure 5.8   First scan differential scanning calorimetry thermograms of 1,4-polybutadiene at various stages of oxidation. All data were from the same thick film, but several samples were harvested from this film and oxidized for various amounts of time in air at 30°C as indicated in the figure. The film was prepared with 200 ppm cobalt neodecanoate using the solution casting method, and the film thickness was 121 µm. The thermograms have been displaced vertically for clarity.

DSC analysis was also performed on 1,4-polybutadiene samples oxidized for various lengths of time. The glass transitions of different samples, approximately 121 µm thick, are shown in Figure 5.8. The unoxidized polybutadiene film has a glass transition temperature at -92ºC. This value is slightly higher than the reported value of -103ºC in *cis*-1,4-polybutadiene by Kanaya[47], and such differences are probably due to differences in the content of *cis*-, *trans*-, and *vinyl*- structures in the polymer considered by Kanaya and in this study. After two days of oxidation in air at 30ºC, the T_g remains the same, but the step change in heat flow (i.e., the heat flow shift) at T_g

96

decreases from 0.12 W/g in an unoxidized sample to 0.08 in a sample oxidized for two days. During the heterogeneous oxidation of 1,4-polybutadiene, the material at the center of the film is much less oxidized than that at the surfaces, so the T_g observed is expected to be that of the unoxidized (or slightly oxidized) polymer, since the oxidized polymer is presumably much less mobile than the unoxidized material. With increasing oxidation time and oxygen mass uptake, the oxidized region in 1,4-polybutadiene films becomes thicker. After 6 days of oxidation, a 120 µm thick film has an oxygen uptake of about 14 wt%[27]. As discussed before, a fully oxidized thin film sorbs about 30 wt % oxygen during oxidation. Presumably, the oxidized layer in thicker films sorbs the same amount of oxygen, so the effective volume fraction of oxidized material is around 46%. At this point, the DSC analysis showed a slight increase in T_g (-86ºC) and an obvious decrease in heat flow shift (0.024W/g). However, longer oxidation times did not lead to further oxidation; a sample oxidized in air for 30 days showed very similar T_g (-84ºC) and heat flow shift (0.024W/g). The heat flow shift in Figure 5.8 is correlated with oxidized polybutadiene content in Figure 5.9. The content of oxidized polybutadiene was calculated as the ratio of oxygen uptake at the time the DSC experiment was conducted divided by the maximum oxygen uptake observed in this sample. There is a strong correlation between these two variables. This observation also supports the existence of heterogeneous oxidation in these samples, with oxidation replacing flexible, mobile polybutadiene (which undergoes a step change in heat capacity at its T_g) with highly rigid, immobile oxidized polybutadiene (which has no thermal events over the entire temperature range probed by the DSC, from -180 to +250 °C).

97
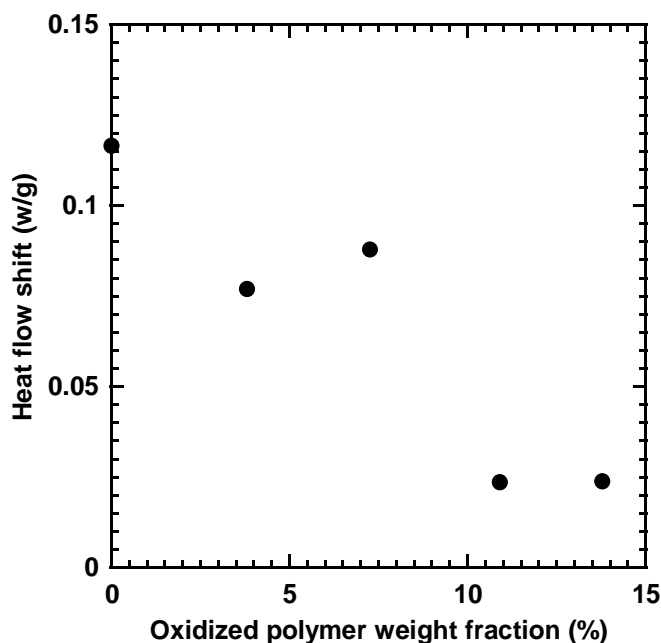
Figure 5.9   Correlation between effective oxidized polymer weight fraction and the heat flow shift at the Tg from Figure 5.8. The heat flow shift at the Tg was determined using the TA Instrument Universal Analysis 2000 software provided by the DSC manufacturer. The effective oxidized polymer weight fraction was calculated by dividing the oxygen mass uptake in the polymer film (obtained from Figure 5.1(A), data from 117 µm thick sample) by the oxygen mass uptake in a fully oxidized thin film, which is 30% based on the data in Figure 5.3(A).

5.2.3   *Gas Permeability in Unoxidized and Oxidized 1,4-Polybutadiene Films*

Oxidation in polymers typically decreases gas permeability. Adam[37, 38, 48] reported oxygen permeability decrease after photo-oxidation of 1,2, 1,4-PB and SBS block copolymers with increasing extent of oxidation, and Clough[4] reported permeability decreases in thermally oxidized rubbers. Our oxygen scavenging materials also showed a significant permeability decrease upon oxidation.

Permeability experiments were conducted in a constant volume permeation system[49]. The permeability of a film was calculated using the following equation[50]:

$$P_A = \frac{V \cdot l}{p_1 \cdot A \cdot R \cdot T} \left[\left(\frac{dp_2}{dt} \right)_{ss} - \left(\frac{dp_2}{dt} \right)_{leak} \right] \tag{5.6}$$

where V is the downstream volume (cm^3), l is the film thickness (cm), p_1 is the upstream absolute pressure (cmHg), A is the film area (cm^2), T is absolute temperature (K), R is the gas constant (0.278 cmHg cm^3/(cm^3(STP)K)), and $(dp_2/dt)_{ss}$ and $(dp_2/dt)_{leak}$ are the pseudo-steady state rates of pressure rise in the downstream volume at a fixed upstream pressure and under vacuum (cmHg/s), respectively. Typically, a plot of the downstream pressure versus time is linear after the time lag period, so the rate of change in downstream pressure with time, $(dp_2/dt)_{ss}$ in Equation (5.6), is a constant value. Thus, the permeability, which is proportional to $(dp_2/dt)_{ss}$, does not change during the measurement. However, in the oxygen permeability experiments reported in this work, $(dp_2/dt)_{ss}$ is not constant. Downstream pressure did increase, but the rate of increase slowed over time, demonstrating that the flux of the film was decreasing. Because the downstream pressure change rate was decreasing during measurement, it was difficult to obtain a constant $(dp_2/dt)_{ss}$ value for permeability calculation. In this case, a stopwatch was used to record the elapsed time for a unit pressure increase and this transient rate of downstream pressure rise was used to estimate permeability according to Equation (5.6).
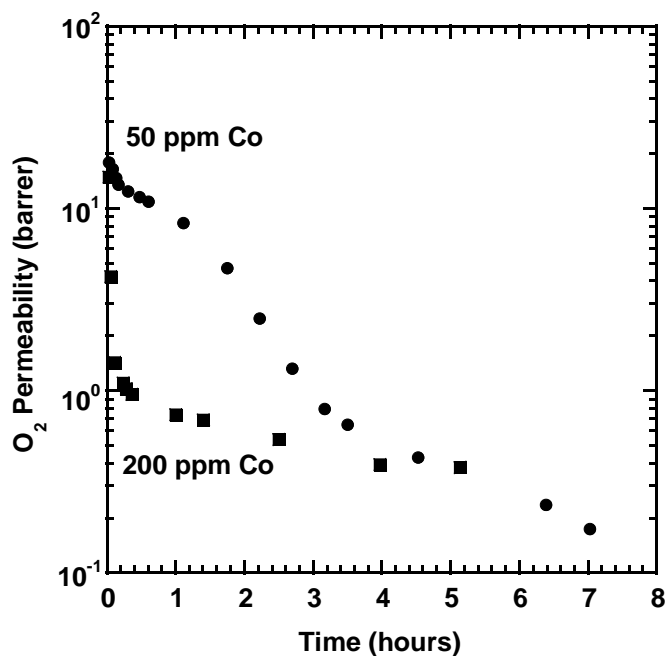
Figure 5.10   Oxygen permeability of 1,4-polybutadiene films containing 50 and 200 ppm of cobalt neodecanoate. Oxygen permeability was measured at 35ºC. The upstream pressure was 3 atm. The film thickness was 113 µm (50 ppm) and 125 µm (200 ppm).

Figure 5.10 demonstrates the oxygen permeability reduction over time in samples containing 50 and 200 ppm of cobalt neodecanoate. The oxygen pressure feed on the upstream face of the sample was 30 psig (3.04 atm), which is 15 times higher than the oxygen partial pressure in air. Therefore, oxidation was faster in the 1,4-polybutadiene film during measurements than at ambient conditions. In both samples, the permeability decreased steadily from the time the permeability measurement began; the permeability decrease is much faster for the sample with higher cobalt catalyst concentration. After 10 hours, the downstream rate of pressure change is very near the leak rate of the permeation system, and the calculated permeability was only 0.2 barrers, which is close to the

100

detection limit of this equipment for a film of this thickness. The film had the distinct

yellow color of oxidized polybutadiene when it was removed from the cell following the

permeability measurement, and the mechanical properties changed from soft to rigid and

brittle, which was also observed with films oxidized in air.
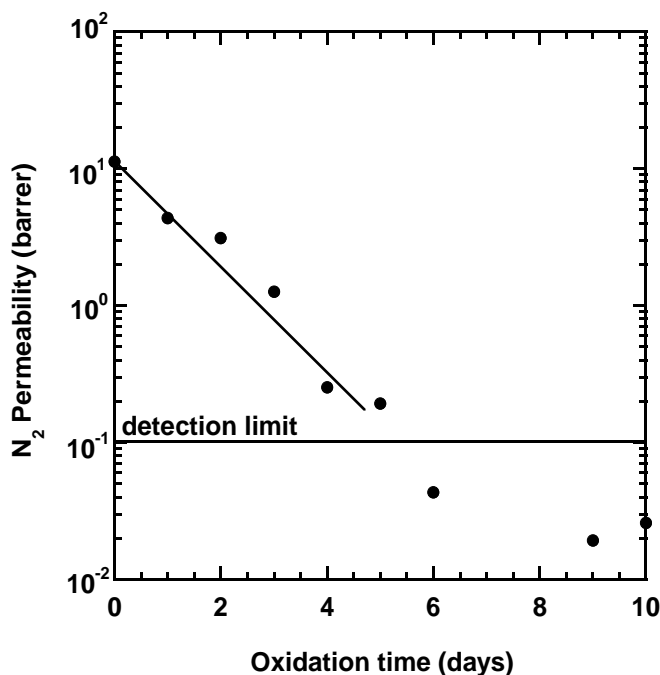
Figure 5.11   Nitrogen permeability of 1,4-polybutadiene films containing 200 ppm of
cobalt neodecanoate. Films were oxidized in air for various lengths of time,
and the N_2 permeability coefficients were measured at 35ºC. The film
thickness was 108 μm.

Since the oxygen permeability changed constantly during testing, we performed

nitrogen permeability experiments on the 1,4-polybutadiene films; the permeation

coefficients of films oxidized for various times are presented in Figure 5.11. In this case,

the metal-catalyzed 1,4-polybutadiene films were oxidized in air, using the protocol

described earlier, for a pre-determined time, then loaded into a permeation cell for N_2 permeability measurements. During measurement, the permeation cell was either under vacuum (for leak tests) or filled with pure nitrogen (for permeation tests), so that the extent of the film's oxidation should be the same before and after measurement. However, if the films were oxidized in air for more than 5 days, the nitrogen permeability would be lower than the detection limit.

If the two phase model showed in Figure 5.5 is right, then the permeability in a thick film can be estimated using the series resistance model. The permeability of a layered film system can be expressed using the permeability of individual layers and thickness of each layer in that film[51]. For a film that has the layered structure showed in Figure 5.5, the permeability of the entire film is given by:

$$\frac{L}{P_{comp}} = \frac{2L_c}{P_o} + \frac{L_{no}}{P_{no}} \tag{5.7}$$

where P_{comp}, P_o and P_{no} are the permeability coefficients of the entire film, the oxidized layer, and the non-oxidized layer, respectively; L, L_c and L_{no} are the thicknesses of the entire film, the critical oxidized layer, and the non-oxidized layer.

Consequently, the permeability of the entire film, P_{comp}, can be expressed as:

$$P_{comp} = \frac{P_o \times (2L_c + L_{no})}{2L_o + \frac{P_o}{P_{no}} \times L_{no}} \tag{5.8}$$

In this case, if the permeability of the oxidized layer is much smaller than the permeability of non-oxidized material (i.e., the permeability of pure 1,4-polybutadiene),

and the thicknesses of the oxidized and the non-oxidized layers are similar, then

$\dfrac{P_o}{P_{no}} L_{no} \ll L_c$, and the equation can be simplified to:

$$P_{comp} = \frac{P_o \times (2L_c + L_{no})}{2L_c} = P_o \times (1 + \frac{L_{no}}{2L_c}) \tag{5.9}$$

The permeability of the entire film will be very similar to that of the oxidized layer. Thus, measuring the permeability of the oxidized material is useful in determining the permeability change in 1,4-polybutadiene films due to oxidation.

Since the oxidized 1,4-polybutadiene has much lower gas permeability than that of the unoxidized polymer, the flux though an oxidized film at the same upstream pressure will be very small, and the downstream pressure change will be hard to detect. To circumvent this issue, we made permeability measurements in thin films. Initially, we measured nitrogen permeability of thin films and compared the results with permeability of a 115 µm thick 1,4-polybutadiene film. The results are shown in Figure 5.12. The thin films are 1.7 µm and 3.1 µm thick, respectively. Both oxygen and nitrogen permeability were measured at low feed pressure (below 3 atm) to accommodate the film's fragility.
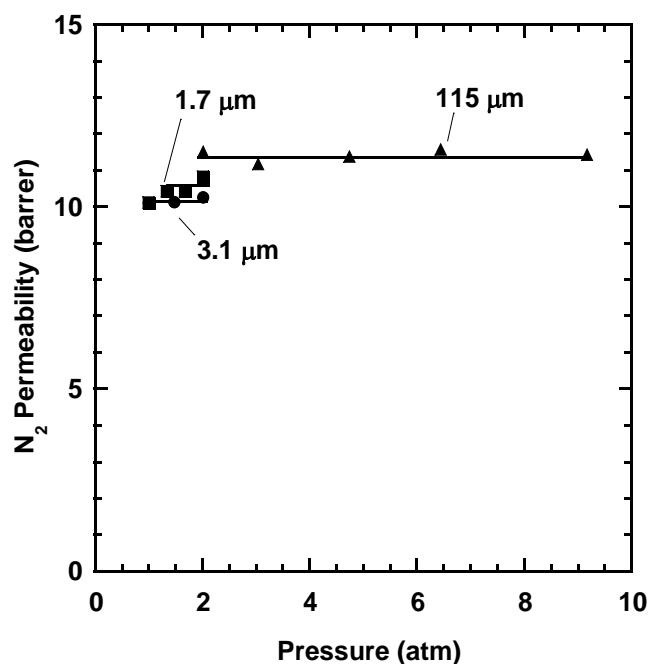
Figure 5.12   Nitrogen permeability at 35°C in unoxidized 1,4-polybutadiene films of different thicknesses.

As Figure 5.12 shows, the permeabilities of thin films and thick films are close but not identical.   One possible cause may arise from our thickness measurement techniques. In thick film measurements, a cover glass was applied to both sides of the films, providing sufficient support to prevent changes in polymer thickness under pressure from the tip of the measuring instrument.   However, when using the profilometer, only one side of the film was supported by a silicon wafer.   The profilometer tip scanned from the unsupported side to collect film thickness data. Even though the force applied on the tip is very small, it could still cause deformation because unoxidized 1,4-polybutadiene films are very soft. The measured thickness would thus be

slightly smaller than the actual thickness, which would explain the apparent permeability

coefficients in the thin films being slightly lower than those in thicker films.
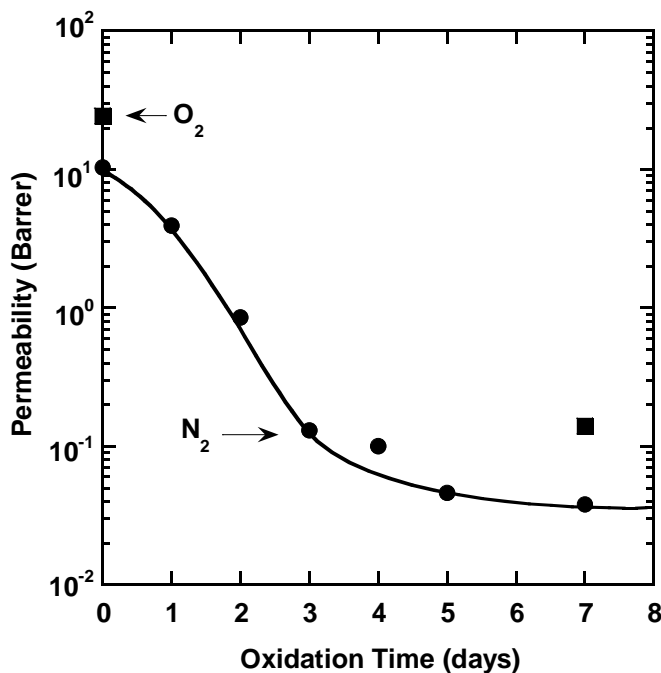
Figure 5.13   Influence of oxidation time on nitrogen (●) and oxygen (■) permeability
in spin-coated 1,4-polybutadiene thin films.   The film thickness was
around 3 μm. The permeability measurements were conducted at 35ºC.

To measure nitrogen permeability change during oxidation, films were oxidized

in air for a certain period, then loaded into the permeation system for measurement.

Oxygen permeability was obtained only for unoxidized and fully oxidized (i.e., once

oxygen mass uptake did not increase with time) films because oxygen permeability

changes during the measurement otherwise. Permeability data are presented as a function

of oxidation time in Figure 5.13. After two days of oxidization, the nitrogen permeability

in the thin film decreased by one order of magnitude, and it decreased by another order of magnitude after 4 days.

Since the permeability coefficient of oxygen and nitrogen in fully oxidized and unoxidized 1,4-polybutadiene were obtained in Figure 13, and the oxidized layer thickness (28 µm) was obtained from Figure 5.4, the permeability in an oxidized thick films having a two-phase structure can be estimated using Equation (5.8) or (5.9). The thickness of films used in Figure 5.10 (200 ppm sample) and Figure 5.11 were used in the model, and the estimated P_{comp} were presented in Table 5.3. The estimated P_{comp} and the measured permeability $P_{measure}$ in oxidized films were in the same range, showing the heterogeneous oxidation hypothesis provides a reasonable explanation of the permeability decrease in thick films.

Table 5.3   Calculation of P_{comp} of films in Figures 5.10 and 5.11 using Equations (5.8) and (5.9). Oxidized layer thicknesses (28 µm) was estimated from Figure 5.4. P_o and P_{no} of oxygen and nitrogen were obtained from Figure 5.13.

	L (µm)	L_c (µm)	L_{no} (µm)	P_o (barrer)	P_{no} (barrer)	P_{comp} (barrer)*	$P_{measure}$ (barrer)
Oxygen (Figure 5.10)	125	28	69	0.14	24.3	0.31	0.42
Nitrogen (Figure 5.11)	108	28	52	0.038	10.3	0.073	0.025**

* Both Equations (5.8) and (5.9) lead to the same P_{comp} value.
** This value is already below the detection limit of permeation system, which is about 0.1 barrer.

5.3 Conclusions

In cobalt-catalyzed 1,4-polybutadiene, auto-oxidation in air exhibits a period of acceleration and then slows down. The reduction of the oxidation rate can be attributed to two concomitant causes: a decreasing number of reactive sites in the substrate, and the diffusion limitation of oxidation in the film. Oxidation is homogeneous in thin films and heterogeneous if the film is thick enough (i.e. more than two times the critical oxidized layer thickness, which was determined to be about 28 µm at the conditions considered in this study). The oxygen uptake data were well described by a simple two-phase model that restricts oxidation to only the film surfaces and only allows oxidation to a depth equal to the critical thickness. Nitrogen permeability in 1,4-polybutadiene decreases more than two orders of magnitude, from 10 barrer in an unoxidized film to 0.04 barrer in a fully oxidized film. Similar oxygen permeability changes were observed before and after oxidization of 1,4-polybutadiene films, which makes the oxidized film a much better barrier material. The permeability coefficients for oxygen and nitrogen in unoxidized and fully oxidized thin films were used, with the two-phase model, to estimate permeability in a thick film, and the results were similar to the experimental value obtained from the permeation experiment. The existence of oxidized layers which protect a relatively unoxidized core from further oxidation suggests that the use of thin layers of polybutadiene might provide efficient use of the polymer in oxygen scavenging packaging applications.

5.4   References

1. M. L. Rooney. Active packaging in polymer films. In: Rooney M. L., editor. Active food packaging, vol. 4. Blackie Academic & Professional, London, 1995, 74-110.

2. W. J. Koros. Barrier polymers and structures: overview. In: Koros W. J., editor. Barrier Polymers and Structures. American Chemical Society, Washington, DC, 1990, 1-22.

3. J. Wise, K. T. Gillen, and R. L. Clough. Quantitative model for the time development of diffusion-limited oxidation profiles. *Polymer*, **1997**, 38(8), 1929-1944.

4. R. L. Clough and K. T. Gillen. Oxygen diffusion effects in thermally aged elastomers. *Polymer Degradation and Stability*, **1992**, 38(1), 47-56.

5. R. G. Bauman and S. H. Maron. Oxidation of polybutadiene. I. Rate of oxidation. *Journal of Polymer Science*, **1956**, 22, 1-12.

6. S. W. Bigger and O. Delatycki. New approach to the measurement of polymer photooxidation. *Journal of Polymer Science Part A: Polymer Chemistry*, **1987**, 25(12), 3311-3323.

7. M. Coquillat, J. Verdu, X. Colin, L. Audouin, and R. Neviere. Thermal oxidation of polybutadiene. Part 1: Effect of temperature, oxygen pressure and sample thickness on the thermal oxidation of hydroxyl-terminated polybutadiene. *Polymer Degradation and Stability*, **2007**, 92(7), 1326-1333.

8. S. P. Fairgrieve and J. R. MacCallum. Diffusion-controlled oxidation of polymers: A mathematical model. *Polymer Degradation and Stability*, **1985**, 11(3), 251-265.

9. S. G. Kiryushkin and Y. A. Shlyapnikov. Diffusion-controlled polymer oxidation. *Polymer Degradation and Stability*, **1989**, 23(2), 185-192.

10. M. Menard and R. W. Paynter. Fick's law of diffusion depth profiles applied to the degradation of oxidized polystyrene during ARXPS analysis. *Surface and Interface Analysis*, **2005**, 37(5), 466-471.

11. T. Shimotori, E. L. Cussler, and W. A. Arnold. Diffusion of mobile products in reactive barrier membranes. *Journal of Membrane Science*, **2007**, 291(1-2), 111-119.

12. C. Sinturel and N. C. Billingham. A theoretical model for diffusion-limited oxidation applied to oxidation profiles monitored by chemiluminescence in hydroxy-terminated polybutadiene. *Polymer International*, **2000**, 49(9), 937-942.

13. S. E. Solovyov. Theory of transient permeation through reactive barrier films I. Steady state theory for homogeneous passive and reactive media. *International Journal of Polymeric Materials*, **2005**, 54, 71-91.

14. S. E. Solovyov. Theory of transient permeation through reactive barrier films II. Two layer reactive passive structures with dynamic interface. *International Journal of Polymeric Materials*, **2005**, 54, 93-115.

15. S. E. Solovyov. Theory of transient permeation through reactive barrier films III. Solute ingress dynamics and model lag times. *International Journal of Polymeric Materials*, **2005**, 54, 117-139.

16. S. Carranza, D. R. Paul, and R. T. Bonnecaze. Design formulae for reactive barrier membranes. *Chemical Engineering Science*, **2010**, 65(3), 1151-1158.

17. S. Carranza, D. R. Paul, and R. T. Bonnecaze. Analytic formulae for the design of reactive polymer blend barrier materials. *Journal of Membrane Science*, Submitted.

18. N. Nagai, T. Matsunobe, and T. Imai. Infrared analysis of depth profiles in UV-photochemical degradation of polymers. *Polymer Degradation and Stability*, **2005**, 88(2), 224-233.

19. D. J. Nagle, M. Celina, L. Rintoul, and P. M. Fredericks. Infrared microspectroscopic study of the thermo-oxidative degradation of hydroxy-terminated polybutadiene/isophorone diisocyanate polyurethane rubber. *Polymer Degradation and Stability*, **2007**, 92(8), 1446-1454.

20. L. Audouin and J. Verdu. Change in mechanical properties of low-density polyethylene during radiochemical aging. *ACS Symposium Series*, **1991**, 475, 473-484.

21. P. J. Cahill and S. Y. Chen. Oxygen scavenging condensation copolymers for bottle and packaging articles. U. S. Patent, 6,509,436, **2003**

22. D. V. Speer, C. R. Morgan, W. P. Roberts, and R. K. Ramesh. Compositions, articles and methods for scavenging oxygen which have improved physical properties. U. S. Patent, 5,399,289, **1995**

23. D. V. Speer and W. P. Roberts. Oxygen scavenging compositions for low temperature use. U. S. Patent, 5,310,497, **1993**

24. D. V. Speer, W. P. Roberts, and C. R. Morgan. Method and compositions for oxygen scavenging. U. S. Patent, 5,211,875, **1993**

25. J. M. Tibbitt, G. E. Rotter, D. P. Sinclair, G. T. Brooks, and R. T. Behrends. Oxygen scavenging monolayer bottles. United States Patent Application Publication, US 2002/0183488, **2002**

26. M. L. Tsai and A. K. Murali. Oxygen scavenging polymer compositions containing ethylene vinyl alcohol copolymers. U. S. Patent, 6,793,994, **2004**

27. H. Li, K. K. Tung, D. R. Paul, and B. D. Freeman. Characterization of oxygen scavenging films based on 1,4-polybutadiene. In preparation.

28. H. Li, D. K. Ashcraft, B. D. Freeman, M. E. Stewart, M. K. Jank, and T. R. Clark. Non-invasive headspace measurement for characterizing oxygen-scavenging in polymers. *Polymer*, **2008**, 49(21), 4541-4545.

29. A. S. Kuzminskii, I. A. Shokhin, and R. M. Belitzkaya. The nature of structural changes of butadiene rubbers caused by high temperatures (100-200°C). *Rubber Chemistry and Technology*, **1952**, 25, 33-35.

30. G. J. Armerongen. Influence of structure of elastomers on their permeability to gases. *Journal of Polymer Science*, **1950**, 5(3), 307-332.

31. H. J. Bixler and O. J. Sweeting. Barrier properties of polymer films. In: Bixler H. J. and Sweeting O. J., editors. Science and Technology of Polymer Films. Wiley-Interscience, New York City, New York, 1971, 1-130.

32. B. Mailhot and J. L. Gardette. Polystyrene photooxidation 2. A pseudo wavelength effect. *Macromolecules*, **1992**, 25(16), 4127-4133.

33. B. Mailhot and J. L. Gardette. Polystyrene photooxidation 1. Identification of the IR-absorbing photoproducts formed at short and long wavelength. *Macromolecules*, **1992**, 25(16), 4119-4126.

34. S. W. Beavan. Mechanistic studies on the photo-oxidation of commercial poly(butadiene). *European Polymer Journal*, **1974**, 10, 593-603.

35.   M. Piton and A. Rivaton. Photooxidation of polybutadiene at long wavelengths (λ>300nm). *Polymer Degradation and Stability*, **1996**, 53(3), 343-359.

36.   R. V. Gemmer and M. A. Golub. Applications of Polymer Spectroscopy Academic Press, New York 1978, 79.

37.   C. Adam, J. Lacoste, and J. Lemaire. Photo-oxidation of elastomeric materials. 1. Photooxidation of polybutadienes. *Polymer Degradation and Stability*, **1989**, 24(3), 185-200.

38.   C. Adam, J. Lacoste, and J. Lemaire. Photo-oxidation of elastomeric materials. 2. Photo-oxidation of styrene-butadiene copolymer. *Polymer Degradation and Stability*, **1989**, 26(3), 269-284.

39.   J. A. Coffman. Highly cross-linked polybutadiene. *Journal of Industrial and Engineering Chemistry*, **1952**, 44, 1421-1428.

40.   J. M. Mohr, D. R. Paul, T. E. Mlsna, and R. J. Lagow. Surface fluorination of composite membranes 1. Transport-properties. *Journal of Membrane Science*, **1991**, 55(1-2), 131-148.

41.   J. M. Mohr, D. R. Paul, Y. Taru, T. E. Mlsna, and R. J. Lagow. Surface fluorination of composite membranes 2. Characterization of the fluorinated layer. *Journal of Membrane Science*, **1991**, 55(1-2), 149-171.

42.   G. Papet, L. Audouin, L. Rackova, and J. Verdu. Diffusion controlled radiochemical oxidation of low-density polyethylene 2. Kinetic modeling. *Radiation Physics and Chemistry*, **1989**, 33(4), 329-335.

43.   C. B. Bucknall and D. G. Street. Fracture behavior of rubber-modified thermophastics after aging. *Journal of Applied Polymer Science*, **1968**, 12(6), 1311-1320.

44.   G. M. Ruhnke and L. F. Biritz. Fast, quantitative method of measuring the natural and artificial aging behavior of ABS material. *Plastics & Polymers*, **1972**, 40(147), 118-124.

45.   R. L. Clough, K. T. Gillen, and C. A. Quintana. Heterogeneous oxidative degradation in irradiated polymers. *Journal of Polymer Science, Polymer Chemistry Edition*, **1985**, 23(2), 359-377.

46. P. So and L. J. Broutman. The effect of surface embrittlement on the mechanical behavior of rubber-modified polymers. *Polymer Engineering and Science*, **1982**, 22(14), 888-894.

47. T. Kanaya, T. Kawaguchi, and K. Kaji. Local dynamics of cis-1, 4-polybutadiene near the glass transition temperature T_g. *Physica B: Condensed Matter*, **1992**, 182(4), 403-408.

48. C. Adam, J. Lacoste, and J. Lemaire. Photooxidation of elastomeric materials. 4. Photooxidation of 1,2-polybutadiene. *Polymer Degradation and Stability*, **1990**, 29(3), 305-320.

49. V. I. Bondar, B. D. Freeman, and I. Pinnau. Gas transport properties of poly(ether-b-amide) segmented block copolymers. *Journal of Polymer Science Part B-Polymer Physics*, **2000**, 38(15), 2051-2062.

50. H. Lin and B. D. Freeman. Permeation and diffusion. In: Czichos H., Smith L. E., and Saito T., editors. Handbook of Materials Measurement Methods. Springer, New York, 2006, 371-387.

51. J. M. S. Henisa and M. K. Tripodi. Composite hollow fiber membranes for gas separation: the resistance model approach. *Journal of Membrane Science*, **1981**, 8(3), 233-246.

Chapter 6: Effect of Oxidation Conditions on Oxygen Scavenging Properties

6.1   Introduction

Oxidation in 1,4-polybutadiene films is a competition between the consumption and replenishment of oxygen in the film[1, 2] (i.e., reacting oxygen with the reactive sites and diffusion of oxygen into the film). Therefore, oxidation can be controlled by the oxidation rate and the diffusion coefficient of oxygen through the polymer[3]. The oxidation conditions can affect either or both of these parameters [1, 4-9].

As discussed in previous chapters, increasing catalyst concentration will increase the reaction rate, with no significant effect on diffusion, while increasing the film thickness will affect only the diffusion of oxygen. However, reaction conditions, such as oxygen partial pressure in the environment surrounding the sample and oxidation temperature, can influence both reaction and diffusion. Consequently, it is important to understand the effects of such conditions on oxygen uptake in scavenging films.

Chapter 4 showed that in purified 1,4-polybutadiene, the oxidation rate and oxygen mass uptake in 1,4-polybutadiene films strongly depend on catalyst concentration. In Chapter 5, the sandwich structure characteristic of heterogeneous oxidation, with an oxidized surface and unoxidized film core regions, was characterized. Oxygen and nitrogen permeability changes during oxidation were also studied. This chapter extends these observations to consider how the oxygen content in the environment surrounding the polymer film and temperature affect the oxidation timescale and oxygen mass uptake

in 1,4-polybutadiene films.

6.2   Results and Discussion

6.2.1   Effect of Reaction Temperature in Thick Films

In general, the reaction rate increases with increasing temperature.   Thus increasing the storage temperature in the oxygen uptake experiment will yield faster oxidation reactions[1].   At higher temperature, the mobility of gas molecules also increases, which means that diffusion of gas penetrants through a polymer film will be faster[10].

In this study, the reaction temperatures considered were -20, 5, 30, and 45ºC. Samples oxidized at 30 ºC and 45 ºC were stored in Mason jars and placed in a controlled temperature chamber equipped with an electric fan and heaters.   Temperature was measured by both a thermocouple and a thermometer.   Samples oxidized at 5ºC were stored in Mason jars in a refrigerator; samples for the -20ºC tests were kept in the freezer of a refrigerator.   These samples were removed from their storage environments only for OxySense® measurements.   Mason jars were stored in the predetermined temperatures for one day, and polymer films were loaded into the jars under the same conditions as for storage to allow samples to reach target temperatures as quickly as possible.   The oxygen uptake data were measured using the OxySense® apparatus.   Figure 6.1 presents the influence of temperature on oxygen mass uptake in 1,4-polybutadiene films containing 200 ppm of cobalt neodecanoate.   The film thickness was around 100 µm in all cases.
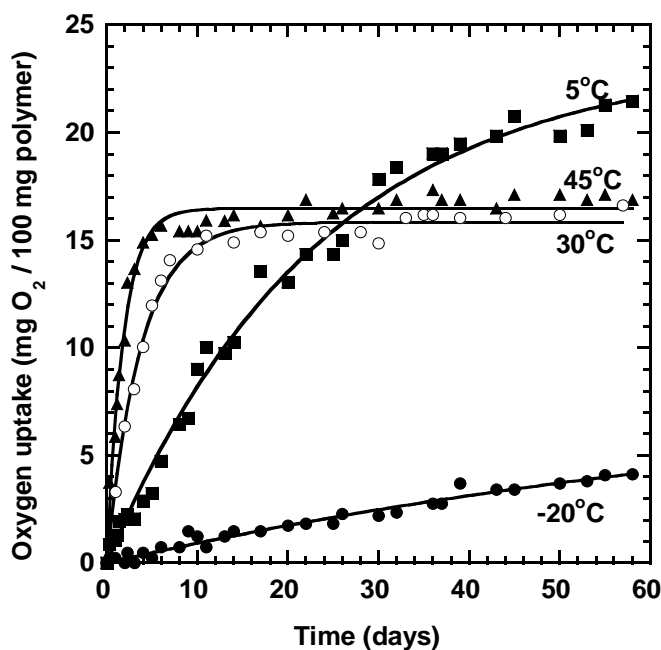
Figure 6.1   Effect of oxidation temperature on oxygen mass uptake in 1,4-polybutadiene films oxidized in air. Samples contained 200 ppm of cobalt neodecanoate. The film thickness was approximately 100 µm. Oxygen mass uptake values were measured using the OxySense® apparatus.

Samples stored at -20ºC exhibited very slow oxygen uptake, even after 60 days. Both the oxidation reaction rate and diffusion of oxygen into the polymer would be low at this temperature, making oxygen mass uptake very slow. The sample stored at 5ºC had a long oxidation process relative to that of the other samples. The oxygen mass uptake increased slowly but steadily, exceeding 20 wt % after 50 days. Samples oxidized at 45ºC exhibited oxidation kinetics and uptake levels similar to those of samples oxidized at 30ºC, but the oxidation period was somewhat shorter (i.e., oxidation was faster) and slightly higher oxygen mass uptake was obtained in the samples oxidized at 45ºC. For 1,4-polybutadiene films oxidized at 30ºC and 45ºC, most of the oxygen mass uptake

115

occurred during the first several days because of the generation of low permeability, highly oxidized surface layers which effectively limits the amount of oxidation that can occur subsequently[4, 11]. The lines through the data in Figure 6.1 represent fits of the oxidation model introduced in Chapter 5. The oxidation timescale and the maximum oxygen mass uptake parameters from this model are recorded in Table 6.1.

Table 6.1 Model parameters m_0 and τ used to describe the experimental data in Figure 6.1

Reaction Temperature (ºC)	45	30	5	-20
m_0 (wt %)	16.5	15.8	23.5	8.6
τ (days)	1.2	3.8	23	88

In Figures 6.2 and 6.3, oxygen mass uptake in films of different thicknesses are reported for samples oxidized at 45ºC and 5ºC. Free standing films were stored in Mason jars at different temperatures. To determine the oxygen mass uptake in the fully oxidized layer, thin films were spin-coated onto silicon wafers, and their oxidation properties were measured. Thin films oxidized at 45ºC were measured using an analytical balance. For thin films oxidized at 5ºC, the temperature difference between the storage and measuring conditions caused small water droplets to form on the films during measurement, so the oxygen uptake was verified using the OxySense® apparatus. The silicon wafers were cut into pieces smaller than 5cm^2 and stored in Mason jars for the OxySense® test. The volume of the silicon wafers was subtracted from that of the Mason jar for the mass uptake calculations.
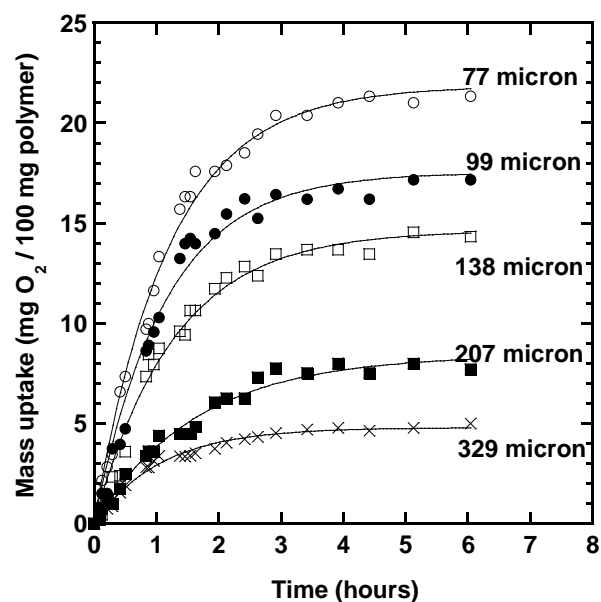
(A)
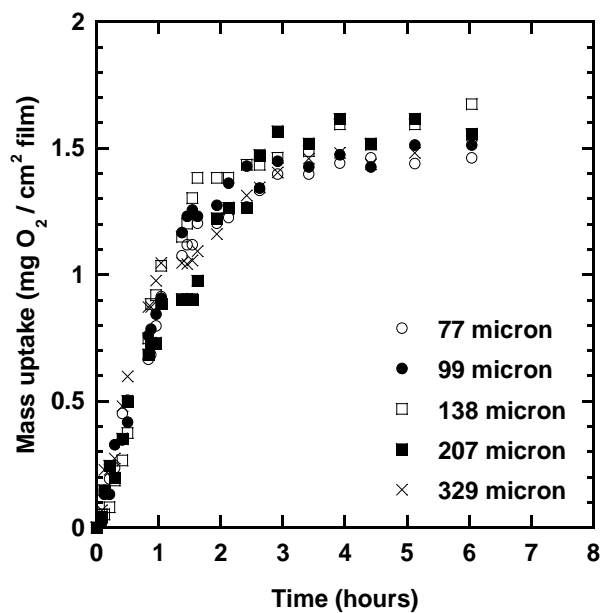
(B)

Figure 6.2   Oxygen mass uptake in films containing 200 ppm of cobalt and oxidized at 45ºC in air. Oxygen mass uptake values were normalized by: (A) polymer mass and (B) polymer film area.
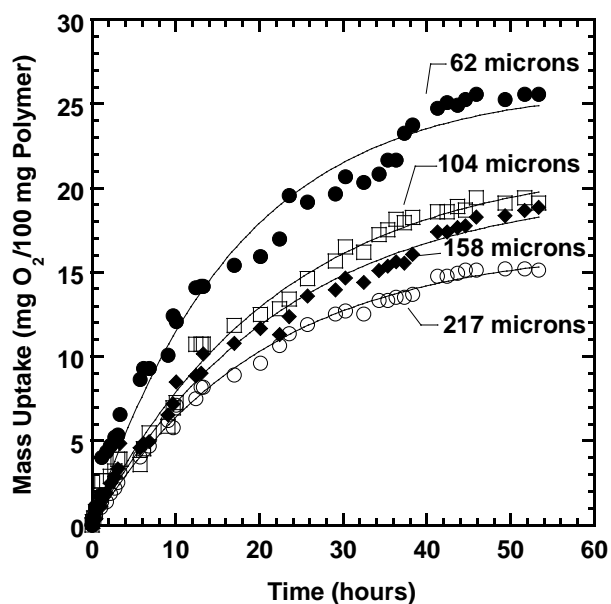
(A)
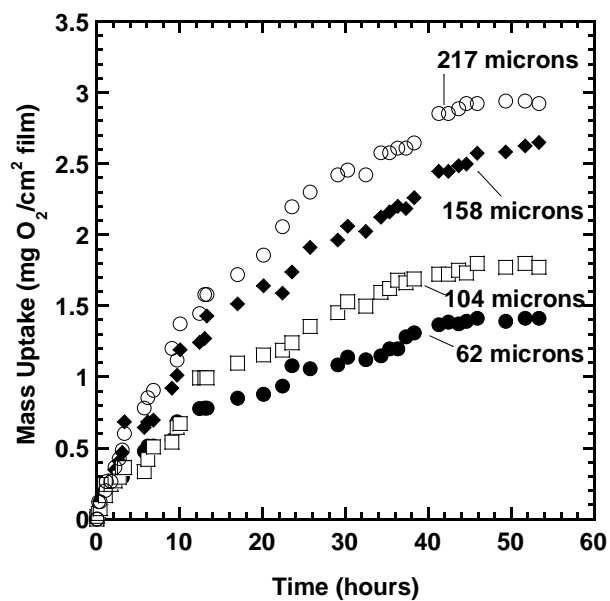
(B)

Figure 6.3   Oxygen mass uptake in films containing 200 ppm of cobalt, and oxidized at 5°C in air. Oxygen mass uptake values were normalized by: (A) polymer mass and (B) polymer film area.

118

Figure 6.2 shows that oxygen mass uptake per unit polymer mass increases as film thickness decreases. When oxygen uptake was normalized by film area (rather than mass), all films had similar oxygen uptake values, around 1.5 mg O_2/100 cm^2 polymer. As shown in Figure 5.1, this value is very similar to the value obtained for samples oxidized at 30ºC, which was about 1.3 mg O_2/100 cm^2 polymer. In each case, the oxidation time scale, τ, is slightly more than 1 day, which is shorter than that for films oxidized at 30ºC (around 4 days)[12].

Table 6.2 Model parameters m_0 and τ used to describe the experimental data in Figures 6.2 and 6.3

oxidized at 45ºC					
Film Thickness (µm)	77	99	138	207	329
m_0 (wt %)	21.8	17.5	14.6	8.41	4.79
τ (days)	1.20	1.14	1.28	1.24	1.07

oxidized at 5ºC				
Film Thickness (µm)	62	104	158	217
m_0 (wt %)	26.1	21.7	20.2	16.6
τ (days)	17.2	20.2	22.6	20.5

The final oxygen uptake, m_0, and the oxidation timescale in PB films oxidized at 45ºC and 5ºC are presented in Table 6.2. In samples oxidized at 5ºC, the oxygen mass

uptake per unit polymer mass had higher m_0 values in thinner films. However, in Figure 6.3(B), the curves for oxygen uptake normalized by film area did not collapse to a single curve, as they did in the 30 and 45ºC cases. Therefore, the oxidation kinetics are somewhat different in this case. As discussed previously, if the polymer film is homogeneously oxidized, oxygen mass uptake per unit polymer mass would be independent of film thickness. On the other hand, heterogeneous oxidation (i.e., the two-phase model discussed earlier) would lead to oxygen uptake per unit film area being independent of film thickness as long as the thickness was greater than twice the critical oxidized layer thickness. In Figure 6.3(A), as thickness decreases, oxygen mass uptake per unit mass decreases, suggesting that oxidation is not completely homogeneous. As shown in Figure 6.3(B), when oxygen uptake is normalized by film area, oxygen mass uptake decreases as thickness decreases, suggesting that oxidation is not completely heterogeneous either. Therefore, oxidation in 1,4-polybutadiene films at 5ºC is not simply homogeneous or heterogeneous but may be intermediate between these extremes.

The oxidization in thicker films at 45ºC is analogous to that in films oxidized at 30ºC. That is, the oxygen absorption curves normalized per unit area of polymer overlap, as shown in Figure 6.2(B). The oxidation curves of films oxidized at 5ºC did not overlap, as shown in Figure 6.3, when normalized either by polymer mass or film surface area. In the thick films oxidized at 5ºC, the oxygen uptake values per unit mass of polymer decrease as film thickness increases, but the oxygen uptake per unit area increases as film thickness increases. The oxygen uptake values for samples oxidized at 5ºC are much higher than those of films oxidized at 30 or 45ºC. For example, the oxygen uptake value

120

in a 217 µm thick film oxidized at 5ºC is around 3 mg of oxygen per cm^2 of PB, which is about 2 times higher than the values obtained in films of about the same thickness that were oxidized at 30 or 45ºC (1.3 and 1.5 mg/cm^2 PB, respectively).

As discussed earlier, more rapid oxidization due to higher catalyst loading may lead to a thinner oxidized layer and reduce the oxygen mass uptake in the polymer film. However, this does not happen when the higher oxidation rate is caused by higher oxidation temperature, e.g., 45ºC. The oxygen mass uptake values, normalized either by unit polymer mass or by unit polymer area, are similar to the oxygen uptake in films oxidized at 30ºC. Increased temperature not only enhances the oxidation reaction rate that helps to generate the oxidized layer faster, but also enhances gas permeability in polymers. Celina[7] studied oxygen permeability of elastomers at various temperatures. Over the range from 25 to 65ºC; oxygen permeability increased more than one order of magnitude in black Viton rubber, and about a factor of 5 in neoprene (polychloroprene).

Figure 6.4 presents SEM images of the cross sections of films oxidized at 45 and 5ºC. As with the films oxidized at 30ºC, an oxidized surface layer can be observed in films oxidized at 45ºC. The layer thickness is around 50 µm—thicker than that shown in Figure 5.5, which is about 40 µm. However, the cross section structure is different in samples oxidized at 5ºC.
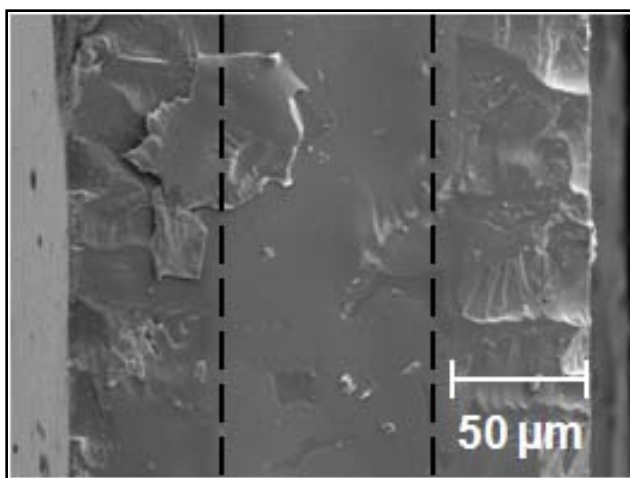
(A)
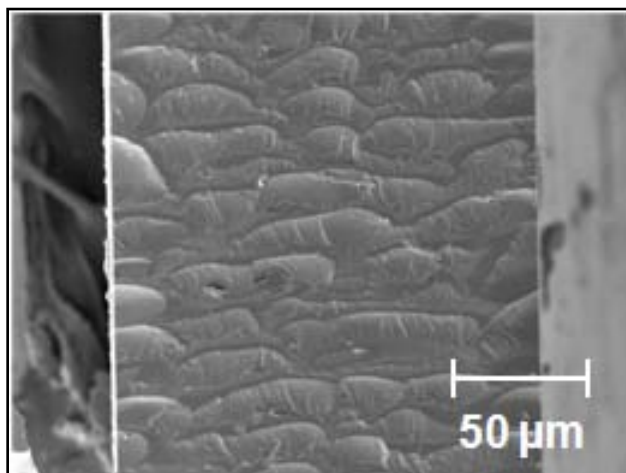
(B)

Figure 6.4   SEM images of cross section of oxidized 1,4-polybutadiene films. Films were doped with 200 ppm of cobalt neodecanoate and oxidized in air at (A) 45ºC, and (B) 5ºC for 60 days. Both samples were microtomed at -125ºC using a diamond knife.

Unlike the other films, the SEM images of films oxidized at 5ºC did not show a layered cross section.   Figure 6.4(B) appears to show a more or less homogeneous structure throughout the thickness of the film, with a scalloped texture, which was

typically observed in highly oxidized surface layers such as that shown in Figure 6.4(A). Because the film thickness is 150 µm in Figure 6.4(B), the critical thickness must be greater than 75 µm.

Even though the scalloped structure extends throughout the cross session, the film may not be completely homogeneously oxidized. In Figure 6.3 the oxygen uptake curves did not overlap in either figure. If oxidation was exactly homogeneous, the data in Figure 6.3 (A) should overlap. On the contrary, if completely heterogeneous oxidation occurs, the data in Figure 6.3 (B) should overlap. However, neither of these limits was observed. The oxidization in samples oxidized at 5ºC may be approximately homogeneous at the early stages of oxidation, and heterogeneous after the oxidation has proceeded for a considerable period of time, long enough for the oxygen permeability to decreases significantly. Because the complete oxidation process is most likely a mixture of homogeneous and heterogeneous oxidation, the oxygen mass uptake curves follow neither homogenous nor heterogeneous oxidation. For this reason, the oxygen uptake per unit mass of polymer at 5ºC is higher than those in films oxidized at higher temperatures, but somewhat lower than the oxygen uptake in spin-coated thin films oxidized at 5ºC, as will be shown below.
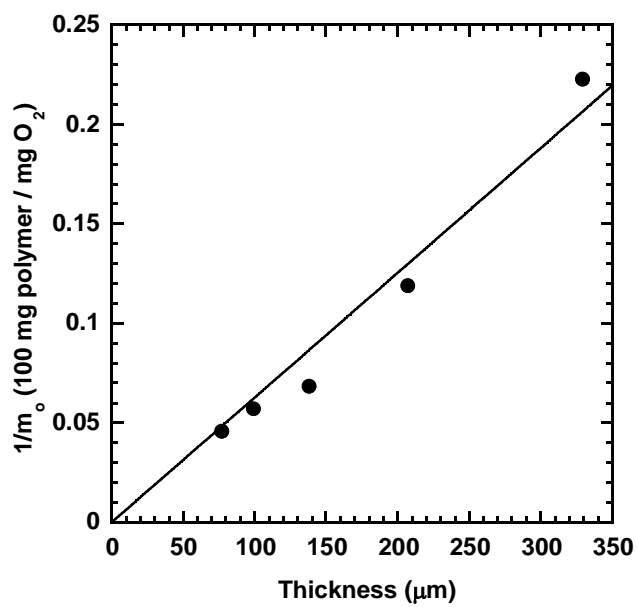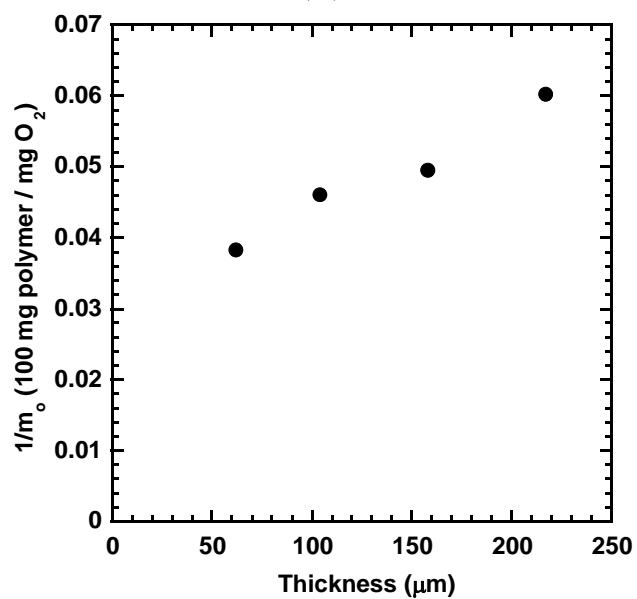
Figure 6.5   Effect of film thickness on reciprocal of final oxygen mass uptake, m_0. Films were oxidized at (A) 45°C and (B) 5°C. The best fit line in (A) is based on Equation (5.6), where the slope of the line is equal to $\dfrac{1}{2L_c \cdot m_{o_{max}}}$.

The L_c value estimated from this slope is about 29 µm. The least squares line in (B) did not pass through (0,0) so it did not fit the model.

The method suggested in Chapter 5, based on Equation (5.6), was also used to estimate the critical layer thickness. The data for samples oxidized at 45ºC (c.f. Figure 6.5(A)) were well described by this model. The oxidized layer thickness, based on the slope and the oxygen uptake in fully oxidized thin films, is about 29 µm. However, as shown in Figure 6.5(B), the mass uptake obtained from films oxidized at 5ºC did not fit the model, probably because oxidation was more homogeneous in this sample.

6.2.2   *Effect of Reaction Temperature in Thin Films*

To further study the influence of reaction temperature on oxygen mass uptake and oxidation, oxygen uptake experiments were conducted using spin coated thin films. The oxygen uptake curves of thin films oxidized at 45ºC and 5ºC are presented in Figures 6.6 (A) and (B). Spin coated films were prepared at three thicknesses for each temperature. Samples oxidized at 45ºC had an oxidation timescale in the range of half a day; the final mass uptakes were around 35 wt % in each sample. PB films oxidized at 5ºC had a much longer oxidation timescale, and the oxygen mass uptake was slightly lower, a little less than 30 wt % after 60 days. The final oxygen uptake and oxidation time scale of thin films oxidized at different temperatures are shown in Table 6.3. Compared with thick films oxidized at sample temperature, thin films oxidized at 45ºC showed a much higher oxygen mass uptake, while thin films oxidized at 5ºC also showed higher oxygen uptake but the difference is much smaller than samples oxidized at 45ºC. This also demonstrates that the oxidation in thick films oxidized at 5ºC would be more homogeneous than any other samples that we measured before.
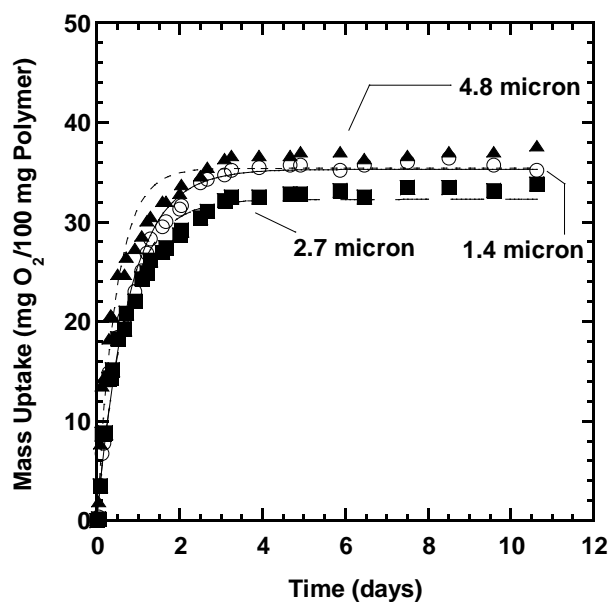
(A)
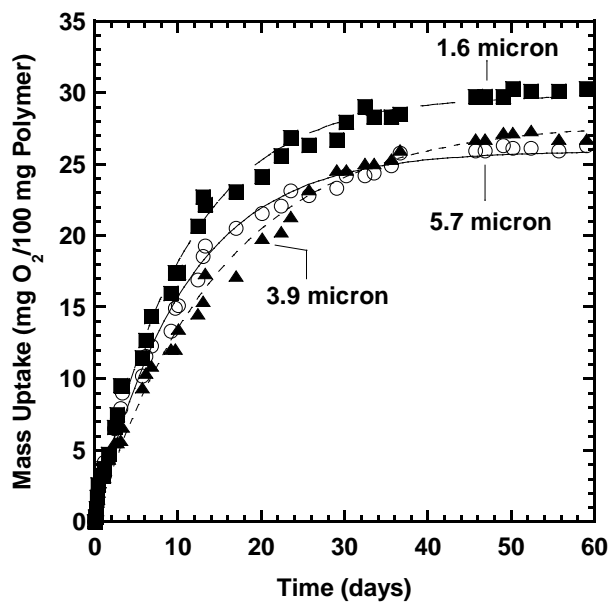
(B)

Figure 6.6   Oxygen mass uptakes in thin films containing 200 ppm of cobalt and oxidized at (A) 45ºC. and (B) 5ºC

Table 6.3   Model parameters used to describe the experimental data in Figure 6.6

Oxidized at 45ºC			
Film Thickness (µm)	1.4	2.7	4.8
m_0 (wt %)	35.3	32.3	35.4
τ (days)	0.67	0.69	0.57

Oxidized at 5ºC			
Film Thickness (µm)	1.6	3.9	5.7
m_0 (wt %)	25.9	29.8	27.9
τ (days)	13.7	12.7	16.1

Since the films were very thin, the effect of oxygen diffusion on oxygen uptake was minimized in these films, because the oxygen in these films would reach steady state practically instantly.   The difference in oxidation timescale of thin films oxidized at different temperatures is expected to be caused by the different reaction rate.   The oxidation timescale, τ, in thin films oxidized at 45ºC, is only half of the τ values of thin films oxidized at 30ºC, as shown in Table 5.2. The τ values of thin films oxidized at 5ºC is about 10 times longer than those of films oxidized at 30ºC.

The different oxidation temperatures also lead to changes in oxygen uptake in highly oxidized thin films. Based on the m_0 values listed in Tables 5.2 and 6.3, the oxygen uptake values slightly increased as oxidation temperature increased. Although increasing reaction temperature would not lead to big differences in oxidation product species, the oxidation at different temperatures might shift the mixture of oxidation

products[8].   For example, increasing oxidation temperature could lead to more carboxylic acid structures formed during oxidation[8].

6.2.3   Effect of Oxygen Content in Environment

Chapter 5 showed that higher oxygen feed pressure leads to more rapid permeability decreases with time in 1,4-polybutadiene films during oxidation.   Films oxidized in air required 5-7 days to reach full oxidation, while the oxidation time in a permeation cell with 3 atm of oxygen was only 10 hours.

Environmental oxygen mole fraction was controlled in this experiment.   Free-standing films were prepared by solution casting, as described earlier.   Mason[®] jars and film samples were transferred to a glove box pre-filled with a specially ordered gas mixture containing different percentages of O_2 and N_2.   The total pressure inside the glove box was 1 atm, as measured by a pressure gauge.   Samples were stored in Mason[®] jars in the glove box, so the original oxygen content in these sealed jars was equal to the oxygen content in the glove box.   Oxygen uptake data were obtained using the OxySense[®] system.   Oxygen mass uptake results for films oxidized at different oxygen partial pressures are prsented in Figure 6.7.
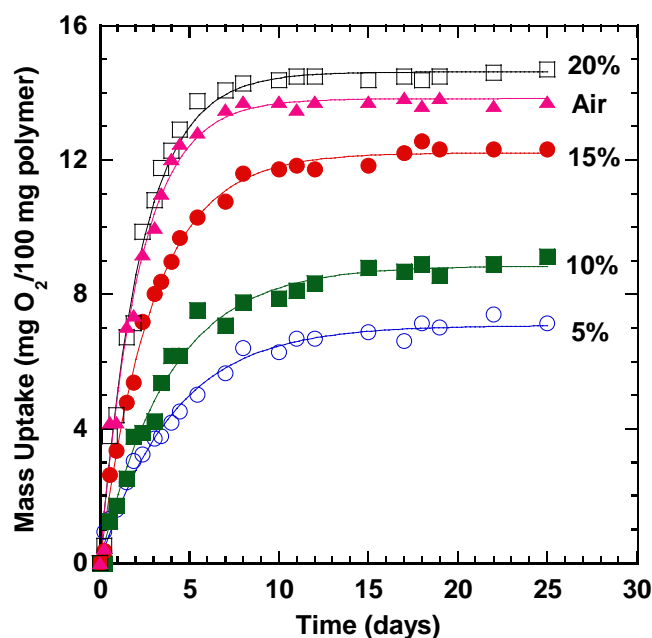
Figure 6.7   Oxygen mass uptake curves of films oxidized in environments containing different oxygen mole fractions at a total pressure of 1 atm. Films were doped with 200 ppm of cobalt neodecanoate and oxidized at 30ºC. Film thicknesses were around 120 µm. Oxygen uptake values were calculated from data obtained by the OxySense® apparatus. The curves represent least squares fits of Equation (5.2) to the data.

The model parameters for the data presented in Figure 6.7 are presented in Figure 6.8. As oxygen content in the surrounding environment increases, the oxygen uptake by the PB film increases. Similar behavior was reported in diffusion-controlled polymer oxidation[13], and it is reported that L_c increases as oxygen content in the surrounding environment increases[14]. In thermally oxidized 1,4-polybutadiene, there is a critical partial pressure of oxygen above which the oxidation kinetics are almost independent of oxygen partial pressure[1]. However, this behavior was not observed in this research. The oxidization timescale, τ, decreases as oxygen content in the surrounding environment

increases, indicating a faster oxidation occurs. For packaging applications, the oxygen partial pressure is usually at a low level, which may far from the critical pressure level that reported in literature (about 5MPa in the thermal oxidation study).
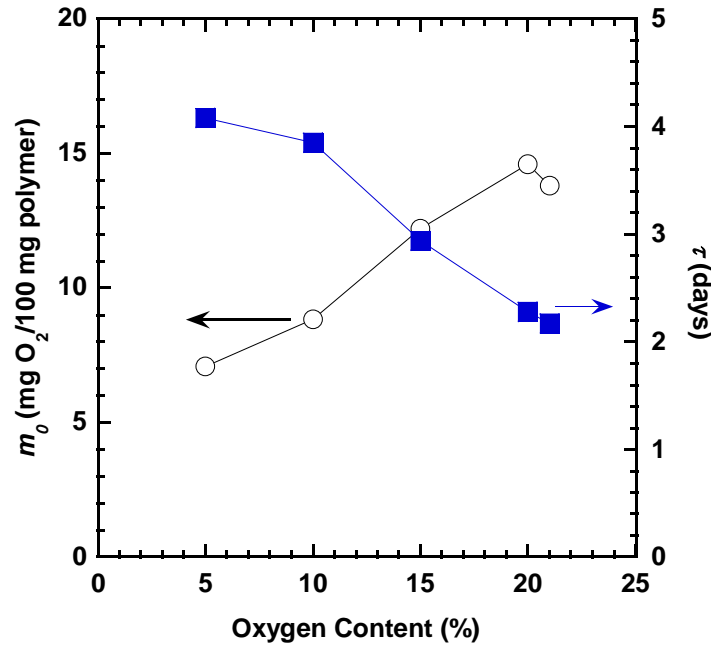
Figure 6.8   Model parameters m_0 (○) and τ (■) used to describe the experimental data in Figure 6.7

6.3   Conclusions

This chapter describes the oxygen scavenging properties of 1,4-polybutadiene oxidized at different temperatures and oxygen partial pressures. Polybutadiene films were oxidized at 45ºC, 30ºC, 5ºC and -20ºC, and experimental results showed different oxidation kinetics and final oxygen uptake values. Compared with samples oxidized at 30ºC, samples oxidized at 45ºC had a similar oxygen uptake but faster oxidation rate.

The two-phase model was still suitable for describing the observed oxidation behavior at 45ºC, showing the formation of a highly oxidized layer. However, this model could not fit the oxidation data at 5ºC. The oxidation in films at 5ºC was more homogeneous; the oxidation timescale was much longer and oxygen uptakes in thick films were higher than those in films oxidized at 30 or 45ºC. The reaction conditions for oxygen partial pressure variation were limited so that the oxygen mole fraction was lower than 21% (and total pressure was maintained at 1 atmosphere). Under these circumstances, increasing oxygen partial pressure leads to faster oxidation and higher oxygen uptake.

6.4   References

1.   M. Coquillat, J. Verdu, X. Colin, L. Audouin, and R. Neviere. Thermal oxidation of polybutadiene. Part 1: Effect of temperature, oxygen pressure and sample thickness on the thermal oxidation of hydroxyl-terminated polybutadiene. *Polymer Degradation and Stability*, **2007**, 92(7), 1326-1333.

2.   M. C. Ferrari, S. Carranza, R. T. Bonnecaze, K. K. Tung, B. D. Freeman, and D. R. Paul. Modeling of oxygen scavenging for improved barrier behavior: Blend films *Journal of Membrane Science*, **2009**, 329(1-2), 183-192.

3.   R. L. Clough and K. T. Gillen. Oxygen diffusion effects in thermally aged elastomers. *Polymer Degradation and Stability*, **1992**, 38(1), 47-56.

4.   C. Adam, J. Lacoste, and J. Lemaire. Photo-oxidation of elastomeric materials. 1. Photooxidation of polybutadienes. *Polymer Degradation and Stability*, **1989**, 24(3), 185-200.

5.   C. Adam, J. Lacoste, and J. Lemaire. Photo-oxidation of elastomeric materials. 2. Photo-oxidation of styrene-butadiene copolymer. *Polymer Degradation and Stability*, **1989**, 26(3), 269-284.

6.   C. Adam, J. Lacoste, and J. Lemaire. Photooxidation of elastomeric materials. 4. Photooxidation of 1,2-polybutadiene. *Polymer Degradation and Stability*, **1990**, 29(3), 305-320.

7.   M. Celina and K. T. Gillen. Oxygen permeability measurements on elastomers at temperatures up to 225 degrees C. *Macromolecules*, **2005**, 38(7), 2754-2763.

8.   M. Piton and A. Rivaton. Photooxidation of polybutadiene at long wavelengths (λ>300nm). *Polymer Degradation and Stability*, **1996**, 53(3), 343-359.

9.   M. Piton and A. Rivaton. Photo-oxidation of ABS at long wavelengths (λ>300 nm). *Polymer Degradation and Stability*, **1997**, 55(2), 147-157.

10.   H. Lin and B. D. Freeman. Gas solubility, diffusity and permeability in poly(ethylene oxide). *Journal of Membrane Science*, **2004**, 239, 105-117.

11.   R. G. Bauman and S. H. Maron. The oxidation of polybutadiene. II. Property changes during oxidation. *Journal of Polymer Science*, **1956**, 22, 203-212.

12.   H. Li, K. K. Tung, D. R. Paul, and B. D. Freeman. Effect of thickness on auto-oxidation in cobalt-catalyzed 1,4-polybutadiene films. In preparation.

13.   S. G. Kiryushkin and Y. A. Shlyapnikov. Diffusion-controlled polymer oxidation. *Polymer Degradation and Stability*, **1989**, 23(2), 185-192.

14.   L. Audouin, V. Langlois, J. Verdu, and J. C. M. Debruijn. Role of oxygen diffusion in polymer aging - kinetic and mechanical aspects. *Journal of Materials Science*, **1994**, 29(3), 569-583.

Chapter 7: Gas Permeation Properties of Poly(urethane-urea)s Containing Different Polyethers

7.1   Introduction

Polyurethanes and poly(urethane-urea)s are linear block copolymers composed of flexible and rigid segments[1]. They usually have a micro-phase separated structure due to the incompatibility between the soft and hard segments[2].   The gas transport performance is affected by the concentration as well as the chemical structures of the hard and soft segments.[3-5]. Generally, gas permeability of polyurethane membranes increases as polyether diol molecular weight increases (i.e., as soft segment content increases)[5]. The effect of hard-segment content on gas separation properties has also been explored[6].

Gas separation using polymeric membranes has attracted significant interest in recent decades because it can be more energy-efficient than other separation techniques[7-9]. Among gas separation applications, interest has increased in membranes for CO_2 gas separation due to the wide variety of potential applications[10], such as CO_2/H_2 separation in synthesis gas purification, CO_2/N_2 in carbon capture, CO_2/CH_4 in natural gas purification, CO_2/O_2 in food packaging, etc.[10-12]. Poly(ethylene oxide) (PEO) has been identified as having interesting gas separation properties, particularly for polar, quadrupolar, or acid gas (*e.g.,* CO_2, H_2S) removal from non-polar gases (*e.g.,* H_2, N_2, and CH_4)[10-12].   The polar ether oxygen in PEO interacts favorably with CO_2 molecules, which contributes to high selectivity towards CO_2 by membranes comprising

PEO[10]. Based on these composite characteristics, PEO has been used in many material platforms for CO_2-based gas separations, such as crosslinked PEO[11, 13-16], Pebax[17-20], PEO-polyester[21, 22], PEO-PI[23, 24] and PEO blends[25].

In many applications of interest, water is also present. However, PEO is water-sensitive, and linear, uncrosslinked PEO is, in fact, water soluble. In preparing membranes for gas separation applications, materials with good humidity resistance and favorable gas separation properties are of interest. In this regard, poly(tetramethylene ether glycol) (Terathane®) and poly(propylene glycol) (PPG) both have ether structures similar to that of PEO and may interact with CO_2, leading to high CO_2 solubility in the polymer. However, they are more hydrophobic than PEO and so may have better stability in humid environments than PEO-based materials. Additionally, the gas transport properties of such materials have been less thoroughly studied than those of PEO-based systems. Therefore, in this study, similar molecular weights of PPG and Terathane® were used as soft segments, and the effect of chemical structure on gas permeability in these poly(urethane-urea)s was studied. Control materials based on PEO were also synthesized for comparison.

7.2 Polymer Synthesis and Film Preparation

Polyether molecular weights were determined prior to synthesis by hydroxyl (OH) group titration using ASTM D 4274-05, Method C[26]. Hydroxyl groups react with excess phthalic anhydride; the unreacted anhydride was back titrated using dilute sodium

hydroxide solution. The isocyanate content in monomers and prepolymers was determined using ASTM D 5155-01, Method B[27]. Isocyanate groups react with excess dibutyl amine, and the unreated amine was back titrated using dilute hydrochloric acid.

The basis scheme of the polymer synthesis is presented in Figure 7.1. 20.21 grams (0.010 mol) of Terathane® 2000 and 120 ml of *N,N*-dimethylacetamide (DMAc) were charged to a 500 ml three-necked flask equipped with mechanical stirrer, a dropping funnel, and a nitrogen outlet. The mixture was stirred under the protection of nitrogen until the Terathane® was totally dissolved. At room temperature, 5.50 grams (0.022 mol) of MDI, dissolved in 30 ml of DMAc, were added to the Terathane®/DMAc solution dropwise over a five-minute period. The solution was slowly heated to 90°C and held at this temperature for 2 hours under nitrogen. Afterwards, the solution was cooled to room temperature. Then, 0.66 gram (0.011 mol) of EDA, dissolved in 20 ml of DMAc, was added to the solution dropwise under mechanical stirring. The amount of added chain extender (i.e., EDA) did not reach its stoichiometric endpoint (i.e., 0.012 mol) because the polymerization mixture had already become too viscous to be easily stirred using the mechanical stirrer. The solution was then held at 40°C for 2 hours under a nitrogen atmosphere. Excess diethylamine (0.20 g, 0.003 mol) was then added to react with the remaining N=C=O groups and terminate the polymer chains, and the reaction was continued for two more hours at 40°C in nitrogen. The solution was monitored by FTIR until no N=C=O absorption peak (2200 cm^{-1}) was detected. The reaction was then stopped, and the solution was allowed to cool to room temperature.

After cooling, the polyurethane solution was coagulated by slowly pouring it into 1L of methanol (5X volume) under stirring, and white precipitated strings were obtained. The precipitated polymer was left in methanol overnight and then cut into small pieces using a blender. The polymer pieces were filtered and washed again with methanol. The resulting polymer was dried at room temperature in air overnight, then in a vacuum oven at 140˚C for 48 hours to remove residual DMAc.

In other syntheses, Terathane® 2900, PEG 2000, PPG 2700, and PEG 2000/Terathane® 2000 mixture (1:1 mixture by weight) were used instead of Terathane® 2000. In each synthesis, 0.010 mole of diol (e.g., 29.0 grams of Terathane® 2900) was used. The other reagent amounts and synthesis steps remained the same as indicated above. Table 7.1 shows the chemical structure of polyether diols and the soft segment weight fractions in the resulting polymers. Samples containing PPG 2700, Terathane® 2900, Terathane® 2000, mixed PEG 2000/Terathane® 2000, and PEG 2000 were labeled as I, II, III, IV and V, respectively. These identifiers are used in the following discussion.

OCN—R—NCO

\+

HO—R'—OH

Ratio 2.2:1

$$OCN—R—\underset{\underset{H}{|}}{N}—\underset{\overset{\parallel}{O}}{C}—O—R'—O—\underset{\overset{\parallel}{O}}{C}—\underset{\underset{H}{|}}{N}—R—NCO$$

Prepolymer

$$H_2N\diagup\diagdown NH_2$$

$$OCN\sim\sim\sim\underset{\underset{H}{|}}{N}—\underset{\overset{\parallel}{O}}{C}—\underset{\underset{H}{|}}{N}\diagup\diagdown\underset{\underset{H}{|}}{N}—\underset{\overset{\parallel}{O}}{C}—\underset{\underset{H}{|}}{N}\sim\sim\sim NCO$$

$$\diagup N \diagdown \underset{H}{\overset{N}{|}}$$

R= [benzene ring — CH₂ — benzene ring structure]

R'= $-\left(CH_2CH_2O\right)_n CH_2CH_2-$

$-\left(CH_2\underset{\overset{|}{CH_3}}{CHO}\right)_n CH_2\underset{\overset{|}{CH_3}}{CH}-$

$-\left((CH_2)_4O\right)_n (CH_2)_4-$
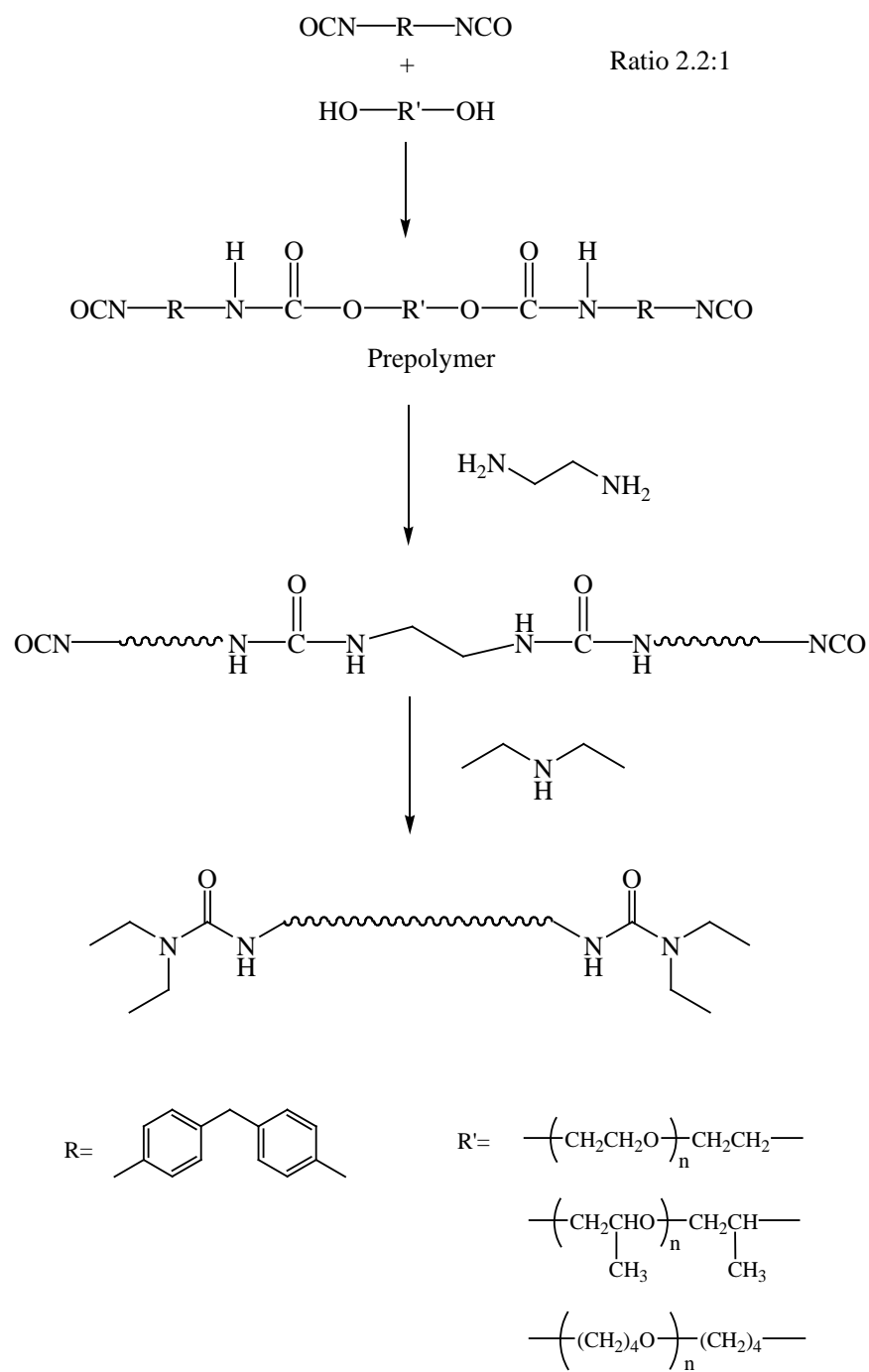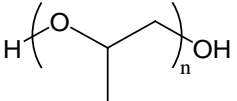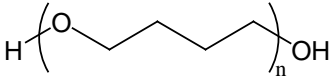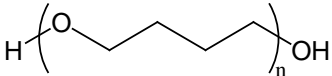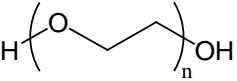
Figure 7.1   The chemical structures and synthesis steps used to prepare poly(urethane-urea)s.

137

Table 7.1   Composition of the different polyurethane/polyurea block copolymers and their physical properties

Sample code	Diol	Soft segment chemical structure	Soft segment content (wt %)	Water uptake (wt %)
I	PPG 2700		83.1	17 ± 2
II	Terathane® 2900		84.3	10 ± 1
III	Terathane® 2000		78.4	11 ± 1
IV	Terathane® 2000 : PEG 2000 = 1:1		78.4	34 ± 2
V	PEG 2000		78.4	132 ± 9

138

Poly(urethane-urea) films were prepared from a DMAc solution using a solution casting method. Polyurethanes were dissolved in DMAc at 20 wt % solids and then passed through a filter with 5 µm pores under pressure. The filtered solution was cast onto a glass plate preheated to 80ºC and then vacuum dried at 100ºC for 6 hours to remove most of the DMAc, then at 160ºC for two hours to further remove DMAc. The film was then cooled to room temperature in vacuum and detached from the glass plate. Because of its high polarity, even rigorous drying protocols may not be sufficient to remove all of the residual DMAc, and the presence of such residual solvent may influence permeability measurement results. Therefore, in addition to the drying protocol described above, the films were then solvent exchanged by soaking overnight in a large excess of ethanol. DMAc and ethanol are miscible, and ethanol can swell the polymer samples but not dissolve them. Thus, any DMAc left in the film can solvent exchange with the ethanol when the film swelled. Afterwards, the film was dried in air until most of the ethanol evaporated, then dried in vacuum at 160ºC for 6 hours to remove all remaining traces of ethanol. As will be discussed, the removal of residual DMAc and ethanol from the film was confirmed by TGA because no related weight loss was observed. Membrane thickness was measured using a Mitutoyo Litematic VL-50A measuring instrument (Mitutoyo Corporation, Japan). This thickness gauge is

specifically designed for use with soft materials, such as rubbery polymers, and employs a low-force micrometer to measure thickness. The thickness of the dry films varied from 80 to 130 μm.

7.3   Results and Discussion

7.3.1   Polymer Characterization

The chemical structures of the poly(urethane-urea)s were verified using FT-IR spectroscopy. As shown in Figure 7.2, all samples demonstrated characteristic urethane urea absorption peaks. The amide (-NH) structure in urethane/urea linkages was observed at 3330 cm^{-1} in each spectrum. Peaks between 1730 cm^{-1} and 1710 cm^{-1} correspond to the free carbonyl groups and H-bonded urethane carbonyl groups[28]. The peak around 1645 cm^{-1} correspond to the H-bonded urea carbonyl groups[28]. C-N-H bending in the urethane linkges can be observed around 1545 cm^{-1}[29]. Due to the high molecular weight and high soft segment content (between 78 and 84%), a strong sharp peak appears around 1095 cm^{-1} that is ascribed to the C-O-C stretching of the ether group in polyethers[30]. The 2200-2400 cm^{-1} region remained clear, demonstrating that no unreacted isocyanate groups remained[31]..
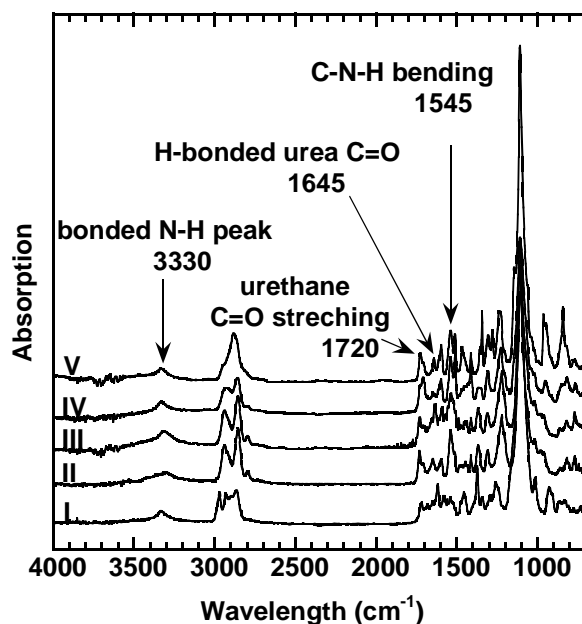
Figure 7.2   FT-IR spectra of synthesized poly(urethane-urea)s.

TGA was used to investigate the thermal stability of these poly(urethane-urea)s

and to verify the absence of solvent in the samples. There was no indication of any mass

loss that could be ascribed to the loss of solvent, so the drying protocol has likely

removed all solvent from the polymers. All TGA curves presented in Figure 7.3 show

similar weight loss, which began between 200ºC and 250ºC, indicating the onset of

polymer decomposition. The H-bonded urea links were suggested to provide improved

better thermal stability in poly(urethane-urea)s relative to polyurethanes[32, 33], but

thermal degradation following breaking of H-bonds should not be cause weight loss in

these poly(urethane-urea)s because the H-bond dissociation temperature is much lower

(no more than 130ºC)[34]. The thermal degradation in MDI-based poly(urethane-urea)s was suggested to start with cleavage of N-H and C-H bonds in the hard segments[35], and the weight loss caused by decomposition of MDI-based hard segments in polyurethanes was observed at about 245ºC[36]. The rapid weight loss between 250ºC and 440ºC was associated with decomposition of the soft segments[37]. Based on the TGA curves showed in Figure 7.3, the five percent weight loss temperatures for all samples were determined and are recorded in Table 7.2. These temperatures are very similar (284ºC-291ºC) because of the similarity among the chemical structures of the polymers in this study. Moreover, they are consistent with temperatures reported for other poly(urethane-urea) copolymers[29, 38].
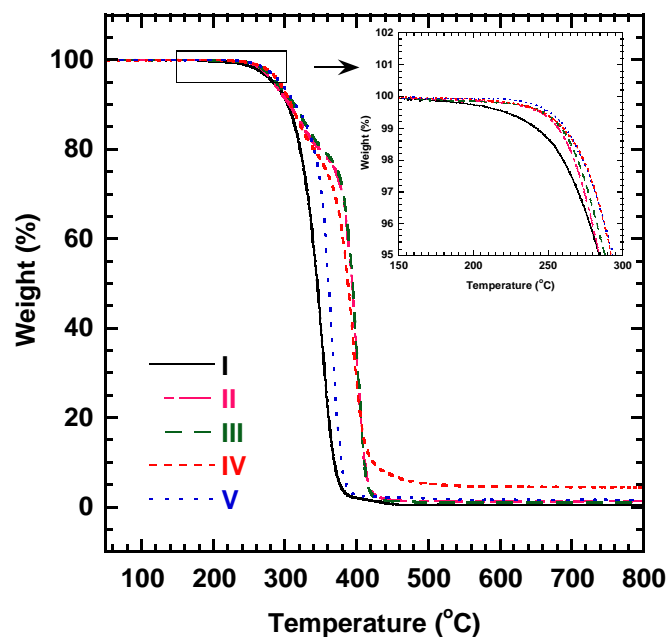
Figure 7.3   TGA curves of poly(urethane-urea) films. The heating rate was 5°C/min.

DSC thermograms of poly(urethane-urea) films are presented in Figure 7.4, and Table 7.2 summarizes the thermal transitions from these DSC scans. DSC data were taken during the first heating of the poly(urethane-urea) samples. The glass transition temperatures of the soft segments are of interest because they are related to microphase separation in such segmented poly(urethane-urea)s; if the microphase separation between hard and soft segments is incomplete, the T_g of the soft segments will often increase beyond the value associated with the T_g of a polymer composed of pure soft segments[39]. The hard segment T_g sometimes cannot be observed because of the

143

relatively weak signal of this glass transition temperature and incomplete microphase

separation in the hard segment domains[24].

Table 7.2 The thermal properties of poly(urethane-urea)s and pure polyether diols measured using DSC and TGA

Sample code	ρ (g/cm^3)	FFV	T_g (°C)	T_m (°C)	5% Weight Loss Temperature (°C)
I	1.019	0.200	-63.4	N/A	284
II	1.050	0.161	-70.1	12.3	284
III	1.082	0.148	-74.9	4.5	288
IV	1.117	0.151	-81.5/-28.4[*]	10.4	291
V	1.214	0.127**	-44.4	37.3	291

* Sample IV exhibited two glass transition temperatures because there are two polyethers.
**All FFV values were calculated using the density listed in this Table, except for that of sample V. In this case, the estimated amorphous density, 1.207 g/cm^3, used was calculated FFV using Equation (7.5). The soft segment and hard segment molar ratios in the amorphous phase were also recalculated for the group contribution method to eliminate the influence of the crystalline region on the calculation of V_o. This calculation assumes that only PEO segments crystallize.

Sample I (PPG-based) exhibits only a glass transition temperature; all other

samples showed both glass transition and melting points. The glass transition

temperature of sample I, -63.4°C, is near the T_g of pure polypropylene glycol (-70°C) [39]

but lower than the reported T_g in crosslinked PPG systems (-43°C) [40] and PPG

containing polyurethanes (-35.7ºC and -39.8ºC) [29]. However, sample I has much

higher soft segment content (83.1 wt %) than that of other polyurethanes reported in the

literature, which are usually restricted to soft segment contents below 65 %[4, 24, 29, 41].

Our DSC measurements showed that the hard and soft segment phases should be well

phase-separated in sample I because the thermal transition temperature is quite close to

that of pure PPG, reflecting very little phase mixing of hard and soft segment domains.

Similar behavior was observed in the Terathane®-based poly(urethane-urea)s (i.e.,

samples II, III, and IV). The melting temperature in samples II and III are 12.3ºC and

4.5ºC, respectively, consistent with the reported melting temperatures of the Terethane®

phase in Terathane®-based polyurethanes[41, 42]. The reported glass transition

temperatures of Terathane® soft segments, however, varies from -38.7ºC to -80.8ºC[2,

41-43], depending on the polyether molecular weight, hard segment content, and the

nature and amount of any additional polyether components in polyurethanes and

poly(urethane-urea)s. Based on our DSC experiments, the glass transition temperatures

of II and III are -71.8ºC and -70.1ºC, respectively, close to the values (-75ºC and -76.2ºC)

for polyurethanes containing 74.2 wt % soft segment with a polyether molecular weight

of 2400 and 2030, reported by Galland and Lam[41].
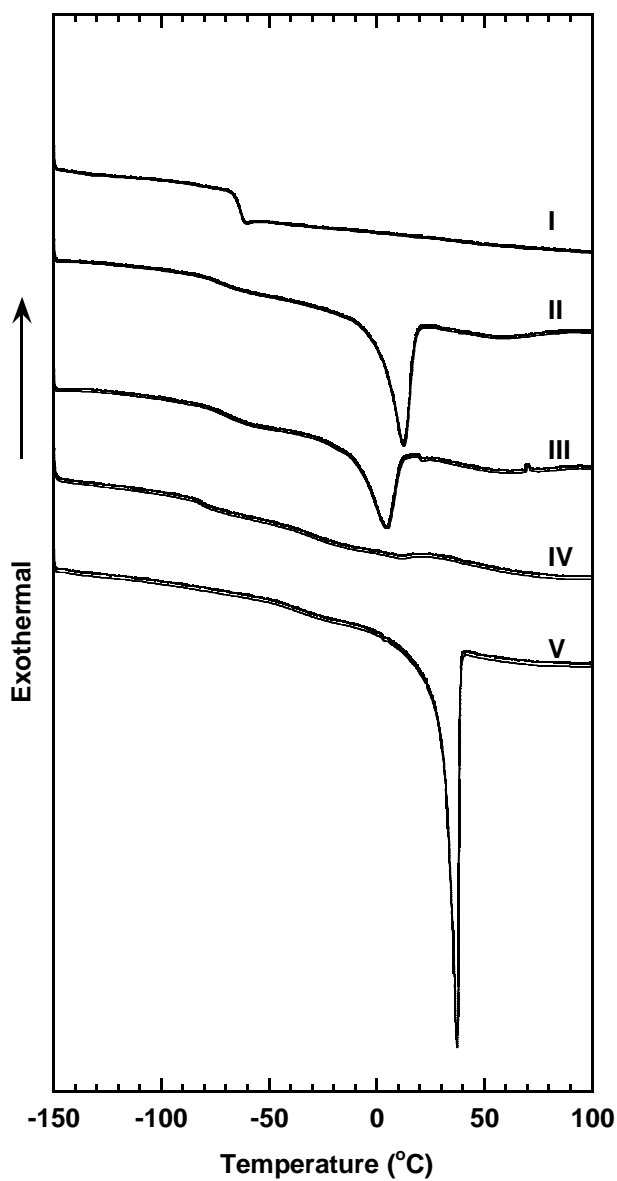
Figure 7.4   Differential scanning calorimetry (DSC) thermograms of poly(urethane-urea) samples prepared using solution casting.   The heating rate was 10°C/min. The thermograms have been displaced vertically for clarity.

146

In sample IV, two glass transition temperatures were observed at -78.9ºC (Terathane®) and -28.4ºC (PEG) showing that the soft segments were phase separated. A very weak transition was also observed between 10-15ºC that may due to low levels of crystallinity in one of the soft segment phases. However, the enthalpy (less than 1 J/g) is much smaller than that of either Terathane®-based (around 20 J/g) or PEG-based (51 J/g) poly(urethane-urea)s, and there was no observation of a melting transition of the other soft segment phase, showing that mixing the two polyethers disrupts crystallinity in the final product. Such a situation is desirable for preparing highly permeable polymers, since crystallinity typically reduces gas permeability[10]. Similar results were reported by Jiang[37] in polyurethanes containing PEG/PDMS soft segment mixtures.

As Figure 7.4 shows, sample V is the only polymer having a semi-crystalline structure above room temperature. DSC analysis showed that the melting point is 37ºC, slightly lower than the melting temperature of the pure PEG 2000 starting material, which was 51ºC based on DSC analysis. In semi-crystalline polymers, gas molecules are presumed to permeate only through amorphous regions[44]. Thus, it is of interest to determine the crystallinity in any sample, such as sample V, which may have some crystallinity at the temperature of gas permeation studies. Even though there are potentially urethane/urea linkages from the hard segments dissolving in the soft segment

147

region, we presume that the crystalline phase contains only polyether structures because of the well-organized packing of molecules in crystals. Moreover, WAXD data, to be discussed below, supports the assignment of the crystalline region to be composed of PEG crystals. Therefore, the weight fraction crystallinity in the crystals, χ_C (g crystals/g soft segment material), was estimated as follows[45]:

$$\chi_C = \frac{\Delta H}{\Delta H_C} \tag{7.1}$$

where ΔH is the melting enthalpy obtained from the DSC melting peak area, and ΔH_C is the melting enthalpy of 100% crystalline polyethylene oxide. The weight fraction of crystallinity in the entire poly(urethane-urea), $\chi_C^{'}$ (g crystals/g polymer), can be estimated based on the soft segment content listed in Table 7.2 and χ_C in the soft segments. The ΔH_C value used for PEG in this calculation, 166.4 J/g, was suggested by Simon and Rutherford[46]. From DSC analysis, the ΔH value of sample V was 56.1 J/g. Using this value in Equation (7.2) yields a crystallinity of 33.7 wt % in the PEG soft segments and 26.4 wt % crystallinity in sample V.

Volume fraction crystallinity, ϕ_c, can be calculated as follows[47]:

$$\phi_C = \left(\frac{\rho}{\rho_c}\right)\chi_C^{'} \tag{7.2}$$

or[44]:

$$\phi_C = \frac{\rho - \rho_a}{\rho_c - \rho_a} \tag{7.3}$$

where ρ is the measured poly(urethane-urea) density, ρ_c is the density of crystalline PEO

at room temperature (1.234 g/cm^3[46]), and ρ_a is the density of amorphous regions in the

poly(urethane-urea) sample. The film density of sample V, according to Table 7.2, is

1.214 g/cm^3. Using this value in Equation (7.2) yields a volume fraction crystallinity of

26.0%. From this calculation, one may estimate the density of the amorphous regions of

this sample, ρ_a, to be 1.207 g/cm^3 based on Equation (7.3). This value will be used to

calculate fractional free volume in the amorphous regions of this sample.

WAXD was also conducted to characterize the morphology in these samples.

Figure 7.5 presents the X-ray diffraction spectra of these poly(urethane-urea)s. The

reflection peak ascribed to the amorphous regions of the samples was observed at 2θ

values of approximately 19.5º, which is similar to reported values in other poly(urethane-

urea)s[48]. Except for sample V, all other samples showed only an amorphous halo. In

sample V, two sharp peaks appear at $2\theta = 19.2º$ and $2\theta = 23.3º$, respectively, which are

ascribed to crystalline PEO structures in the polymer[49]. The weight fraction of the

crystalline region in this sample was estimated from the WAXD data as follows[47]:

$$\chi_C = \frac{I_C}{I_C + I_A} \tag{7.4}$$

where I_A and I_C were the integrated areas under the amorphous and crystalline peaks, respectively. Based on Equation (7.4) and the WAXD pattern, the crystalline weight fraction of sample V would be 22%. The weight fraction and volume fraction crystallinity values obtained from DSC and WAXD analysis appear in Table 7.3. Typically, the amount of crystallinity estimated from DSC and WAXD will not agree perfectly, because different assumptions are used to determine crystallinity values from these different techniques[47, 50]. For example, Equation (7.4) is based on the assumption that all polymer chains in the crystalline region contribute to I_c, and only chains in the amorphous region contribute to I_a. However, the estimated crystallinity values based on the WAXD measurements are sometimes lower than the crystallinity estimated using other methods such as DSC and density. Such lower crystallinity values are ascribed to the existence of a transition region between the crystalline and amorphous regions[51], or defects in crystalline regions[52]. Therefore, we used the DSC crystallinity value in the amorphous phase density and FFV calculation. However, the WAXD data are in reasonable agreement with the crystallinity values from DSC.
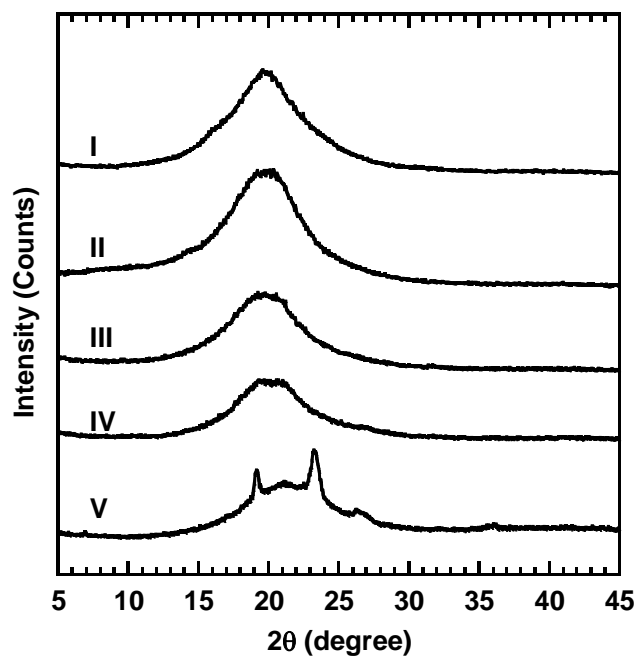
Figure 7.5   WAXD analyses of poly(urethane-urea) films.   The curves have been displaced vertically for clarity.

Table 7.3   Volume and weight percent crystallinity in sample V (PEG 2000 based)

Technique for estimating crystallinity	χ_c (%)	ϕ_c (%)
DSC	26.4	26.0
WAXD	22	22

ϕ_c values were estimate from χ_c values using Equation (7.3).

7.3.2 Density and FFV

The amount of free volume in the polymer matrix is an important parameter influencing gas transport properties[53]. Fractional free volume can be estimated as follows[54]:

$$FFV = \frac{V_{sp} - V_0}{V_{sp}} \approx \frac{V_{sp} - 1.3V_w}{V_{sp}} \qquad (7.5)$$

where V_{sp} is the polymer specific volume at the temperature of interest, V_0 is the occupied volume of polymer at 0K, which is estimated as 1.3 times the van der Waals volume (V_w) calculated by group distribution methods[55, 56]. With the exception of Sample V, the poly(urethane-urea)s presented in this work are totally amorphous at or above room temperature. The densities of these materials at ambient conditions are presented in Table 7.2. Table 7.2 also provides the fractional free volumes of these samples, calculated as described above. For the case of Sample V, which is semi-crystalline at ambient conditions, the estimated amorphous phase density was used in the FFV calculation. Based on the amorphous polymer density and estimated van der Waals volume, sample I has the highest FFV (0.200), which may be due to the extra $-CH_3$ groups along the main chain of the soft segments. Interestingly, this FFV value is very close to the FFV (around 0.190) in crosslinked PPG materials[40]. In samples II and III, an increase in Terathane® molecular weight (from 2000 to 2900) increases the soft

152

segment content and, consequently, increases FFV from 0.148 to 0.161. For the FFV of sample IV, a 50/50 ratio of Terathane$^®$ and PEG was used to calculate V_w values for the soft segments, and the FFV is similar to that of sample III. The FFV in sample V, however, cannot be simply calculated using the film density and van der Waals volume obtained from the group distribution method based on the total polymer composition. Since part of the PEG chains are sequestered in crystals, the chemical composition of the amorphous phase must be recalculated to account for this fact. Based on the χ_c value estimated from DSC analysis (as shown in Table 7.3), the mole ratio of soft to hard segments in the amorphous phase is 1.46:1, and the FFV in the amorphous phase is 0.127, which is lower than that of the other poly(urethane-urea)s in this work.

7.3.3 Water Uptake

Water uptake values for poly(urethane-urea) samples are also reported in Table 7.1. The sample synthesized from PEG 2000 (sample V) has around 130 wt % water uptake, while the water uptake is only about 35 wt % for sample IV, which contains 50% PEG 2000 and 50% Terathane$^®$ 2000 soft segments. For comparison, in crosslinked amorphous PEG systems, the water uptake can vary from 110% to about 350%, depending on the preparation conditions[57]. Clearly, water uptake depends strongly on

the polyethylene oxide content. A more detailed study of this phenomenon is provided

elsewhere[58, 59]. Although PPG and Terathane® have similar ether structures in the

polymer main chain, the water uptakes for these polymers are much lower. Sample I

(PPG-based) has only 17 wt % water uptake, and samples II and III (Terathane®-based)

are only around 10 wt %. The water uptake data illustrate that PPG and Terathane®

containing materials are much less hydrophilic than those based on PEO and should,

therefore, be much less sensitive to humidity.

7.3.4   Gas Transport Properties

Figure 7.6 presents the pure gas permeability coefficients of six gases (N_2, O_2, H_2,

He, CH_4 and CO_2) in poly(urethane-urea) membranes at 35ºC as a function of upstream

pressure. The permeability coefficient change *vs*. upstream pressure is similar to that in

rubbery polymers[60]. That is, the permeability coefficients of permanent gases, such as

N_2, O_2, H_2, CH_4 and He, are essentially independent of upstream pressure, and the

permeability of CO_2 increases somewhat with increasing upstream pressure. The

relationship between permeability and upstream pressure can be described by the

following empirical model[61]:

$$P_A = P_{A,0}(1 + m\Delta p) = P_{A,0}(1 + mp_2) \tag{7.6}$$

where P_A is the permeability coefficient at an upstream pressure, p_2; $P_{A,0}$ is the permeability coefficient at $p_2 = 0$ (i.e., infinite dilution); m is an adjustable constant; and Δp is the pressure difference between the upstream and downstream faces of the film, $\Delta p = p_2 - p_1$. In this study, the downstream pressure was much lower than the upstream pressure, so the downstream pressure can be neglected, and Δp can be replaced by p_2. Infinite dilution permeability coefficients for different gases in these poly(urethane-urea) block copolymers were calculated using Equation (7.6), and the results are recorded in Table 7.4.

(A)   (B)
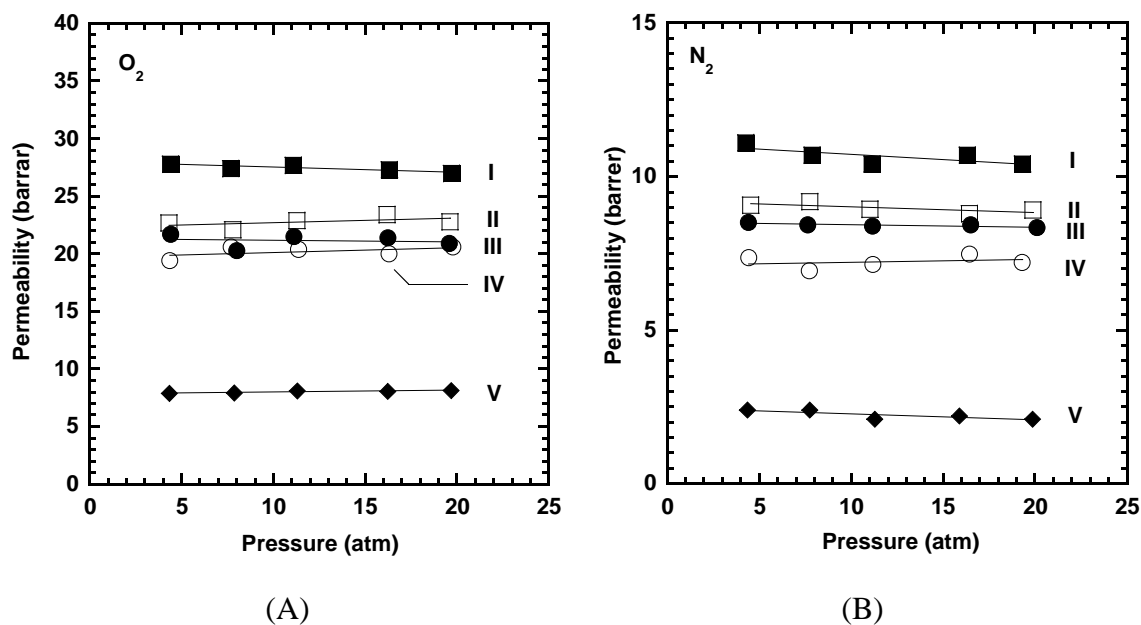
Figure 7.6 To next page →
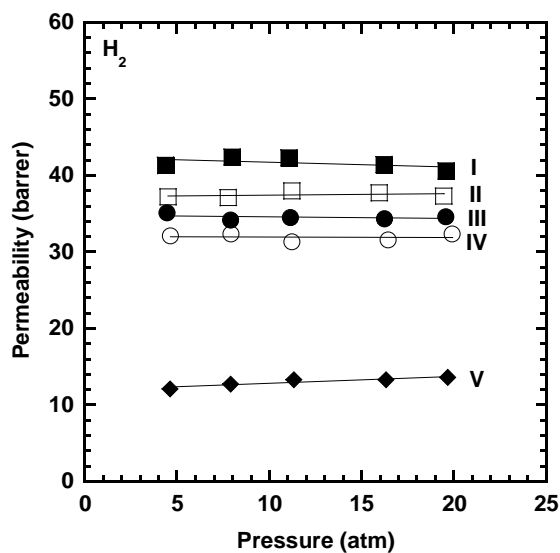
(C)
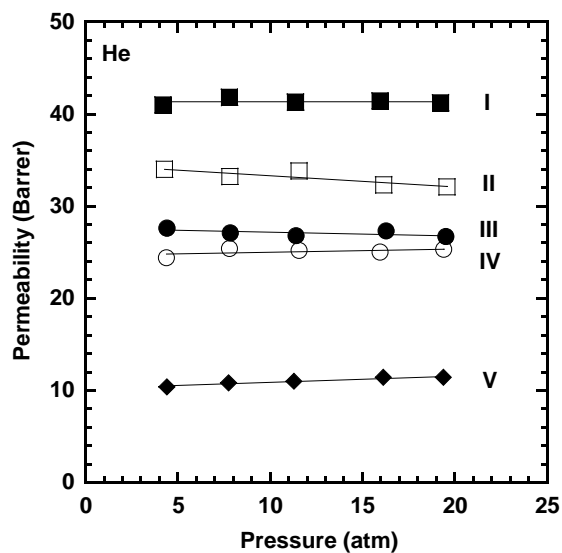
(D)
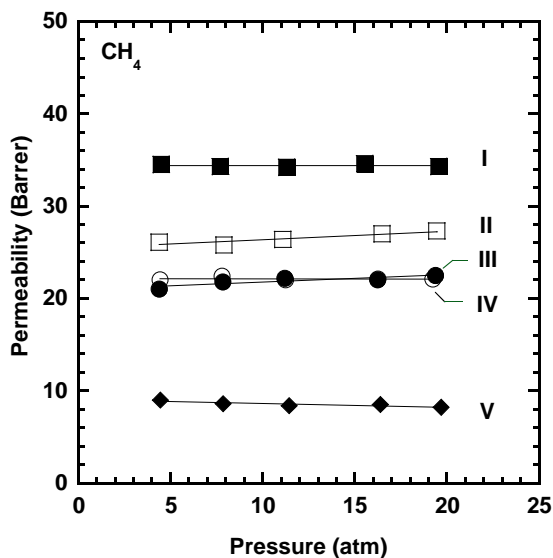
(E)
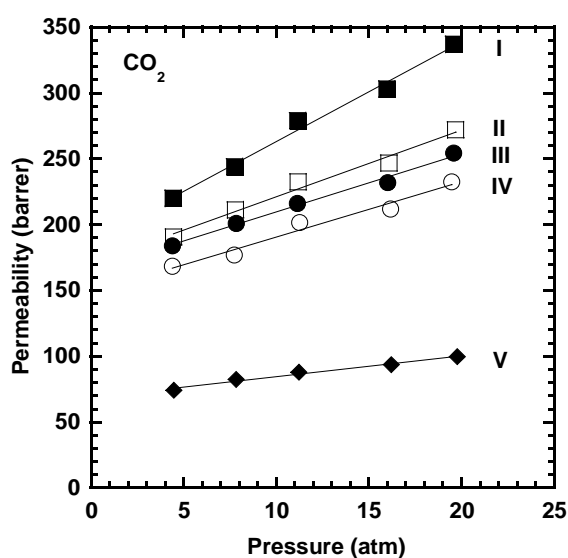
(F)

Figure 7.6   Pure gas permeability of: (A) O_2, (B) N_2, (C) H_2, (D) He, (E) CH_4, and (F) CO_2 in polymer films prepared from samples I (■), II (□), III (●), IV (○) and V (♦) as a function of upstream pressure at 35°C.

Table 7.4   Pure gas permeability in poly(urethane-urea) films at 35°C and infinite dilution

Polymer	$P_{A,0}$ (Barrer)						Permeability Selectivity				
	O_2	N_2	H_2	He	CH_4	CO_2	CO_2/H_2	CO_2/N_2	CO_2/O_2	CO_2/CH_4	O_2/N_2
I	28	11	42	41	34	190	4.5	17	6.8	5.5	2.5
II	22	9.2	37	35	25	170	4.6	19	7.7	6.7	2.4
III	21	8.5	35	28	20	170	4.8	20	7.8	7.9	2.5
IV	20	7.2	32	25	22	150	4.3	21	7.6	6.9	2.7
V	8.0	2.4	12	10	9.1	69	5.8	29	8.6	7.6	3.3

Gas permeability increases as FFV increases. For example, sample I has the highest FFV (0.200), and it also has the highest infinite dilution permeability to all gases. Sample II has higher permeability than sample III. The higher soft chain molecular weight increases soft segment content, enhances FFV and leads to increased permeability[41]. Sample V has lower gas permeability than all other materials, perhaps due to the semi-crystalline structure in the PEG soft segments and low FFV in the amorphous phase. The permeability measurements were conducted at 35°C, which is in the window where some of the PEG crystals melt. Based on the melting enthalpy from the DSC scan at temperatures up to 35°C, it appears that about 40% of the crystals would have melted, so approximately 60% of the crystalline material would remain during the permeation measurement. So the crystallinity at the conditions of the permeability measurements was around 13% by volume of the PEG soft segments and 10-11% by volume based in the polymer. PEG 2000-based sample V has permeability coefficients similar to those of amorphous crosslinked PEO [11] but larger than those of semi-crystalline PEO[44]. For example, the nitrogen permeability coefficients (35ºC) in sample V, crosslinked PEO and semi-crystalline PEO were 2.4 Barrer, 2.1 Barrer, and 0.24 Barrer, respectively. This divergence may be due to the great differences in the extent of crystallinity (71 vol. % in semi-crystalline PEO, but only 10-11 vol. % in sample V). Compared to sample V, sample IV only contains 50 wt % PEG 2000 in the soft segments, and replacing the other 50% of the polyether with Terathane® 2000 results in a more amorphous structure at room temperature and higher FFV in the amorphous phase, as shown in Figure 7.5 and Table 7.2. This change in the soft segment

composition leads to a significant increase, by more than a factor of two, in permeability. For example, the N_2 infinite dilution permeability increases from 2.4 Barrer in sample V to 7.2 Barrer in sample IV, while the CO_2 infinite dilution permeability increases from 69 Barrer to 150 Barrer.

The permeability coefficients decrease in the following order:

$$CO_2 > H_2 > He > CH_4 \approx O_2 > N_2.$$

Unlike gas transport in glassy polymers, in rubbery polymers the diffusion coefficient is somewhat less affected by penetrant size because of the polymer's relatively high free volume and flexible chain nature[40]. Penetrants with higher critical temperature are usually more condensable and have higher solubility coefficients. Thus, in poly(urethane-urea)s based on polyether diols, CO_2 is often more permeable than smaller penetrants, such as H_2, because the much higher CO_2 solubility (relative to that of H_2) more than offsets the somewhat lower diffusion coefficient of CO_2. H_2 and He, which are the smallest gases considered, were more permeable than all other gases except CO_2[44]. In the permeability results presented in this study, except for hydrogen and helium, the order of the permeability coefficients reflects the order of decreasing gas critical temperature, which is often associated with a decrease in gas solubility in the polymers[60].

The permeability selectivities for different gas pairs are also shown in Table 7.4. Sample I has the highest gas permeability but low selectivity values. Samples II and III have permeabilities close to those of sample I but better gas separation properties than those of sample I. Sample V has the best O_2/N_2 permeability selectivity as well as the

highest CO_2 separation properties from other gases. However, it has the lowest permeability coefficients. This result may be due to some residual crystallinity in the sample during the permeation measurements as well as the higher hard segment content in the amorphous phase. The hard segment content is related to the morphology and microphase-separation in the soft segment regions[24, 62]. The rigid urethane/urea linkages are reported to act as fillers or physical crosslinks in polyurethanes[63]. Various studies[5, 41, 63, 64] have reported that increasing hard segment content (i.e. decreasing soft segment content) reduces permeability and *vice versa*.

The lower overall CO_2 permeability selectivity in PPG and Terathane®-based poly(urethane-urea)s is somewhat balanced by higher CO_2 permeability, as shown in Figure 7.7. Sample I, which has lower CO_2 selectivity over other gases, maintains higher CO_2 permeability relative to the other poly(urethane-urea)s. Since low FFV usually leads to a decrease in gas permeability but an increase in diffusivity selectivity[65], there is often a trade-off between permeability and selectivity [66, 67]. In rubbery polymers containing PEO or PPO links, the change in FFV does not strongly decrease CO_2 permeability selectivity, as it would in glassy polymers, because the diffusion coefficient is not strongly affected by penetrant molecular size, and the permeability selectivity is determined mainly by differences in solubility selectivity[15, 40].
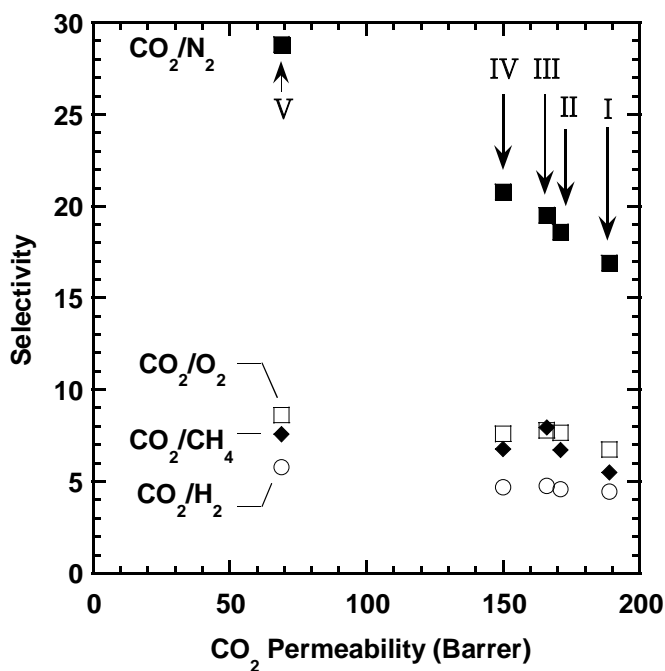
Figure 7.7   Pure gas selectivities of CO_2/N_2 (■), CO_2/O_2 (●), CO_2/CH_4 (♦), and CO_2/H_2 (○) in poly(urethane-urea) membranes as a function of CO_2 permeability at 35°C.

As shown in Figure 7.7, only CO_2/N_2 selectivity showed a decrease with increasing CO_2 permeability; CO_2 separation properties over other gases are less strongly affected than is the infinite dilution CO_2 permeability. The CO_2/H_2 selectivity values are presented as a function of CO_2 permeability in Figure 7.8 along with reported values from other polymer materials[66]. Unlike cases where the separation is based on strong size-sieving ability, the positive slope of the upper bound indicates that high CO_2 permeability and high CO_2/H_2 selectivity may be achieved simultaneously. The slightly higher CO_2/H_2 permeability selectivity of sample I, as shown in Figure 7.8 may be attributed to the better solubility of CO_2 in PEG than in PPG and Terathane®

161

polymers[23]. All CO_2/H_2 selectivity values are close to the upper bound, showing that the materials have interesting CO_2/H_2 separation properties.
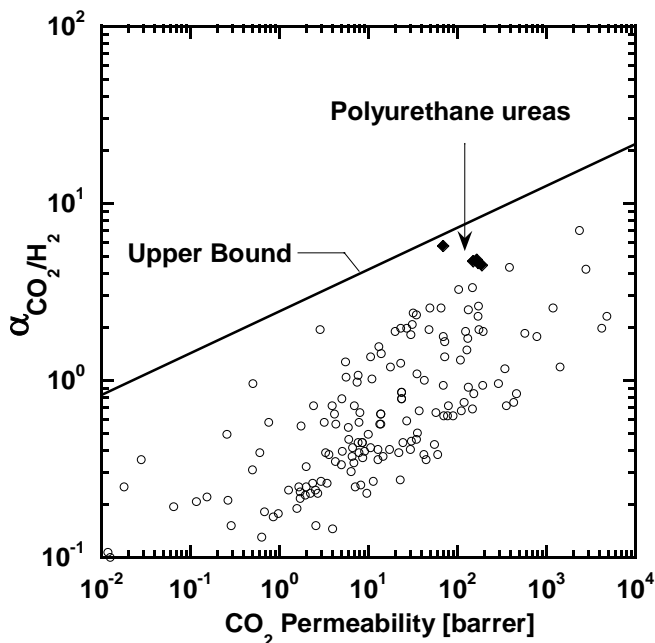
Figure 7.8   Comparison of CO_2/H_2 selectivity vs. CO_2 permeability of poly(urethane-urea)s prepared in the present study (▼) with other polymers (○)from the literature[11]. Data at lower CO_2 permeability values correspond to lower CO_2 partial pressures in the feed gas and vice versa. The upper bound provided from the literature [11] was drawn based on a model prediction [66].

7.4   Conclusions

The physical and gas transport properties of a systematic series of poly(urethane-urea)s were determined. The presence of different polyether diols affects thermal transitions as well as the fractional free volume and leads to changes in gas transport performance. Samples synthesized from PEG 2000 have a semi-crystalline structure at

room temperature. The crystallization reduces soft segment content in the amorphous phase and leads to lower permeability. However, replacing half of the PEG soft segments with Terathane$^{®}$ results in an essentially amorphous material and increases gas permeability approximately three-fold. PPG-based poly(urethane-urea) has the highest FFV, as well as the highest permeability, but the CO_2 selectivity over other gases decreases slightly. The Terathane$^{®}$-based polymers also have good gas permeability and better CO_2 separation properties than PPG-based materials. Both PPG- and Terathane$^{®}$-based polymers exhibit much lower water uptake than PEG base materials (about 150 wt % in PEG-based, 17 wt % in PPG-based and 10 wt % in Terathane$^{®}$-based polymer), showing that in an environment with high humidity, these materials may achieve more stable separation properties than those of materials based PEG.

7.5   References

1.   D. Dieterich, E. Grigat, W. Hahn, H. Hespe, and H. G. Schmelzer. Principles of polyurethane chemistry and special applications. In: Oertel G., editor. Polyurethane Handbook: Chemistry Raw Materials Processing Application Properties. Hanser Gardner Publication, Cicinnati, OH, 1994, 11-31.

2.   S. Abouzahr and G. L. Wilkes. Structure property studies of polyester- and polyether-based MDI-BD segmented polyurethanes: Effect of one- vs. 2-stage polymerization conditions. *Journal of Applied Polymer Science*, **1984**, 29(9), 2695-2711.

3.   M. Pegoraro, L. Zanderighi, A. Penati, F. Severini, F. Bianchi, N. Cao, R. Sisto, and C. Valentini. Polyurethane membranes from polyether and polyester diols for gas fractionation. *Journal of Applied Polymer Science*, **1991**, 43(4), 687-697.

4.   L. S. Teo, J. F. Kuo, and C. Y. Chen. Study on the morphology and permeation property of amine group-contained polyurethanes. *Polymer*, **1998**, 39(15), 3355-3364.

5.   P. M. Knight and D. J. Lyman. Gas permeability of various block copolyether urethanes. *Journal of Membrane Science*, **1984**, 17(3), 245-254.

6.   M. Yoshino, K. Ito, H. Kita, and K.-I. Okamoto. Effect of Hard-Segment Polymers on CO_2/N_2 Gas-Separation Properties of Poly(ethylene oxide)-segmented Copolymers. *Journal of Polymer Science: Part B: Polymer Physics*, **2000**, 38, 1707-1715.

7.   M. B. Shiflett and H. C. Foley. Ultrasonic deposition of high-selectivity nanoporous carbon membranes. *Science*, **1999**, 285(5435), 1902-1905.

8.   J. M. S. Henis and M. K. Tripodi. The developing technology of gas separating membranes. *Science*, **1983**, 220(4592), 11-17.

9.   R. W. Baker, J. G. Wijmans, and J. H. Kaschemekat. The design of membrane vapor-gas separation systems. *Journal of Membrane Science*, **1998**, 151(1), 55-62.

10.   H. Q. Lin and B. D. Freeman. Materials selection guidelines for membranes that remove CO_2 from gas mixtures. *Journal of Molecular Structure*, **2005**, 739(1-3), 57-74.

11.   H. Q. Lin, E. Van Wagner, B. D. Freeman, L. G. Toy, and R. P. Gupta. Plasticization-enhanced hydrogen purification using polymeric membranes. *Science*, **2006**, 311(5761), 639-642.

12.   H. Lin and B. D. Freeman. Gas and vapor solubility in cross-linked poly(ethylene glycol diacrylate). *Macromolecules*, **2005**, 38(20), 8394-8407.

13.   S. Kelman, H. Q. Lin, E. S. Sanders, and B. D. Freeman. CO_2/C_2H_6 separation using solubility selective membranes. *Journal of Membrane Science*, **2007**, 305(1-2), 57-68.

14.   H. Q. Lin, T. Kai, B. D. Freeman, S. Kalakkunnath, and D. S. Kalika. The effect of cross-linking on gas permeability in cross-linked poly(ethylene glycol diacrylate). *Macromolecules*, **2005**, 38(20), 8381-8393.

15.   H. Q. Lin, E. Van Wagner, J. S. Swinnea, B. D. Freeman, S. J. Pas, A. J. Hill, S. Kalakkunnath, and D. S. Kalika. Transport and structural characteristics of

crosslinked poly(ethylene oxide) rubbers. *Journal of Membrane Science*, **2006**, 276(1-2), 145-161.

16. H. Lin, E. Van Wagner, R. Raharjo, B. D. Freeman, and I. Roman. High-performance polymer membranes for natural-gas sweetening. *Advanced Materials*, **2006**, 18(1), 39-44.

17. V. I. Bondar, B. D. Freeman, and I. Pinnau. Gas sorption and characterization of poly(ether-b-amide) segmented block copolymers. *Journal of Polymer Science Part B-Polymer Physics*, **1999**, 37(17), 2463-2475.

18. V. I. Bondar, B. D. Freeman, and I. Pinnau. Gas transport properties of poly(ether-b-amide) segmented block copolymers. *Journal of Polymer Science Part B-Polymer Physics*, **2000**, 38(15), 2051-2062.

19. J. H. Kim and Y. M. Lee. Gas permeation properties of poly(amide-6-b-ethylene oxide)-silica hybrid membranes. *Journal of Membrane Science*, **2001**, 193(2), 209-225.

20. V. Barbi, S. S. Funari, R. Gehrke, N. Scharnagl, and N. Stribeck. SAXS and the gas transport in polyether-block-polyamide copolymer membranes. *Macromolecules*, **2003**, 36(3), 749-758.

21. S. J. Metz, M. H. V. Mulder, and M. Wessling. Gas-permeation properties of poly(ethylene oxide) poly(butylene terephthalate) block copolymers. *Macromolecules*, **2004**, 37(12), 4590-4597.

22. W. Yave, A. Car, S. S. Funari, S. P. Nunes, and K. V. Peinemann. CO_2-philic polymer membrane with extremely high separation performance. *Macromolecules*, **2010**, 43(1), 326-333.

23. K. Okamoto, M. Fujii, S. Okamyo, H. Suzuki, K. Tanaka, and H. Kita. Gas permeation properties of poly(ether imide) segmentd copolymers. *Macromolecules*, **1995**, 28(20), 6950-6956.

24. M. Yoshino, K. Ito, H. Kita, and K. I. Okamoto. Effects of hard-segment polymers on CO_2/N_2 gas separation properties of poly(ethylene oxide) segmented copolymers. *Journal of Polymer Science Part B-Polymer Physics*, **2000**, 38(13), 1707-1715.

25. A. Car, C. Stropnik, W. Yave, and K. V. Peinemann. Pebax (R)/polyethylene glycol blend thin film composite membranes for CO_2 separation: Performance with mixed gases. *Separation and Purification Technology*, **2008**, 62(1), 110-117.

26. ASTM D4274-05 Standard Test Methods for Testing Polyurethane Raw Materials: Determination of Hydroxyl Numbers of Polyols. 2001.

27. ASTM D5155-07 Standard Test Methods for Polyurethane Raw Materials: Determination of the Isocyanate Content of Aromatic Isocyanates. 2007.

28. T. O. Ahn, I. S. Choi, H. M. Jeong, and K. Cho. Thermal and mechanical properties of thermoplastic polyurethane elastomers from different polymerization methods. *Polymer International*, **1993**, 31, 329-333.

29. H. B. Park, C. K. Kim, and Y. M. Lee. Gas separation properties of polysiloxane/polyether mixed soft seogment urethane urea membranes. *Journal of Membrane Science*, **2002**, 204(1-2), 257-269.

30. J. M. Orban, T. M. Chapman, W. R. Wagner, and R. Jankowski. Easily grafted polyurethanes with reactive main chain functional groups. Synthesis, characterization, and antithrombogenicity of poly(ethylene glycol)-grafted poly(urethanes). *Journal of Polymer Science Part a-Polymer Chemistry*, **1999**, 37(17), 3441-3448.

31. T. Tawa and S. Ito. Preparation and reactions of hydrophilic isocyanate micelles dispersed in water. *Colloid and Polymer Science*, **2005**, 283(7), 731-737.

32. F. M. B. Coutinho and M. C. Delpech. Degradation profile of films cast from aqueous polyurethane dispersions. *Polymer Degradation and Stability*, **2000**, 70(1), 49-57.

33. L. S. Teo, C. Y. Chen, and J. F. Kuo. Fourier transform infrared spectroscopy study on effects of temperature on hydrogen bonding in amine-containing polyurethanes and poly(urethane-urea)s. *Macromolecules*, **1997**, 30(6), 1793-1799.

34. E. Yilgor, E. Burgaz, E. Yurtsever, and I. Yilgor. Comparison of hydrogen bonding in polydimethylsiloxane and polyether based urethane and urea copolymers. *Polymer*, **2000**, 41(3), 849-857.

35. Y. M. Song, W. C. Chen, T. L. Yu, K. Linliu, and Y. H. Tseng. Effect of isocyanates on the crystallinity and thermal stability of polyurethanes. *Journal of Applied Polymer Science*, **1996**, 62(5), 827-834.

36.   Y. T. Shieh, H. T. Chen, K. H. Liu, and Y. K. Twu. Thermal degradation of MDI-based segmented polyurethanes. *Journal of Polymer Science Part a-Polymer Chemistry*, **1999**, 37(22), 4126-4134.

37.   X. Jiang, J. F. Ding, and A. Kumar. Polyurethane-poly(vinylidene fluoride) (PU-PVDF) thin film composite membranes for gas separation. *Journal of Membrane Science*, **2008**, 323(2), 371-378.

38.   R. A. Azzam, S. K. Mohamed, R. Tol, V. Everaert, H. Reynaers, and B. Goderis. Synthesis and thermo-mechanical characterization of high performance polyurethane elastomers based on heterocyclic and aromatic diamine chain extenders. *Polymer Degradation and Stability*, **2007**, 92(7), 1316-1325.

39.   J. P. Santerre and J. L. Brash. Microstructure of polyurethane ionomers derivatized with dodecylamine and polyethylene oxide in the hard segment. *Journal of Applied Polymer Science*, **1994**, 52(4), 515-523.

40.   R. D. Raharjo, H. Q. Lin, D. E. Sanders, B. D. Freeman, S. Kalakkunnath, and D. S. Kalika. Relation between network structure and gas transport in crosslinked poly(propylene glycol diacrylate). *Journal of Membrane Science*, **2006**, 283(1-2), 253-265.

41.   G. Galland and T. M. Lam. Permeability and diffusion of gases in segmented polyurethanes: structure-properties relations. *Journal of Applied Polymer Science*, **1993**, 50(6), 1041-1058.

42.   B. C. Chun, T. K. Cho, M. H. Chong, and Y. C. Chung. Structure-property relationship of shape memory polyurethane cross-linked by a polyethyleneglycol spacer between polyurethane chains. *Journal of Materials Science*, **2007**, 42(21), 9045-9056.

43.   S. Abouzahr, G. L. Wilkes, and Z. Ophir. Structure property behavior of segmented polyether MDI butanediol based urethanes: Effect of composition ratio. *Polymer*, **1982**, 23(7), 1077-1086.

44.   H. Lin and B. D. Freeman. Gas solubility, diffusity and permeability in poly(ethylene oxide). *Journal of Membrane Science*, **2004**, 239, 105-117.

45.   S. Sunderrajan, B. D. Freeman, C. K. Hall, and I. Pinnau. Propane and propylene sorption in solid polymerelectrolytes based on poly(ethylene oxide). *Journal of Membrane Science*, **2001**, 182(1-2), 1-12.

46.   F. T. Simon and J. M. Rutherford. Crystallization and melting behavior of polyethylene oxide copolymers. *Journal of Applied Physics*, **1964**, 35(82), 82-86.

47.   S. N. Dhoot, B. D. Freeman, and M. E. Stewart. Sorption and transport of linear alkane hydrocarbons in biaxially oriented polyethylene terephthalate. *Journal of Polymer Science Part B: Polymer Physics*, **2001**, 39(11), 1160-1172.

48.   T. Takahashi, N. Hayashi, and S. Hayashi. Structure and properties of shape-memory polyurethane block copolymers. *Journal of Applied Polymer Science*, **1996**, 60(7), 1061-1069.

49.   N. Ravi, A. Mitra, P. Hamilton, and F. Horkay. Characterization of the network properties of poly(ethylene glycol)-acrylate hydrogels prepared by variations in the ethanol-water solvent composition during crosslinking copolymerization. *Journal of Polymer Science Part B: Polymer Physics*, **2002**, 40(23), 2677-2684.

50.   C. C. McDowell, B. D. Freeman, and G. W. McNeely. Acetone sorption and uptake kinetic in poly(ethylene terephthalate). *Polymer*, **1999**, 40(12), 3487-3499.

51.   E. W. Fischer and S. Fakirov. Structure and properties of polyethyleneterephthalate crystallized by annealing in the highly oriented state. *Journal of Materials Science*, **1976**, 11(6), 1041-1064.

52.   L. E. Alexander. X-Ray Diffraction Methods in Polymer Science. 2 ed. R. K. Publishing Company, Malabar, Florida, 1985, 137.

53.   B. D. Freeman and I. Pinnau. Polymeric materials for gas separations. In: Freeman B. D. and Pinnau I., editors. Polymer Membranes for Gas and Vapor Separation, vol. 733. ACS Symposium Series, Washington DC, 1999, 1-27.

54.   M. R. Pixton and D. R. Paul. Relationship between structure and transport properties for polymers with aromatic backbones. In: Paul D. R. and Yampol'skii Y. P., editors. Polymeric Gas Separation Membranes. CRC Press, Boca Raton, 1994, 83-154.

55.   A. Bondi. Physical Properties of Molecular Crystals, Liquid, and Glasses John Wiley and Sons, New York, 1968.

56.   D. W. van Krevelen. Properties of Polymers: Their Correlation with Chemical Structure; Their Numerical Estimation and Prediction from Additive Group Contributions Elsevier Science, Amsterdam, 1990.

57. H. Ju, B. D. McCloskey, A. C. Sagle, Y. H. Wu, V. A. Kusuma, and B. D. Freeman. Crosslinked poly(ethylene oxide) fouling resistant coating materials for oil/water separation. *Journal of Membrane Science*, **2008**, 307(2), 260-267.

58. H. Kitano, K. Ichikawa, M. Ide, M. Fukuda, and W. Mizuno. Fourier transform infrared study on the state of water sorbed to poly(ethylene glycol) films. *Langmuir*, **2001**, 17(6), 1889-1895.

59. S. Lusse and K. Arnold. The interaction of poly(ethylene glycol) with water studied by H-1 and H-2 NMR relaxation time measurements. *Macromolecules*, **1996**, 29(12), 4251-4257.

60. T. C. Merkel, V. I. Bondar, K. Nagai, B. D. Freeman, and I. Pinnau. Gas sorption, diffusion, and permeation in poly(dimethylsiloxane). *Journal of Polymer Science Part B: Polymer Physics*, **2000**, 38, 415-434.

61. A. Singh, B. D. Freeman, and I. Pinnau. Pure and mixed gas acetone/nitrogen permeation properties of polydimethylsiloxane [PDMS]. *Journal of Polymer Science Part B: Polymer Physics*, **1998**, 36, 230-289.

62. K. Madhavan and B. S. R. Reddy. Poly(dimethylsiloxane-urethane) membranes: effect of hard segment in urethane on gas transport properties. *Journal of Membrane Science*, **2006**, 283(1-2), 357-365.

63. H. Xiao, Z. H. Ping, J. W. Xie, and T. Y. Yu. Permeation of CO_2 through polyurethane. *Journal of Applied Polymer Science*, **1989**, 40(7-8), 1131-1139.

64. N. Cao, M. Pegoraro, F. Bianchi, and L. Zanderighi. Gas transport properties of polycarbonate-polyurethane membranes. *Journal of Applied Polymer Science*, **1993**, 48(10), 1831-1842.

65. R. D. Raharjo, H. J. Lee, B. D. Freeman, T. Sakaguchi, and T. Masuda. Pure gas and vapor permeation properties of poly[1-phenyl-2-[p-(trimethylsilyl)phenyl]acetylene] (PTMSDPA) and its desilylated analog, poly[diphenylacetylene] (PDPA). *Polymer*, **2005**, 46(17), 6316-6324.

66. B. D. Freeman. Basis of permeability/selectivity tradeoff relations in polymeric gas separation membranes. *Macromolecules*, **1999**, 32(2), 375-380.

67. L. M. Robeson. Correlation of separation factors versus permeability for polymeric membranes. *Journal of Membrane Science*, **1991**, 62(2), 165-185.

Chapter 8: Conclusions and Recommendations

8.1   Conclusions

This dissertation focused on an experimental study of the oxygen scavenging and barrier properties of cobalt-catalyzed 1,4-polybutadiene films and subsequently understanding the effects of reaction rate and oxygen diffusion on oxygen scavenging performance. 1,4-Polybutadiene is readily oxidized upon exposure to even low levels of atmospheric oxygen at room temperature[1-7], and incorporation of a small amount of a transition metal catalyst into oxygen scavenging materials can markedly accelerate oxidation reaction[8-11].   Specifically, by varying the catalyst concentration, film thickness, oxidation temperature and oxygen partial pressure, the reaction rate and/or oxygen diffusion rate could be modified, and the oxygen uptakes in polymer films varied accordingly.

In this study, a non-invasive headspace analysis method was developed to measure the rate and amount of oxygen uptake in oxygen scavenging films. The data were obtained by measuring oxygen headspace concentration above the scavenging polymer with an OxySense® 200T non-invasive oxygen sensor, and, for comparison, oxygen uptake was also measured with an analytical balance. Excellent agreement was observed between the two experiments.

Catalyst-promoted oxidation of commercially available 1,4-polybutadiene was studied to characterize the oxygen scavenging properties of this material. The oxidation

of 1,4-polybutadiene, in the presence of a transition metal salt catalyst, cobalt neodecanoate, was first studied at 30°C. The importance of polymer purification method and residual antioxidant on oxidation properties was determined. Although antioxidants can influence oxygen mass uptake and oxidation rate, they can be removed, with a sufficiently thorough purification process, to the point that they have little or no influence on oxygen uptake and oxidation kinetics. The influence of the polymer purification protocol (i.e., number of purification cycles and time under vacuum) on oxygen uptake and uptake kinetics was explored. Oxygen uptake of 1,4-polybutadiene films was measured as a function of cobalt neodecanoate concentration. In these samples, the films eventually sorb up to 15 weight percent oxygen in films that are approximately 100 µm thick; and the oxidation process occurs over approximately one week. FTIR and XPS analysis suggested that the oxidation was heterogeneous, with the film surface being highly oxidized and the film center being less oxidized. Interestingly, the oxygen uptake exhibited a maximum with catalyst loading, which is believed to be related to the heterogeneous nature of the oxidation process.

This dissertation reports oxygen mass uptake and permeability change during oxidation of 1,4-polybutadiene films. Films containing 200 ppm of cobalt catalyst of different film thicknesses (thickness varied from 66 µm to 344 µm) were oxidized in air. These thick films showed an increase in oxygen uptake per unit polymer mass as film thickness increased, while oxygen uptake per unit film area remained independent of thickness, suggesting that oxidation in films was heterogeneous and proceeded essentially as an oxidized front penetrating into the film from the surfaces exposed to oxygen.

Similar behavior was also observed in samples containing different amounts of cobalt catalyst. In contrast, oxidation in spin coated thin films (thinner than 6 µm) appears to proceed homogeneously, with oxygen uptake per unit mass being essentially independent of thickness. The oxidation in thin films also has higher oxygen mass uptake value (about 30 wt %) and faster oxidation timescale (about 1 day) that that observed in thick films. Two different methods were used to estimate the critical oxidized layer thickness in thick films by analyzing the final oxygen uptakes. Both methods gave similar critical oxidized layer thickness values, which were around 28 µm. The oxygen uptake data were generally well described by a simple model that restricts oxidation to only the film surfaces and only allows oxidation to a depth equal to the critical thickness. SEM images were also conducted on the cross sections of oxidized 1,4-polybutadiene films, a special layered structure was observed that was qualitatively in agreement with the hypothesis of heterogeneous oxidation in thicker films.

In cobalt-catalyzed 1,4-polybutadiene, the oxidation process exhibits a period of acceleration and then slows down. The reduction of the oxidation rate can be attributed to two concomitant causes: a decreasing number of reactive sites in the substrate as oxidation proceeds, and diffusion limitations on the ability of fresh oxygen to penetrate to unoxidized regions of the sample as a result of having to diffuse through highly oxidized surface layers that were relatively impermeable. In this regard, in oxidized thick films, oxygen and nitrogen permeability decreased by approximately two orders of magnitude relative to permeability values in unoxidized samples. Spin coated thin films were prepared, and the permeability coefficient of nitrogen in hihgly oxidized thin films was

172

also measured. Nitrogen permeability in 1,4-polybutadiene thin films decreased more than two orders of magnitude, from 11 Barrer in an unoxidized film to 0.07 Barrer in a highly oxidized film. Similar oxygen permeability changes were also observed before and after oxidization of these thin films, so the oxidized film a much better barrier material than the native, unoxidized polymer. A simple two-phase model, consisting of a highly oxidized surface extending into the sample to a depth corresponding to the critical thickness mentioned above and an unoxidized core, was used to describe the permeability data and estimate oxygen and nitrogen permeability in oxidized 1,4-polybutadiene thick films. If the permeability coefficients for oxygen and nitrogen in highly oxidized thin films and unoxidized films were used as the permeability coefficients in the oxidized surface layer and core region, respectively, the estimated permeability coefficient in thick films are in good agreement with the experimental data, showing that the two-phase model can capture much of the physics of the permeability decrease in thick film oxidation. The existence of oxidized layers which protect a relatively unoxidized core from further oxidation suggests that the use of thin layers of polybutadiene might provide more efficient use of the polymer in oxygen scavenging packaging applications.

This dissertation also reports oxygen scavenging properties of 1,4-polybutadiene oxidized under different temperatures and oxygen partial pressures. Polybutadiene films were oxidized at 45ºC, 30ºC, 5ºC and -20ºC, respectively, and experimental results showed different oxidation kinetics and final oxygen uptake values. Comparing with samples oxidized at 30ºC, samples oxidized at 45ºC gave similar oxygen uptake but a faster oxidation timescale. The two phase model is still suitable for oxidation at 45ºC

showing the formation of a highly oxidized layer. However, this model does not fit the oxidation data obtained at 5ºC. The oxidation in films at 5ºC appears to proceed much more homogenously than that at higher temperatures; the oxidation timescale is much longer and oxygen uptakes in thick films are relatively higher than they are in samples oxidized at higher temperatures. The reaction conditions for oxygen partial pressure variation were limited to oxygen mole fraction in initial atmosphere lower than 21%. Increasing oxygen partial pressure leads to a fast oxidation timescale and higher oxygen uptake.

Polyurethanes and poly(urethane-urea)s are linear block copolymers composed of flexible and rigid segments [12]. They usually have a micro-phase separated structure due to the incompatibility between the soft and hard segments[13]. The gas transport performance is affected by the concentration as well as the chemical structure of the hard and soft segments.[14-16]. The physical and gas transport properties of a systematic series of poly(urethane-urea)s were determined. The presence of different polyether diols affects thermal transitions as well as the fractional free volume and leads to changes in gas transport performance. Samples synthesized from PEG 2000 have a semi-crystalline structure at room temperature. The crystallization reduces soft segment content in the amorphous phase and leads to lower permeability. PPG-based poly(urethane-urea) has the highest FFV, as well as the highest permeability, but the CO_2 selectivity over other gases decreases slightly. The Terathane[®]-based polymers also have good gas permeability and better CO_2 separation properties than PPG-based materials. Both PPG- and Terathane[®]-based polymers exhibit much lower water uptake than PEG base

174

materials (about 150 wt % in PEG-based, 17 wt % in PPG-based and 10 wt % in Terathane®-based polymer), showing that in an environment with high humidity, these materials may achieve more stable separation properties.

8.2   Recommendations for Future Work

Cobalt catalyzed 1,4-polybutadiene films showed very good oxygen scavenging and barrier properties. They can chemically trap large amount of oxygen, and the permeability of the material decreases more than two orders of magnitudes following oxidation. For future research, similar materials could also be considered as oxygen scavenging materials. Oxygen mass uptake capacity and oxidation rate are important factors that need to be considered in food packaging applications. It is reported that 1,2-polybutadiene showed less crosslinking during oxidation[17] which means that such materials would have higher permeability after oxidation but should have higher oxygen uptake capacity. Because of its weak mechanical properties, 1,4-polybutadiene it may be advantageous to blend or copolymerize 1,4-polybutadiene with other polymers such as polystyrene. The blends or copolymers could have phase separated morphology, and the polybutadiene domain size in such materials would be smaller. This would also increase the oxygen mass uptake per unit polymer mass if the characteristic domain size were smaller than the critical thickness observed in these studies. 1,4-Polybutadiene or SBS materials can also be coextruded with other packaging materials such as PS or PET to

generate multilayered packaging films, which may be an important consideration in practical application of these materials.

A two-phase structure was observed in thick oxidized 1,4-polybutadiene films, with highly oxidized film surfaces sandwiching a less oxidized core. The oxidized layers could also be observed by SEM. It is believed the special structure observed in SEM was caused by the mechanical property change in the oxidized layer, since the oxidized polymer is known to become brittle. In the future, it would be of interest to further characterize the mechanical properties of 1,4-polybutadiene or other oxygen scavenging films before and after oxidation. This information could be important for practical packaging applications, where packaging materials that are flexible are often desired.

Although samples oxidized at 30ºC and ambient condition showed good oxygen scavenging and barrier properties, these properties could be better by adjusting the oxidation conditions. Even though samples oxidized at 45ºC and 5ºC also gave high oxygen uptake values, permeability experiments were only conducted on thin and thick films oxidized at 30ºC. This study suggests that sample oxidized at lower temperature lead to more homogeneous oxidation and higher oxygen mass uptake, and the influence of temperature on oxidation and permeation characteristics should be studied in greater detail. Since at different oxidation temperatures, the polymer may produce different oxidation and crosslinking products[7], the permeability coefficient for oxygen and nitrogen could also be different in oxidized layers that were prepared by oxidation at different temperatures. Therefore, it would also be of interest to study in greater detail

the effects of reaction temperature and oxygen partial pressure on gas permeability in thin and thick oxygen scavenging films.

The polyether based poly(urethane-urea)s exhibit interesting gas separation properties. In these materials, gas transport performance is related to the hard and soft segment content and chemical structures. Only 4,4'-methylene diphenyl diisocyanate as used in this study, but more diisocyanate candidates should be considered, such as 2,4-toluene diisocyanate (TDI) and isophorone diisocyanate (IPDI) due to different rigidity in diisocyanates. Lower molecular weight polyethers could also be used to reduce crystallinity in the polymers. The lower molecular weight polyether could lead to lower permeability but may result in a higher permeability selectivity to light gases because of more hard segment dissolving in soft segment regions[18-20]. Additionally, though it is hypothesized that the reduced water uptake of several of these materials would lead to more stable gas separation properties in humid environments, this hypothesis has not been validated experimentally. Therefore, it would be of interest to measure mixed gas separation properties in the presence of humidity to determine whether or not there is a strong correlation between low water uptake and lack of sensitivity of permeation properties to humidity. Finally, all measurements were conducted at 35C, and some important applications involving separation of carbon dioxide may well be conducted at temperatures much higher or lower than 35 C, so it would be of interest to characterize the temperature dependence of permeation properties in these materials. Finally, in this exploratory study, only permeability was measured. It would be of interest to also

measure gas solubility and diffusivity as well to more fully characterize the fundamental

properties of gas transport in this family of materials.

8.3 References

1.   C. Adam, J. Lacoste, and J. Lemaire. Photo-oxidation of elastomeric materials. 1. Photooxidation of polybutadienes. *Polymer Degradation and Stability*, **1989**, 24(3), 185-200.

2.   C. Adam, J. Lacoste, and J. Lemaire. Photo-oxidation of elastomeric materials. 2. Photo-oxidation of styrene-butadiene copolymer. *Polymer Degradation and Stability*, **1989**, 26(3), 269-284.

3.   R. G. Bauman and S. H. Maron. Oxidation of polybutadiene. I. Rate of oxidation. *Journal of Polymer Science*, **1956**, 22, 1-12.

4.   R. G. Bauman and S. H. Maron. The oxidation of polybutadiene. II. Property changes during oxidation. *Journal of Polymer Science*, **1956**, 22, 203-212.

5.   S. W. Beavan. Mechanistic studies on the photo-oxidation of commercial poly(butadiene). *European Polymer Journal*, **1974**, 10, 593-603.

6.   D. J. Nagle, M. Celina, L. Rintoul, and P. M. Fredericks. Infrared microspectroscopic study of the thermo-oxidative degradation of hydroxy-terminated polybutadiene/isophorone diisocyanate polyurethane rubber. *Polymer Degradation and Stability*, **2007**, 92(8), 1446-1454.

7.   M. Piton and A. Rivaton. Photooxidation of polybutadiene at long wavelengths (lambda>300nm). *Polymer Degradation and Stability*, **1996**, 53(3), 343-359.

8.   W. J. Gauthier and D. V. Speer. Method and compositions for improved oxgyen scavenging. U. S. Patent, 5,981,676, **1999**

9.   D. V. Speer, W. P. Roberts, and C. R. Morgan. Method and compositions for oxygen scavenging. U. S. Patent, 5,211,875, **1993**

10.   M. E. Stewart, R. N. Estep, B. B. Gamble, M. D. Cliffton, D. R. Quillen, L. S. Buehrig, V. Govindarajan, and M. J. Dauzvardis. Blends of oxygen scavenging

polyamides with polyesters which contain zinc and cobalt. United States Patent Application Publication, US 2006/0148957, **2006**

11. J. C. Jenkins, R. F. Morrow, and M. E. Stewart. Oxygen-scavenging polyesters useful for packaging. United States Patent Application Publication, US 2008/0161529, **2008**

12. D. Dieterich, E. Grigat, W. Hahn, H. Hespe, and H. G. Schmelzer. Principles of polyurethane chemistry and special applications. In: Oertel G., editor. Polyurethane Handbook: Chemistry-Raw Materials-Processing-Application-Properties. Hanser Gardner Publication, Cicinnati, OH, 1994, 11-31.

13. S. Abouzahr and G. L. Wilkes. Structure property studies of polyester- and polyether-based MDI-BD segmented polyurethanes: Effect of one- vs. 2-stage polymerization conditions. *Journal of Applied Polymer Science*, **1984**, 29(9), 2695-2711.

14. M. Pegoraro, L. Zanderighi, A. Penati, F. Severini, F. Bianchi, N. Cao, R. Sisto, and C. Valentini. Polyurethane membranes from polyether and polyester diols for gas fractionation. *Journal of Applied Polymer Science*, **1991**, 43(4), 687-697.

15. L. S. Teo, J. F. Kuo, and C. Y. Chen. Study on the morphology and permeation property of amine group-contained polyurethanes. *Polymer*, **1998**, 39(15), 3355-3364.

16. P. M. Knight and D. J. Lyman. Gas permeability of various block copolyether urethanes. *Journal of Membrane Science*, **1984**, 17(3), 245-254.

17. C. Adam, J. Lacoste, and J. Lemaire. Photooxidation of elastomeric materials. 4. Photooxidation of 1,2-polybutadiene. *Polymer Degradation and Stability*, **1990**, 29(3), 305-320.

18. K. Madhavan and B. S. R. Reddy. Poly(dimethylsiloxane-urethane) membranes: effect of hard segment in urethane on gas transport properties. *Journal of Membrane Science*, **2006**, 283(1-2), 357-365.

19. H. Xiao, Z. H. Ping, J. W. Xie, and T. Y. Yu. Permeation of CO_2 through polyurethane. *Journal of Applied Polymer Science*, **1989**, 40(7-8), 1131-1139.

20. K. Okamoto, M. Fujii, S. Okamyo, H. Suzuki, K. Tanaka, and H. Kita. Gas permeation properties of poly(ether imide) segmentd copolymers. *Macromolecules*, **1995**, 28(20), 6950-6956.

Bibliography

ASTM D4274-05 Standard Test Methods for Testing Polyurethane Raw Materials: Determination of Hydroxyl Numbers of Polyols. 2005.

ASTM D5155-07 Standard Test Methods for Polyurethane Raw Materials: Determination of the Isocyanate Content of Aromatic Isocyanates. 2007.

Plastics Engineering, **May 1984**, 47.

Y. Abe and Y. Kondoh. Oxygen absorbers. In: Brody A. L., editor. Controlled/Modified Atmosphere/Vacuum Packaging of Foods. Food and Nutrition Press, Trumbull, 1989, 151.

S. Abouzahr and G. L. Wilkes. Structure property studies of polyester- and polyether-based MDI-BD segmented polyurethanes: Effect of one- vs. 2-stage polymerization conditions. *Journal of Applied Polymer Science*, **1984**, 29(9), 2695-2711.

S. Abouzahr, G. L. Wilkes, and Z. Ophir. Structure property behavior of segmented polyether MDI butanediol based urethanes: Effect of composition ratio. *Polymer*, **1982**, 23(7), 1077-1086.

C. Adam, J. Lacoste, and J. Lemaire. Photo-oxidation of elastomeric materials. 1. Photooxidation of polybutadienes. *Polymer Degradation and Stability*, **1989**, 24(3), 185-200.

C. Adam, J. Lacoste, and J. Lemaire. Photo-oxidation of elastomeric materials. 2. Photo-oxidation of styrene-butadiene copolymer. *Polymer Degradation and Stability*, **1989**, 26(3), 269-284.

C. Adam, J. Lacoste, and J. Lemaire. Photooxidation of elastomeric materials. 4. Photooxidation of 1,2-polybutadiene. *Polymer Degradation and Stability*, **1990**, 29(3), 305-320.

C. Adam, J. Lacoste, and J. Lemaire. Photooxidation of elastomeric materials .3. Photooxidation of acrylonitrile butadiene copolymers. *Polymer Degradation and Stability*, **1990**, 27(1), 85-97.

G. Ahlblad, T. Reitberger, B. Terselius, and B. Stenberg. Thermal oxidation of hydroxyl-terminated polybutadiene rubber II. Oxidation depth profiles studied by imaging chemiluminescence. *Polymer Degradation and Stability*, **1999**, 65(2), 185-191.

G. Ahlblad, T. Reitberger, B. Terselius, and B. Stenberg. Thermal oxidation of hydroxyl-terminated polybutadiene rubber I. Chemiluminescence studies. *Polymer Degradation and Stability*, **1999**, 65(2), 179-184.

T. O. Ahn, I. S. Choi, H. M. Jeong, and K. Cho. Thermal and mechanical properties of thermoplastic polyurethane elastomers from different polymerization methods. *Polymer International*, **1993**, 31, 329-333.

L. E. Alexander. X-Ray Diffraction Methods in Polymer Science. 2 ed. R. K. Publishing Company, Malabar, Florida, 1985, 137.

G. C. Allen and A. Aguilo. Metal-ion catalyzed oxidation of acetaldehyde. *Advances in Chemistry Series*, **1968**, 76, 363-381.

T. M. Aminabhavi and N. N. Mallikarjuna. Polymeric membranes: Polymeric nanocomposites: Barrier properties and membrane applications. *Polymer News*, **2004**, 29(6), 193-195.

M. P. Anachkov, S. K. Rakovski, and R. V. Stefanova. Ozonolysis of 1,4-cis-polyisoprene and 1,4-trans-polyisoprene in solution. *Polymer Degradation and Stability*, **2000**, 67(2), 355-363.

G. J. Armerongen. Influence of structure of elastomers on their permeability to gases. *Journal of Polymer Science*, **1950**, 5(3), 307-332.

L. Audouin, V. Langlois, J. Verdu, and J. C. M. Debruijn. Role of oxygen diffusion in polymer aging - kinetic and mechanical aspects. *Journal of Materials Science*, **1994**, 29(3), 569-583.

L. Audouin and J. Verdu. Change in mechanical properties of low-density polyethylene during radiochemical aging. *ACS Symposium Series*, **1991**, 475, 473-484.

R. A. Azzam, S. K. Mohamed, R. Tol, V. Everaert, H. Reynaers, and B. Goderis. Synthesis and thermo-mechanical characterization of high performance polyurethane elastomers based on heterocyclic and aromatic diamine chain extenders. *Polymer Degradation and Stability*, **2007**, 92(7), 1316-1325.

R. W. Baker, J. G. Wijmans, and J. H. Kaschemekat. The design of membrane vapor-gas separation systems. *Journal of Membrane Science*, **1998**, 151(1), 55-62.

G. L. Banks, A. J. Chalk, J. E. Dawson, and J. F. Smith. Catalysis of olefin autoxidation by heavy-metal ions in nonpolar media. *Nature*, **1954**, 174, 274-275.

V. Barbi, S. S. Funari, R. Gehrke, N. Scharnagl, and N. Stribeck. SAXS and the gas transport in polyether-block-polyamide copolymer membranes. *Macromolecules*, **2003**, 36(3), 749-758.

R. G. Bauman and S. H. Maron. Oxidation of polybutadiene. I. Rate of oxidation. *Journal of Polymer Science*, **1956**, 22, 1-12.

R. G. Bauman and S. H. Maron. The oxidation of polybutadiene. II. Property changes during oxidation. *Journal of Polymer Science*, **1956**, 22, 203-212.

G. Beamson and D. Briggs. High resolution XPS of organic polymers John Wiley & Sons Ltd., West Sussex, England, 1992.

S. W. Beavan. Mechanistic studies on the photo-oxidation of commercial poly(butadiene). *European Polymer Journal*, **1974**, 10, 593-603.

A. T. Betts and N. Uri. Conversion of metal catalysts into inhibitors of autoxidation. *Makromolekulare Chemie*, **1966**, 95, 22-39.

A. T. Betts and N. Uri. Catalyst-inhibitor conversion in autoxidation reactions. *Advances in Chemistry Series*, **1968**, 76, 160-181.

P. R. Bevington and D. K. Robinson. Data Reduction and Error Analysis for the Physical Sciences, 3rd ed. McGraw-Hill, Inc., New York, 2003.

S. W. Bigger and O. Delatycki. New approach to the measurement of polymer photooxidation. *Journal of Polymer Science Part A: Polymer Chemistry*, **1987**, 25(12), 3311-3323.

N. C. Billingham and T. J. Walker. Autoxidation of poly(4-methyl-1-pentene). I. Role of diffusion in autoxidation kinetics. *Journal of Polymer Science, Polymer Chemistry*, **1975**, 13(5), 1209-1222.

H. J. Bixler and O. J. Sweeting. Barrier Properties of Polymer Films. In: Bixler H. J. and Sweeting O. J., editors. Science and Technology of Polymer Films. Wiley-Interscience, New York City, New York, 1971, 1-130.

J. F. Black. Metal-catalyzed autoxidation. The unrecognized consequences of metal-hydroperoxide complex formation. *Journal of the American Chemical Society*, **1978**, 100(2), 527-535.

J. L. Bolland. Kinetic studies in the chemistry of rubber and related materials. I. The thermal oxidation of ethyl linoleate. *Proceedings of the Royal Society of London. Series A, Mathematical and Physical Sciences*, **1946**, A186(1005), 218-236.

V. I. Bondar, B. D. Freeman, and I. Pinnau. Gas sorption and characterization of poly(ether-b-amide) segmented block copolymers. *Journal of Polymer Science Part B-Polymer Physics*, **1999**, 37(17), 2463-2475.

V. I. Bondar, B. D. Freeman, and I. Pinnau. Gas transport properties of poly(ether-b-amide) segmented block copolymers. *Journal of Polymer Science Part B: Polymer Physics*, **2000**, 38(15), 2051-2062.

A. Bondi. Physical Properties of Molecular Crystals, Liquid, and Glasses John Wiley and Sons, New York, 1968.

D. E. Bornside, C. W. Macosko, and L. E. Scriven. On the modeling of spin coating. *Journal of Imaging Technology*, **1987**, 13(4), 122-130.

C. R. Boss and J. C. W. Chien. Oxygen diffusion limitation in autoxidation of polypropylene. *Journal of Polymer Science, Part A-1: Polymer Chemistry*, **1966**, 4(6), 1543-1551.

K. Brandon, M. Beggan, P. Allen, and F. Butler. The performance of several oxygen scavengers in varying oxygen environments at refrigetrated temperatures: implications for low-oxygen modified atmosphere packaging of meat. *International Journal of Food Science and Technology*, **2009**, 44, 188-196.

J. Brandrup, E. H. Immergut, and E. A. Grulke. Polymer Handbook Fourth Edition John Wiley & Sons, Inc., New York City, New York, 1999.

A. L. Brody. Modified atomsphere packaging of seafoods. In: Brody A. L., editor. Controlled/Modified Atmosphere/Vacuum Packaging of Foods. Food and Nutrition Press, Trumbull, 1989, 59-60.

C. B. Bucknall and D. G. Street. Fracture behavior of rubber-modified thermophastics after aging. *Journal of Applied Polymer Science*, **1968**, 12(6), 1311-1320.

P. J. Cahill and S. Y. Chen. Oxygen scavenging condensation copolymers for bottle and packaging articles. U. S. Patent, 6,509,436, **2003**

N. Cao, M. Pegoraro, F. Bianchi, and L. Zanderighi. Gas transport properties of polycarbonate-polyurethane membranes. *Journal of Applied Polymer Science*, **1993**, 48(10), 1831-1842.

A. Car, C. Stropnik, W. Yave, and K. V. Peinemann. PEG modified poly(amide-b-ethylene oxide) membranes for CO_2 separation. *Journal of Membrane Science*, **2008**, 307(1), 88-95.

A. Car, C. Stropnik, W. Yave, and K. V. Peinemann. Pebax (R)/polyethylene glycol blend thin film composite membranes for CO_2 separation: Performance with mixed gases. *Separation and Purification Technology*, **2008**, 62(1), 110-117.

S. Carranza, D. R. Paul, and R. T. Bonnecaze. Analytic formulae for the design of reactive polymer blend barrier materials. *Journal of Membrane Science*, Submitted.

S. Carranza, D. R. Paul, and R. T. Bonnecaze. Design formulae for reactive barrier membranes. *Chemical Engineering Science*, **2010**, 65(3), 1151-1158.

M. Celina and K. T. Gillen. Oxygen permeability measurements on elastomers at temperatures up to 225 degrees C. *Macromolecules*, **2005**, 38(7), 2754-2763.

M. Celina, A. C. Graham, K. T. Gillen, R. A. Assink, and L. M. Minier. Thermal degradation studies of a polyurethane propellant binder. *Rubber Chemistry and Technology*, **2000**, 73(4), 678-693.

M. Celina, J. M. Skutnik Elliott, R. A. Winters, R. A. Assink, and L. M. Minier. Correlation of antioxidant depletion and mechanical performance during thermal degradation of an HTPB elastomer. *Polymer Degradation and Stability*, **2006**, 91, 1870-1879.

M. C. Celina and R. A. Assink. Polymer durability and radiation effects American Chemical Society, Washington, DC, 2007.

A. J. Chalk and J. F. Smith. Catalysis of cyclohexane autoxidation by trace metals in nonpolar media. II. Metal salts in the presence of chelating agents. *Transactions of the Faraday Society*, **1957**, 53, 1235-1245.

T. Y. Ching, K. Katsumoto, S. P. Current, and L. P. Theard. Compositions having ethylenic backbone and benzylic, allylic, or ether-containing side-chains, oxygen scavenging compositions containing same, and process for making these compositions by esterification or transesterification of a polymer melt. U. S. Patent, 5,627,239, **1997**

B. C. Chun, T. K. Cho, M. H. Chong, and Y. C. Chung. Structure-property relationship of shape memory polyurethane cross-linked by a polyethyleneglycol spacer between polyurethane chains. *Journal of Materials Science*, **2007**, 42(21), 9045-9056.

D. R. Clarke, S. Suresh, and I. M. Ward. Surface analysis of polymers by XPS and static SIMS Cambridge University Press, Cambridge, United Kingdom, 1998.

R. L. Clough and K. T. Gillen. Oxygen diffusion effects in thermally aged elastomers. *Polymer Degradation and Stability*, **1992**, 38(1), 47-56.

R. L. Clough, K. T. Gillen, and C. A. Quintana. Heterogeneous oxidative degradation in irradiated polymers. *Journal of Polymer Science, Polymer Chemistry Edition*, **1985**, 23(2), 359-377.

M. A. Cochran, R. Folland, J. W. Nicholas, and M. E. R. Robinson. Packaging. U. S. Patent, 5,021,515, **1991**

J. A. Coffman. Highly cross-linked polybutadiene. *Journal of Industrial and Engineering Chemistry*, **1952**, 44, 1421-1428.

M. Coquillat, J. Verdu, X. Colin, L. Audouin, and M. Celina. A kinetic evaluation of the thermal oxidation of a phenol stabilised polybutadiene. *Polymer Degradation and Stability*, **2008**, 93(9), 1689-1694.

M. Coquillat, J. Verdu, X. Colin, L. Audouin, and R. Neviere. Thermal oxidation of polybutadiene. Part 1: Effect of temperature, oxygen pressure and sample thickness on the thermal oxidation of hydroxyl-terminated polybutadiene. *Polymer Degradation and Stability*, **2007**, 92(7), 1326-1333.

M. Coquillat, J. Verdu, X. Colin, L. Audouin, and R. Neviere. Thermal oxidation of polybutadiene. Part 2: Mechanistic and kinetic schemes for additive-free non-crosslinked polybutadiene. *Polymer Degradation and Stability*, **2007**, 92(7), 1334-1342.

M. Coquillat, J. Verdu, X. Colin, L. Audouin, and R. Neviere. Thermal oxidation of polybutadiene. Part 3: Molar mass changes of additive-free non-crosslinked polybutadiene. *Polymer Degradation and Stability*, **2007**, 92(7), 1343-1349.

F. M. B. Coutinho and M. C. Delpech. Degradation profile of films cast from aqueous polyurethane dispersions. *Polymer Degradation and Stability*, **2000**, 70(1), 49-57.

C. F. Cullis and H. S. Laver. The effect of metal oxides on the oxidation of polybutadiene. *European Polymer Journal*, **1978**, 14, 575-580.

A. V. Cunliffe and A. Davis. Photooxidation of thick polymer samples. Part II. The influence of oxygen diffusion on the natural and artificial weathering of polyolefins. *Polymer Degradation and Stability*, **1982**, 4(1), 17-37.

E. L. Cussler, S. E. Hughes, W. J. Ward, and R. Aris. Barrier membranes. *Journal of Membrane Science*, **1988**, 38(2), 161-174.

L. Cuve, J. P. Pascault, G. Boiteux, and G. Seytre. Synthesis and properties of polyurethanes based on polyolefin. 1. Rigid polyurethanes and amorphous segmented polyurethanes prepared in polar-solvents under homogeneous conditions. *Polymer*, **1991**, 32(2), 343-352.

M. J. Cyr. Polyether containing polymers for oxygen scavenging. U. S. Patent, 6455620 B1, **2002**

H. A. Daynes. The Permeability of Rubber and Methods of Testing It. *Transactions, Institution of the Rubber Industry*, **1928**, 3, 428-453.

S. N. Dhoot, B. D. Freeman, and M. E. Stewart. Sorption and transport of linear alkane hydrocarbons in biaxially oriented polyethylene terephthalate. *Journal of Polymer Science Part B: Polymer Physics*, **2001**, 39(11), 1160-1172.

S. N. Dhoot, B. D. Freeman, and M. E. Stewart. Barrier Polymers. In: Kroschwitz J. I., editor. Encyclopedia of Polymer Science and Technology, vol. 5. Wiley-Interscience, New York, 2003, 193-263.

D. Dieterich, E. Grigat, W. Hahn, H. Hespe, and H. G. Schmelzer. Principles of polyurethane chemistry and special applications. In: Oertel G., editor. Polyurethane Handbook: Chemistry-Raw Materials-Processing-Application-Properties. Hanser Gardner Publication, Cicinnati, OH, 1994, 11-31.

S. P. Fairgrieve and J. R. MacCallum. Diffusion-controlled oxidation of polymers: A mathematical model. *Polymer Degradation and Stability*, **1985**, 11(3), 251-265.

W. R. Falla, M. Mulski, and E. L. Cussler. Estimating diffusion through flake-filled membranes. *Journal of Membrane Science*, **1996**, 119(1), 129-138.

C. J. Farrell and B. C. Tsai. Oxygen Scavenger. U. S. Patent, 4,536,409, **1985**

M. C. Ferrari, S. Carranza, R. T. Bonnecaze, K. K. Tung, B. D. Freeman, and D. R. Paul. Modeling of oxygen scavenging for improved barrier behavior: Blend films *Journal of Membrane Science*, **2009**, 329(1-2), 183-192.

E. W. Fischer and S. Fakirov. Structure and properties of polyethyleneterephthalate crystallized by annealing in the highly oriented state. *Journal of Materials Science*, **1976**, 11(6), 1041-1064.

B. D. Freeman. Basis of permeability/selectivity tradeoff relations in polymeric gas separation membranes. *Macromolecules*, **1999**, 32(2), 375-380.

B. D. Freeman and I. Pinnau. Polymeric materials for gas separations. In: Freeman B. D. and Pinnau I., editors. Polymer Membranes for Gas and Vapor Separation, vol. 733. ACS Symposium Series, Washington DC, 1999, 1-27.

M. Frounchi, S. Dadbin, Z. Salehpour, and M. Noferesti. Gas barrier properties of PP/EPDM blend nanocomposites. *Journal of Membrane Science*, **2006**, 282(1+2), 142-148.

G. Galland and T. M. Lam. Permeability and diffusion of gases in segmented polyurethanes: structure-properties relations. *Journal of Applied Polymer Science*, **1993**, 50(6), 1041-1058.

W. J. Gauthier and D. V. Speer. Method and compositions for improved oxgyen scavenging. U. S. Patent, 5,981,676, **1999**

R. V. Gemmer and M. A. Golub. Applications of Polymer Spectroscopy Academic Press, New York 1978, 79.

K. Ghosal and B. D. Freeman. Gas separation using polymer membranes: an overview. *Polymers for Advanced Technologies*, **1994**, 5, 673-697.

K. T. Gillen, M. Celina, R. L. Clough, and J. Wise. Extrapolation of accelerated aging data - Arrhenius or erroneous? *Trends in Polymer Science*, **1997**, 5(8), 250-257.

K. T. Gillen and R. L. Clough. Rigorous experimental confirmation of a theoretical-model for diffusition-limited oxidation. *Polymer*, **1992**, 33(20), 4358-4365.

D. Gomes, K.-V. Peinemann, S. P. Nunes, W. Kujawski, and J. Kozakiewicz. Gas transport properties of segmented poly(ether siloxane urethane ureaP membranes. *Journal of Membrane Science*, **2006**, 281, 747-753.

B. G. S. Goss, I. Blakey, M. D. Barry, and G. A. George. Modelling of infectious spreading in heterogeneous polymer oxidation II. Refinement of stochastic model and calibration using chemiluminescence of polypropylene. *Polymer Degradation and Stability*, **2001**, 74(3), 523-532.

U. Graham. On the absorption and dialytic separation of gases by colloid septa Part I.-Action of a septum of caoutchouc. *Philosophical Magazine*, **1866**, 32, 401-420.

J. Greener. Moisture permeability through multilayered barrier films as applied to flexible OLED display. *Journal of Applied Polymer Science*, **2007**, 106, 3534-3542.

M. Guyader, L. Audouin, X. Colin, J. Verdu, and S. Chevalier. Epoxides in the thermal oxidation of polybutadiene. *Polymer Degradation and Stability*, **2006**, 91(11), 2813-2815.

J. M. S. Henis and M. K. Tripodi. Composite hollow fiber membranes for gas separation: the resistance model approach. *Journal of Membrane Science*, **1981**, 8(3), 233-246.

J. M. S. Henis and M. K. Tripodi. The developing technology of gas separating membranes. *Science*, **1983**, 220(4592), 11-17.

K. Hodge. Diffusion of Oxygen and Carbon Dioxide in Thermally Crystallized Syndiotactic Polystyrene. *Journal of Polymer Science: Part B: Polymer Physics*, **2001**, 39, 2519-2538.

Y. S. Hu, V. Prattipati, S. Mehta, D. A. Schiraldi, A. Hiltner, and E. Baer. Improving gas barrier of PET by blending with aromatic polyamides. *Polymer*, **2005**, 46(8), 2685-2698.

Y. Huang and D. R. Paul. Experimental methods for tracking physical aging of thin glassy polymer films by gas permeation. *Journal of Membrane Science*, **2004**, 244(1-2), 167-178.

Y. Huang, X. Wang, and D. R. Paul. Physical aging of thin glassy polymer films: Free volume interpretation. *Journal of Membrane Science*, **2006**, 277(1-2), 219-229.

M. Iring, T. Kelen, and F. Tudos. Thermal oxidation of polyolefins. II. Effect of layer thickness on the rate of oxidation in the melt phase. *European Polymer Journal*, **1975**, 11(9), 631-636.

J. C. Jenkins, R. F. Morrow, and M. E. Stewart. Oxygen-scavenging polyesters useful for packaging. United States Patent Application Publication, US 2008/0161529, **2008**

W. A. Jenkins and J. P. Harrington. Packaging Foods with Plastics. Technomic Publishing Co., Lancaster, 1991, 326-327.

X. Jiang, J. F. Ding, and A. Kumar. Polyurethane-poly(vinylidene fluoride) (PU-PVDF) thin film composite membranes for gas separation. *Journal of Membrane Science*, **2008**, 323(2), 371-378.

H. Ju, B. D. McCloskey, A. C. Sagle, Y. H. Wu, V. A. Kusuma, and B. D. Freeman. Crosslinked poly(ethylene oxide) fouling resistant coating materials for oil/water separation. *Journal of Membrane Science*, **2008**, 307(2), 260-267.

Y. Kamiya and K. U. Ingold. The metal-catalyzed autoxidation of Tetralin. IV. The effect of solvent and temperature. *Canadian Journal of Chemistry*, **1964**, 42(11), 2424-2433.

T. Kanaya, T. Kawaguchi, and K. Kaji. Local dynamics of cis-1, 4-polybutadiene near the glass transition temperature T_g. *Physica B: Condensed Matter*, **1992**, 182(4), 403-408.

S. Kelman, H. Q. Lin, E. S. Sanders, and B. D. Freeman. CO_2/C_2H_6 separation using solubility selective membranes. *Journal of Membrane Science*, **2007**, 305(1-2), 57-68.

D. R. Kemp. Gas sorption in Polymer Membranes containing adsorptive fillers. *Journal of Polymer Science: Polymer Physics Edition*, **1974**, 12, 485-500.

J. H. Kim and Y. M. Lee. Gas permeation properties of poly(amide-6-b-ethylene oxide)-silica hybrid membranes. *Journal of Membrane Science*, **2001**, 193(2), 209-225.

S. G. Kiryushkin and Y. A. Shlyapnikov. Diffusion-controlled polymer oxidation. *Polymer Degradation and Stability*, **1989**, 23(2), 185-192.

H. Kitano, K. Ichikawa, M. Ide, M. Fukuda, and W. Mizuno. Fourier transform infrared study on the state of water sorbed to poly(ethylene glycol) films. *Langmuir*, **2001**, 17(6), 1889-1895.

P. M. Knight and D. J. Lyman. Gas permeability of various block copolyether urethanes. *Journal of Membrane Science*, **1984**, 17(3), 245-254.

W. J. Koros. Barrier Polymers and Structures: Overview. In: Koros W. J., editor. Barrier Polymers and Structures. American Chemical Society, Washington, DC, 1990, 1-22.

W. J. Koros and M. W. Hellums. Gas separation membrane material selection criteria: differences for weakly and strongly interacting feed components. *Fluid Phase Equilibria*, **1989**, 53, 339-354.

A. S. Kuzminskii, I. A. Shokhin, and R. M. Belitzkaya. The nature of structural changes of butadiene rubbers caused by high temperatures (100-200°C). *Rubber Chemistry and Technology*, **1952**, 25, 33-35.

M. E. Ladhabhoy and M. M. Sharma. Absorption of oxygen by 2-ethylhexanaldehyde. *Journal of Applied Chemistry*, **1970**, 20(9), 274-280.

N. K. Lape. Barrier membranes of self-assembled lamellar poly(lactide-isoprene-lactide) triblock copolymers. *Journal of Membrane Science*, **2005**, 259, 1-9.

N. K. Lape, C. F. Yang, and E. L. Cussler. Flake-filled reactive membranes. *Journal of Membrane Science*, **2002**, 209(1), 271-282.

L. H. Lee, C. L. Stacy, and R. G. Engel. Mechanisms of oxidative degradation. II. Effect of metallic salts and metal deactivators on the oxidation of polybutadiene. *Journal of Applied Polymer Science*, **1966**, 10(11), 1717-1724.

L. H. Lee, C. L. Stacy, and R. G. Engel. Mechanisms of oxidative degradaton. I. Oxidation of synthetic rubbers catalyzed by metallic ions. *Journal of Applied Polymer Science*, **1966**, 10(11), 1699-1715.

W. M. Lee. Selection of barrier materials from molecular structure. *Polymer Engineering and Science*, **1980**, 20, 65.

H. Li, D. K. Ashcraft, B. D. Freeman, M. E. Stewart, M. K. Jank, and T. R. Clark. Non-invasive headspace measurement for characterizing oxygen-scavenging in polymers. *Polymer*, **2008**, 49(21), 4541-4545.

H. Li, K. K. Tung, D. R. Paul, and B. D. Freeman. Effect of thickness on auto-oxidation in cobalt-catalyzed 1,4-polybutadiene films. In preparation.

H. Li, K. K. Tung, D. R. Paul, and B. D. Freeman. Characterization of oxygen scavenging films based on 1,4-polybutadiene. In preparation.

H. Lin and B. D. Freeman. Gas solubility, diffusity and permeability in poly(ethylene oxide). *Journal of Membrane Science*, **2004**, 239, 105-117.

H. Lin and B. D. Freeman. Gas and vapor solubility in cross-linked poly(ethylene glycol diacrylate). *Macromolecules*, **2005**, 38(20), 8394-8407.

H. Lin and B. D. Freeman. Permeation and Diffusion. In: Czichos H., Smith L. E., and Saito T., editors. Springer-Handbook of Materials Measurement Methods. Springer, Berlin, 2006, 371-387.

H. Lin, E. Van Wagner, R. Raharjo, B. D. Freeman, and I. Roman. High-performance polymer membranes for natural-gas sweetening. *Advanced Materials*, **2006**, 18(1), 39-44.

H. Q. Lin and B. D. Freeman. Materials selection guidelines for membranes that remove CO_2 from gas mixtures. *Journal of Molecular Structure*, **2005**, 739(1-3), 57-74.

H. Q. Lin, T. Kai, B. D. Freeman, S. Kalakkunnath, and D. S. Kalika. The effect of cross-linking on gas permeability in cross-linked poly(ethylene glycol diacrylate). *Macromolecules*, **2005**, 38(20), 8381-8393.

H. Q. Lin, E. Van Wagner, B. D. Freeman, L. G. Toy, and R. P. Gupta. Plasticization-enhanced hydrogen purification using polymeric membranes. *Science*, **2006**, 311(5761), 639-642.

H. Q. Lin, E. Van Wagner, J. S. Swinnea, B. D. Freeman, S. J. Pas, A. J. Hill, S. Kalakkunnath, and D. S. Kalika. Transport and structural characteristics of crosslinked poly(ethylene oxide) rubbers. *Journal of Membrane Science*, **2006**, 276(1-2), 145-161.

E. A. Lissi and M. V. Encinas. Photoinitiators for Free Radical Polymerization
In: Rabek J. F., editor. Photochemistry and Photophysics, vol. V. CRC Press: Boca Raton, 1991.

S. Lusse and K. Arnold. The interaction of poly(ethylene glycol) with water studied by H-1 and H-2 NMR relaxation time measurements. *Macromolecules*, **1996**, 29(12), 4251-4257.

K. Madhavan and B. S. R. Reddy. Poly(dimethylsiloxane-urethane) membranes: effect of hard segment in urethane on gas transport properties. *Journal of Membrane Science*, **2006**, 283(1-2), 357-365.

B. Mailhot and J. L. Gardette. Polystyrene photooxidation 1. Identification of the IR-absorbing photoproducts formed at short and long wavelength. *Macromolecules*, **1992**, 25(16), 4119-4126.

B. Mailhot and J. L. Gardette. Polystyrene photooxidation 2. A pseudo wavelength effect. *Macromolecules*, **1992**, 25(16), 4127-4133.

S. Matteucci, Y. Yampolskii, B. D. Freeman, and I. Pinnau. Transport of Gases and Vapors in Glassy and Rubbery Polymers. In: Yampolskii Y., Freeman B. D., and Pinnau I., editors. Material Science of Membranes for Gas and Vapor Separation. John Wiley & Sons, New York, 2006, 1-47.

C. C. McDowell, B. D. Freeman, and G. W. McNeely. Acetone sorption and uptake kinetic in poly(ethylene terephthalate). *Polymer*, **1999**, 40(12), 3487-3499.

I. C. McNeill and W. T. K. Stevenson. The structure and stability of oxidized polybutadiene. *Polymer Degradation and Stability*, **1985**, 11(2), 123-143.

I. C. McNeill and W. T. K. Stevenson. Thermal degradation of styrene-butadiene diblock copolymer. Part 1. Characteristics of polystyrene and polybutadiene degradation. *Polymer Degradation and Stability*, **1985**, 10(3), 247-265.

I. C. McNeill and W. T. K. Stevenson. Thermal degradation of styrene-butadiene diblock copolymer. Part 2. Characteristics and mechanism of degradation of the copolymer. . *Polymer Degradation and Stability*, **1985**, 10(4), 319-334.

M. Menard and R. W. Paynter. Fick's law of diffusion depth profiles applied to the degradation of oxidized polystyrene during ARXPS analysis. *Surface and Interface Analysis*, **2005**, 37(5), 466-471.

T. C. Merkel, V. I. Bondar, K. Nagai, B. D. Freeman, and I. Pinnau. Gas sorption, diffusion, and permeation in poly(dimethylsiloxane). *Journal of Polymer Science Part B: Polymer Physics*, **2000**, 38, 415-434.

T. C. Merkel, B. D. Freeman, R. J. Spontak, Z. He, I. Pinnau, P. Meakin, and A. J. Hill. Ultrapermeable, reverse-selective nanocomposite membranes. *Science*, **2002**, 296(5567), 519-522.

S. J. Metz, M. H. V. Mulder, and M. Wessling. Gas-permeation properties of poly(ethylene oxide) poly(butylene terephthalate) block copolymers. *Macromolecules*, **2004**, 37(12), 4590-4597.

G. D. Moggridge. Barrier films using flakes and reactive additives. *Progress in Organic Coatings*, **2003**, 46, 231-240.

J. M. Mohr, D. R. Paul, T. E. Mlsna, and R. J. Lagow. Surface fluorination of composite membranes 1. Transport-properties. *Journal of Membrane Science*, **1991**, 55(1-2), 131-148.

J. M. Mohr, D. R. Paul, Y. Taru, T. E. Mlsna, and R. J. Lagow. Surface fluorination of composite membranes 2. Characterization of the fluorinated layer. *Journal of Membrane Science*, **1991**, 55(1-2), 149-171.

S. Mondal and J. L. Hu. Structural characterization and mass transfer properties of nonporous-segmented polyurethane membrane: Infulence of the hydrophilic segment content and soft segment melting temperature. *Journal of Membrane Science*, **2006**, 276, 16-22.

K. Nagai, S. Tanaka, Y. Hirata, T. Nakagawa, M. E. Arnoldb, B. D. Freeman, D. Lerouxc, D. E. Bettsc, J. M. DeSimonec, and F. A. DiGiano. Solubility and diffusivity of sodium chloride in phase-separated block copolymers of poly(2-dimethylaminoethyl methacrylate), poly(1,1'-dihydroperfluorooctyl methacrylate) and poly(1,1,2,2-tetrahydroperfluorooctyl acrylate). *Polymer*, **2001**, 42(25), 9941-9948.

N. Nagai, T. Matsunobe, and T. Imai. Infrared analysis of depth profiles in UV-photochemical degradation of polymers. *Polymer Degradation and Stability*, **2005**, 88(2), 224-233.

D. J. Nagle, M. Celina, L. Rintoul, and P. M. Fredericks. Infrared microspectroscopic study of the thermo-oxidative degradation of hydroxy-terminated polybutadiene/isophorone diisocyanate polyurethane rubber. *Polymer Degradation and Stability*, **2007**, 92(8), 1446-1454.

E. E. Nuxoll. Layered reactive barrier films. *Journal of Membrane Science*, **2005**, 252, 29-36.

K. Okamoto, M. Fujii, S. Okamyo, H. Suzuki, K. Tanaka, and H. Kita. Gas permeation properties of poly(ether imide) segmentd copolymers. *Macromolecules*, **1995**, 28(20), 6950-6956.

J. M. Orban, T. M. Chapman, W. R. Wagner, and R. Jankowski. Easily grafted polyurethanes with reactive main chain functional groups. Synthesis, characterization, and antithrombogenicity of poly(ethylene glycol)-grafted poly(urethanes). *Journal of Polymer Science Part a-Polymer Chemistry*, **1999**, 37(17), 3441-3448.

G. Papet, L. Audouin, L. Rackova, and J. Verdu. Diffusion controlled radiochemical oxidation of low-density polyethylene 2. Kinetic modeling. *Radiation Physics and Chemistry*, **1989**, 33(4), 329-335.

H. B. Park, C. K. Kim, and Y. M. Lee. Gas separation properties of polysiloxane/polyether mixed soft seogment urethane urea membranes. *Journal of Membrane Science*, **2002**, 204(1-2), 257-269.

D. R. Paul. Effect of Immobilizing Adsorption on the Diffusion Time Lag. *Journal of Polymer Science: Part A-2*, **1969**, 7, 1811-1818.

D. R. Paul. The Diffusion Time Lag in Polymer Membranes containing Adsorptive Fillers. *Journal of Polymer Science: Symposium*, **1973**, 41, 79-93.

M. Pegoraro, L. Zanderighi, A. Penati, F. Severini, F. Bianchi, N. Cao, R. Sisto, and C. Valentini. Polyurethane membranes from polyether and polyester diols for gas fractionation. *Journal of Applied Polymer Science*, **1991**, 43(4), 687-697.

I. Pinnau and Z. J. He. Pure- and mixed-gas permeation properties of polydimethylsiloxane for hydrocarbon/methane and hydrocarbon/hydrogen separation. *Journal of Membrane Science*, **2004**, 244(1-2), 227-233.

193

M. Piton and A. Rivaton. Photooxidation of polybutadiene at long wavelengths (lambda>300nm). *Polymer Degradation and Stability*, **1996**, 53(3), 343-359.

M. Piton and A. Rivaton. Photo-oxidation of ABS at long wavelengths (lambda>300 nm). *Polymer Degradation and Stability*, **1997**, 55(2), 147-157.

M. R. Pixton and D. R. Paul. Relationship between structure and transport properties for polymers with aromatic backbones. In: Paul D. R. and Yampol'skii Y. P., editors. Polymeric Gas Separation Membranes. CRC Press, Boca Raton, 1994, 83-154.

T. K. Poddar and K. K. Sirkar. A hybrid of vapor permeation and membrane-based absorption-stripping for VOC removal and recovery from gaseous emissions. *Journal of Membrane Science*, **1997**, 132(2), 229-233.

A. Polyakova. Oxygen-Barrier Properties of Copolymers Based on Ethylene Terephthalate. *Journal of Polymer Science Part B: Polymer Physics*, **2001**, 39(16), 1889-1899.

A. Polyakova, D. M. Connor, D. M. Collard, D. A. Schiraldi, A. Hiltner, and E. Baer. Oxygen-barrier properties of polyethylene terephthalate modified with a small amount of aromatic comonomer. *Journal of Polymer Science Part B-Polymer Physics*, **2001**, 39(16), 1900-1910.

J. F. Rabek, G. Canback, and B. Ranby. Studies on photooxidation mechanism of polymers 6. Role of commercial thermostabilizers in photostability of polyvinyl-chloride. *Journal of Applied Polymer Science*, **1977**, 21(8), 2211-2223.

J. F. Rabek and D. Lala. Carotenoids as effective stabilizers against photo-oxidation of cis-1,4-polybutadiene. *Journal of Polymer Science Part C-Polymer Letters*, **1980**, 18(6), 427-437.

J. F. Rabek, J. Lucki, and B. Ranby. Comparative studies of reactions of commercial polymers with molecular oxygen, singlet oxygen, atomic oxygen and ozone 1. Reactions with cis-1,4-polybutadiene. *European Polymer Journal*, **1979**, 15(12), 1089-1100.

J. F. Rabek and B. Ranby. Role of singlet oxygen in photooxidative degradation and photostabilization of polymers. *Polymer Engineering and Science*, **1975**, 15(1), 40-43.

J. F. Rabek and B. Ranby. Studies on photooxidation mechanism of polymers 5. Oxidation of polybutadienes by singlet oxygen from microwave discharge and in dye-photosensitized reactions. *Journal of Polymer Science Part a-Polymer Chemistry*, **1976**, 14(6), 1463-1473.

J. F. Rabek and B. Ranby. Studies on the photooxidative mechanism of polymers 7. Role of singlet oxygen in the dye photosensitized oxidation of cis-1.4-polybutadiene and 1,2-polybutadiene and butadiene-styrene copolymers. *Journal of Applied Polymer Science*, **1979**, 23(8), 2481-2491.

R. D. Raharjo, H. J. Lee, B. D. Freeman, T. Sakaguchi, and T. Masuda. Pure gas and vapor permeation properties of poly[1-phenyl-2-[p-(trimethylsilyl)phenyl]acetylene] (PTMSDPA) and its desilylated analog, poly[diphenylacetylene] (PDPA). *Polymer*, **2005**, 46(17), 6316-6324.

R. D. Raharjo, H. Q. Lin, D. E. Sanders, B. D. Freeman, S. Kalakkunnath, and D. S. Kalika. Relation between network structure and gas transport in crosslinked poly(propylene glycol diacrylate). *Journal of Membrane Science*, **2006**, 283(1-2), 253-265.

N. Ravi, A. Mitra, P. Hamilton, and F. Horkay. Characterization of the network properties of poly(ethylene glycol)-acrylate hydrogels prepared by variations in the ethanol-water solvent composition during crosslinking copolymerization. *Journal of Polymer Science Part B: Polymer Physics*, **2002**, 40(23), 2677-2684.

L. Reich and S. S. Stivala. Autoxidation of Hydrocarbons and Polyolefins Marcel Dekker, Inc., New York, 1969.

L. Reich and S. S. Stivala. Elements of Polymer Degradation McGraw-Hill, Inc., New York, 1971.

L. M. Rincon-Rubio, X. Colin, L. Audouin, and J. Verdu. A theoretical model for the diffusion-limited thermal oxidation of elastomers at medium temperatures. *Rubber Chemistry and Technology*, **2003**, 76(2), 460-482.

L. M. Robeson. Correlation of separation factors versus permeability for polymeric membranes. *Journal of Membrane Science*, **1991**, 62(2), 165-185.

M. L. Rooney. Active packaging in polymer films. In: Rooney M. L., editor. Active food packaging, vol. 4. Blackie Academic & Professional, London, 1995, 74-110.

G. M. Ruhnke and L. F. Biritz. Fast, quantitative method of measuring the natural and artificial aging behavior of ABS material. *Plastics & Polymers*, **1972**, 40(147), 118-124.

J. P. Santerre and J. L. Brash. Microstructure of polyurethane ionomers derivatized with dodecylamine and polyethylene oxide in the hard segment. *Journal of Applied Polymer Science*, **1994**, 52(4), 515-523.

J. Scheirs, S. W. Bigger, and N. C. Billingham. A review of oxygen-uptake techniques for measuring polyolefin oxidation. *Polymer Testing*, **1995**, 14(3), 211-241.

W. J. Schrenk. Coextruded Multilayer Polymer Films and Sheets. In: Paul D. R., editor. Polymer Blends, vol. 2. Academic Press, 1978.

M. A. Schubert. Role of Oxigen in biodegradation of poly(etherurethane urea) elastomers. *Journal of Biomedical Materials Research*, **1997**, 34, 519-530.

R. A. Sheldon and J. K. Kochi. Metal-Catalyzed Oxidations of Organic Compounds. Academic Press, Inc. , New York City, New York, 1981, 33-48.

R. A. Sheldon and J. K. Kochi. Metal-Catalyzed Oxidations of Organic Compounds. Academic Press, Inc. , New York City, New York, 1981, 22.

Y. T. Shieh, H. T. Chen, K. H. Liu, and Y. K. Twu. Thermal degradation of MDI-based segmented polyurethanes. *Journal of Polymer Science Part a-Polymer Chemistry*, **1999**, 37(22), 4126-4134.

M. B. Shiflett and H. C. Foley. Ultrasonic deposition of high-selectivity nanoporous carbon membranes. *Science*, **1999**, 285(5435), 1902-1905.

T. Shimotori, E. L. Cussler, and W. A. Arnold. Diffusion of mobile products in reactive barrier membranes. *Journal of Membrane Science*, **2007**, 291(1-2), 111-119.

R. A. Siegel. Characterization of relaxation to steady state in membranes with binding and reaction. *Journal of Membrane Science*, **2005**, 251, 91-99.

R. A. Siegel and E. L. Cussler. Reactive barrier membranes: some theoretical observations regarding the time lag and breakthrough curves. *Journal of Membrane Science*, **2004**, 229(1-2), 33-41.

F. T. Simon and J. M. Rutherford. Crystallization and melting behavior of polyethylene oxide copolymers. *Journal of Applied Physics*, **1964**, 35(82), 82-86.

A. Singh, B. D. Freeman, and I. Pinnau. Pure and mixed gas acetone/nitrogen permeation properties of polydimethylsiloxane [PDMS]. *Journal of Polymer Science Part B: Polymer Physics*, **1998**, 36, 230-289.

C. Sinturel and N. C. Billingham. A theoretical model for diffusion-limited oxidation applied to oxidation profiles monitored by chemiluminescence in hydroxy-terminated polybutadiene. *Polymer International*, **2000**, 49(9), 937-942.

J. M. Smith. Chemical Engineering Kinetics, 2nd edn., McGraw-Hill Inc., New York, 1970, Chapter 12.

J. M. Smith, H. C. Ness, and M. M. Abbott. Introduction to Chemical Engineering Thermodynamics, 5th ed. McGraw-Hill, Inc., New York, 1996.

P. So and L. J. Broutman. The effect of surface embrittlement on the mechanical behavior of rubber-modified polymers. *Polymer Engineering and Science*, **1982**, 22(14), 888-894.

S. E. Solovyov. Theory of transient permeation through reactive barrier films I. Steady state theory for homogeneous passive and reactive media. *International Journal of Polymeric Materials*, **2005**, 54, 71-91.

S. E. Solovyov. Theory of transient permeation through reactive barrier films II. Two layer reactive passive structures with dynamic interface. *International Journal of Polymeric Materials*, **2005**, 54, 93-115.

S. E. Solovyov. Theory of transient permeation through reactive barrier films III. Solute ingress dynamics and model lag times. *International Journal of Polymeric Materials*, **2005**, 54, 117-139.

S. E. Solovyov. Optimized design of multilayer barrier films incorporating a reactive layer. I. Methodology of ingress analysis. *Journal of Applied Polymer Science*, **2006**, 100, 1940-1951.

S. E. Solovyov. Optimized design of multilayer barrier films incorporating a reactive layer. II. Solute dynamics in two-layer films. *Journal of Applied Polymer Science*, **2006**, 100, 1952-1965.

S. E. Solovyov. Optimized design of multilayer barrier films incorporating a reactive layer. III. Case analysis and generalized multilayer solutions. *Journal of Applied Polymer Science*, **2006**, 100, 1966-1977.

Y. M. Song, W. C. Chen, T. L. Yu, K. Linliu, and Y. H. Tseng. Effect of isocyanates on the crystallinity and thermal stability of polyurethanes. *Journal of Applied Polymer Science*, **1996**, 62(5), 827-834.

D. V. Speer, C. R. Morgan, W. P. Roberts, and R. K. Ramesh. Compositions, articles and methods for scavenging oxygen which have improved physical properties. U. S. Patent, 5,399,289, **1995**

D. V. Speer and W. P. Roberts. Oxygen scavenging compositions for low temperature use. U. S. Patent, 5,310,497, **1993**

D. V. Speer, W. P. Roberts, and C. R. Morgan. Method and compositions for oxygen scavenging. U. S. Patent, 5,211,875, **1993**

M. E. Stewart, R. N. Estep, B. B. Gamble, M. D. Cliffton, D. R. Quillen, L. S. Buehrig, V. Govindarajan, and M. J. Dauzvardis. Blends of oxygen scavenging polyamides with polyesters which contain zinc and cobalt. United States Patent Application Publication, US 2006/0148957, **2006**

G. Strupinsky and A. L. Brody. *presented at the Polymers, Laminations and Coating Conference, San Francisco*, **1998 (unpublished)**.

P. M. Subramanian. Barrier Materials by Blending. In: Paul D. R., editor. Polymer Blends, vol. 2. Wiley, 2000.

S. Sunderrajan, B. D. Freeman, C. K. Hall, and I. Pinnau. Propane and propylene sorption in solid polymerelectrolytes based on poly(ethylene oxide). *Journal of Membrane Science*, **2001**, 182(1-2), 1-12.

T. Takahashi, N. Hayashi, and S. Hayashi. Structure and properties of shape-memory polyurethane block copolymers. *Journal of Applied Polymer Science*, **1996**, 60(7), 1061-1069.

T. Tawa and S. Ito. Preparation and reactions of hydrophilic isocyanate micelles dispersed in water. *Colloid and Polymer Science*, **2005**, 283(7), 731-737.

L. S. Teo, C. Y. Chen, and J. F. Kuo. Fourier transform infrared spectroscopy study on effects of temperature on hydrogen bonding in amine-containing polyurethanes and poly(urethane-urea)s. *Macromolecules*, **1997**, 30(6), 1793-1799.

L. S. Teo, J. F. Kuo, and C. Y. Chen. Study on the morphology and permeation property of amine group-contained polyurethanes. *Polymer*, **1998**, 39(15), 3355-3364.

F. N. Teumac. The history of oxygen scavenging bottle closures. In: Rooney M. L., editor. Active food packaging, vol. 8. Blackie Academic & Professional, London, 1995, 193-201.

J. M. Tibbitt, G. E. Rotter, D. P. Sinclair, G. T. Brooks, and R. T. Behrends. Oxygen scavenging monolayer bottles. United States Patent Application Publication, US 2002/0183488, **2002**

A. V. Tobolsky, D. J. Metz, and R. B. Mesrobian. Low temperature autoxidation of hydrocarbons: the phenomenon of maximum rates. *Journal of the American Chemical Society*, **1950**, 72, 1942-1952.

M. L. Tsai and A. K. Murali. Oxygen scavenging polymer compositions containing ethylene vinyl alcohol copolymers. U. S. Patent, 6,793,994, **2004**

G. J. van Amerongen. Influence of structure of elastomers on their permeability to gases. *Journal of Polymer Science*, **1950**, 5, 307-332.

G. J. van Amerongen. Diffusion in elastomers. *Rubber Chemistry and Technology*, **1964**, 37, 1065-1152.

D. W. van Krevelen. Properties of Polymers: Their Correlation with Chemical Structure; Their Numerical Estimation and Prediction from Additive Group Contributions Elsevier Science, Amsterdam, 1990.

L. Vermeiren, F. Devlieghere, M. van Beest, N. de Kruijf, and J. Debevere. Developments in the active packaging of foods. *Trends in Food Science & Technology*, **1999**, 10(3), 77-86.

H. Y. Wang, T. Ugomori, Y. Wang, K. Tanaka, H. Kita, K. I. Okamoto, and Y. Suma. Sorption and pervaporation properties of crosslinked membranes of poly(ethylene oxide imide) segmented copolymer to aromatic/nonaromatic hydrocarbon mixtures. *Journal of Polymer Science Part B-Polymer Physics*, **2000**, 38(13), 1800-1811.

S. M. Wang, J. R. Chang, and R. C. Tsiang. Infrared studies of thermal oxidative degradation of polystyrene-block-polybutadiene-block-polystyrene thermoplastic elastomers. *Polymer Degradation and Stability*, **1996**, 52(1), 51-57.

A. Weill and E. Dechenaux. The spin-coating process mechanism related to polymer solution properties. *Polymer Engineering and Science*, **1988**, 28(15), 945-948.

R. H. Whitfield and D. I. Davies. Novel nitrogen-containing antidegradants for polybutadiene. *Polymer Photochemistry*, **1981**, 1(4), 261-274.

J. G. Wijmans and R. W. Baker. The solution-diffusion model: a review. *Journal of Membrane Science*, **1995**, 107, 1-21.

J. Wise, K. T. Gillen, and R. L. Clough. Quantitative model for the time development of diffusion-limited oxidation profiles. *Polymer*, **1997**, 38(8), 1929-1944.

V. Wroblewski. Ueber die natur der absorption der gase durch flussigkeiten unter hohen drucken. *Ann Physik u Chem*, **1879**, 8, 29-52.

H. Xiao, Z. H. Ping, J. W. Xie, and T. Y. Yu. Permeation of CO_2 through polyurethane. *Journal of Applied Polymer Science*, **1989**, 40(7-8), 1131-1139.

C. Yang, E. E. Nuxoll, and E. L. Cussler. Reactive Barrier Films. *AIChE Journal*, **2001**, 47(2), 295-302.

H. Yasuda, C. E. Lamaze, and L. D. Ikenberry. Permeability of solutes through hydrated polymer membranes. I. Diffusion of sodium chloride. *Die Makromolekulare Chemie*, **1968**, 118(1), 19-35.

W. Yave, A. Car, S. S. Funari, S. P. Nunes, and K. V. Peinemann. CO_2-philic polymer membrane with extremely high separation performance. *Macromolecules*, **2010**, 43(1), 326-333.

W. Yave, A. Car, K. V. Peinemann, M. Q. Shaikh, K. Ratzke, and F. Faupel. Gas permeability and free volume in poly(amide-b-ethylene oxide)/polyethylene glycol blend membranes. *Journal of Membrane Science*, **2009**, 339(1-2), 177-183.

E. Yilgor, E. Burgaz, E. Yurtsever, and I. Yilgor. Comparison of hydrogen bonding in polydimethylsiloxane and polyether based urethane and urea copolymers. *Polymer*, **2000**, 41(3), 849-857.

Y. Yin, L. M. Yang, M. Yoshino, J. H. Fang, K. Tanaka, H. Kita, and K. I. Okamoto. Synthesis and gas permeation properties of star-like poly(ethylene oxide)s using hyperbranched polyimide as central core. *Polymer Journal*, **2004**, 36(4), 294-302.

Y. Yoo. Maleation of poly(3,4-epoxy-1-butene) for accelerated crosslinking in the presence of a redox catalyst. *Journal of Polymer Science: Part A: Polymer Chemistry*, **2002**, 40, 2789-2798.

M. Yoshino, K. Ito, H. Kita, and K. I. Okamoto. Effects of hard-segment polymers on CO_2/N_2 gas separation properties of poly(ethylene oxide) segmented copolymers. *Journal of Polymer Science Part B-Polymer Physics*, **2000**, 38(13), 1707-1715.

B. Zenner, E. Decastro, and J. Ciccone. Ligand extracting composition-containing chelated transition metal immobilised on solid phase, especially for scavenging oxygen in containers. U. S. Patent, 5,096,724, **1992**

P. Zoller and D. Walsh. Standard Pressure-Volume-Temperature Data for Polymers, 1st ed. Technomic Publishing Company, Inc., Lancaster, 1995.

R. A. Zoppi, S. das Neves, and S. P. Nunes. Hybrid films of poly(ethylene oxide-b-amide-6) containing sol-gel silicon or titanium oxide as inorganic fillers: effect of

morphology and mechanical properties on gas permeability. *Polymer*, **2000**, 41(14), 5461-5470.

M. Zulfiqar, A. Quddos, and S. Zulfiqar. Polyurethane networks based on poly(ethylene oxide). *Journal of Applied Polymer Science*, **1993**, 49, 2055-2063.

Vita

Hua Li was born in China, and he is the only child in his family. After graduating from the High School attached to Fudan University, he attended Fudan University (Shanghai, China) and received his Bachelor of Science degree in Applied Chemistry in July 1999 and Master of Science degree in Macromolecular Chemistry and Physics in July 2002. He enrolled in the Department of Chemistry and Biochemistry at The University of Texas at Austin the following summer to pursue a doctoral degree under the guidance of Professor Richard Jones and Professor Benny Freeman.

Permanent address: Room 501, No. 24, Lane 440, Changjiang Road

Shanghai 200431, P. R. China

This dissertation was typed by Hua Li.